NTNU

Norwegian University of
Science and Technology

A thermogravimetric and kinetic study on devolatilization of woody biomass

María Zabalo Alonso

Master's Thesis

Submission date: July 2016

Supervisor: Khanh-Quang Tran, EPT

Co-supervisor: Liang Wang, SINTEF Energy Research
Øyvind Skreiberg, SINTEF Energy Research

Norwegian University of Science and Technology
Department of Energy and Process Engineering

Norwegian University of Science and Technology

Faculty of Engineering Science and Technology
Department of Energy and Process Engineering

EPT-P-2016-157

NTNU

MASTER THESIS PROJECT

For student:

Maria Zabalo Alonso

Spring 2016

English title

A thermogravimetric and kinetic study on devolatilization of woody biomass

Background and objective

Biomass has a large potential to act as a major and sustainable substitution solution for fossil fuels in the future. Woody biomass is one of most abundant biomass resources, which has been used directly for heat and power generation through different thermal conversion routes. Devolatilization is the primary and key step for thermal conversion of the biomass, which has a great impact on char formation and its reactivity. This will affect the overall conversion efficiency of the process.

On the other hand, charcoal produced from woody biomass via carbonization can also be used for energy purpose or as reductant in metallurgical industries. The volatile content of charcoal is normally low, compared to raw biomass, but can be significantly varying depending on carbonization conditions. During carbonization, char formation is associated with the devolatilization of volatile matters. Physical and chemical properties of residual char after devolatilization are not fully understood and need further investigations.

In the present work, the devolatilization behaviours of various woody biomasses at different conditions will be investigated by means of thermogravimetric analysis.

The following tasks are to be considered:

1. Literature survey on devolatilization of woody biomass
    a. Identifying key physical and chemical properties influencing devolatilization behaviors of woody biomass
    b. Identifying critical parameters for devolatilization behaviors of woody biomass
    c. Influence of devolatilization on further conversion (with focus on gasification) of woody biomass
    d. Kinetic modelling and simulation of woody biomass devolatilization
2. Thermogravimetric study on devolatilization behaviours of woody biomass considering the variations of:
    a. Wood species (soft- and hardwood)
    b. Stem wood and forest residue
    c. Particle size and sample mass
3. Kinetic study of devolatilization of woody biomass

-- “ --

Address
N-7034 Trondheim
Norway

Location
K. Hejes vei 1b

Tel. +47 73 59 38 60
Fax +47 73 59 35 80
Org. no. NO 974 767 880

Within 14 days of receiving the written text on the master thesis, the candidate shall submit a research plan for his project to the department.

When the thesis is evaluated, emphasis is put on processing of the results, and that they are presented in tabular and/or graphic form in a clear manner, and that they are analyzed carefully.

The thesis should be formulated as a research report with summary both in English and Norwegian, conclusion, literature references, table of contents etc. During the preparation of the text, the candidate should make an effort to produce a well-structured and easily readable report. In order to ease the evaluation of the thesis, it is important that the cross-references are correct. In the making of the report, strong emphasis should be placed on both a thorough discussion of the results and an orderly presentation.

The candidate is requested to initiate and keep close contact with his/her academic supervisor(s) throughout the working period. The candidate must follow the rules and regulations of NTNU as well as passive directions given by the Department of Energy and Process Engineering.

Risk assessment of the candidate's work shall be carried out according to the department's procedures. The risk assessment must be documented and included as part of the final report. Events related to the candidate's work adversely affecting the health, safety or security, must be documented and included as part of the final report. If the documentation on risk assessment represents a large number of pages, the full version is to be submitted electronically to the supervisor and an excerpt is included in the report.

Pursuant to "Regulations concerning the supplementary provisions to the technology study program/Master of Science" at NTNU §20, the Department reserves the permission to utilize all the results and data for teaching and research purposes as well as in future publications.

The final report is to be submitted digitally in DAIM. An executive summary of the thesis including title, student's name, supervisor's name, year, department name, and NTNU's logo and name, shall be submitted to the department as a separate pdf file. Based on an agreement with the supervisor, the final report and other material and documents may be given to the supervisor in digital format.

☒ Work to be done in lab (Water power lab, Fluids engineering lab, Thermal engineering lab)

☐ Field work

Department of Energy and Process Engineering, 26 January 2016

Olav Bolland

Department Head

Khanh-Quang Tran

Academic Supervisor

Co-supervisors: Liang Wang and Øyvind Skreiberg (SINTEF Energy Research)

MASTER'S THESIS:

A thermogravimetric and kinetic study on devolatilization of woody biomass

Author: Maria Zabalo Alonso

Supervisor: Khanh-Quang Tran

Co-supervisors: Liang Wang, Øyvind Skreiberg

Trondheim, July 2016

Norwegian University of Science and Technology

Faculty of Engineering Science and Technology

Department of Energy and Process Engineering

NTNU
Norwegian University of
Science and Technology

Abstract

Biomass is a promising energy resource for a more sustainable global energy outlook. Thermochemical conversion of biomass is a very attractive and important technology for energy generation and production of value-added products such as charcoal. With the aim of studying the internal processes taking place when thermochemical conversion of biomass takes place, in this Master's Thesis a thermogravimetric analysis of woody biomass samples was developed. Woody biomass samples underwent pyrolysis experiments, with the main goal of the development of the kinetic modeling and simulation of the decomposition process. Also, the effect of various experimental parameters was studied for achieving increasing char yield values in pyrolysis processes.

Pyrolysis experiments of hardwood (birch and oak) and softwood (spruce) samples were developed by means of a thermogravimetric analyzer. Besides, two types of samples were studied for each of the mentioned species: stem wood samples and forest residue samples, composed by tops and branches of the trees (named as GROT, the corresponding Norwegian acronym). By means of changing particle size and sample mass of the samples, it was analyzed whether this parameters affected the kinetics of the samples and so, whether reactions were fully kinetically controlled or some heat and mass transfer limitations were needed to be considered. For this, three different kinetic approaches were employed. From the results obtained, it was concluded that the considered experimental parameters had some effects on the kinetics of the samples, as not negligible differences were registered in the values of the kinetic parameters obtained under different experimental conditions. Besides, the heterogeneous nature of GROT samples was also proved in terms of kinetics, in contrast with the high level of repeatability of the stem wood samples. Regarding the study of the char yield, it was concluded that higher char yield values were obtained when developing the pyrolysis experiments in an atmosphere of generated volatiles, rather than in a pure, nitrogen atmosphere. The effect of ash forming elements favoring char yield was also observed, with GROT samples giving the highest values. It was also registered an odd behavior of oak stem wood and GROT samples, which is further explained in this Thesis.

Sammendrag

I dag står biomasse som en lovende energikilde i den hensikt å oppnå en mer bærekraftig global energiutsiktene. Konkret er termokjemisk konvertering av biomasse en meget attraktiv teknologi for energiproduksjon og for fremstilling av trekull. Målet var å studere de indre prosesser som skjer i termokjemisk konvertering av biomasse. I denne masteroppgaven ble det utviklet for å Termogravimetrisk analyse av trevirke prøver. Trevirke prøvene tok pyrolyse eksperimenter, med hovedmål for utviklingen av den kinetiske modellering og simulering av nedbryting prosessen. Effekten av ulike eksperimentelle parametre ble undersøkt også for å oppnå høyere røye ytelsesverdier i pyrolyseprosesser .

Table of contents

List of Figures

List of Tables

List of abbreviations and acronyms

A	ash content [%]
A	pre-exponential factor or frequency factor [min^{-1}]
A_i, A_j	pre-exponential factor or frequency factor of the i^{th} or j^{th} pseudo-component [min^{-1}]
ASTM	American Standard Test Method
α	degree of conversion [-]
β	heating rate, dT/dt [K min^{-1}]
c_i, c_j	contribution that the i^{th} or j^{th} pseudo-component makes to the decomposition process
(concentration of component)$_j$	presence of the j^{th} pseudo-component in the initial sample
DAEM	Distributed Activation Energy Model
DTG curve	first derivative of the mass loss curve obtained from the Thermogravimetric Analyzer
dα/dt	conversion rate, as function of time [min^{-1}]
dα/dT	conversion rate, as function of temperature [K^{-1}]
$d\alpha_j/dT$	conversion rate of the j^{th} pseudo-component, as function of temperature [K^{-1}]
-dY/dT	first temperature derivative of the mass loss curve
$(-dY/dT)_{exp}$	experimentally obtained first temperature derivative of the mass loss curve
$(-dY/dT)_{calc}$	theoretically calculated first temperature derivative of the mass loss curve
E	activation energy [kJ/mol]
E_i, E_j	activation energy of the i^{th} or j^{th} pseudo-component [kJ/mol];
E_0	mean value of the activation energy when using the DAEM [kJ/mol];
E_{0i}, E_{0j}	mean value of the activation energy of the i^{th} or j^{th} pseudo-component when using the DAEM [kJ/mol];
FC	Fixed Carbon content [%]
FIT	fit quality obtained for the modeling by means of the Least Square Method [%]
FWO	Flynn and Wall (method)
f(α)	conversion function dependent on the reaction mechanism
f(E)	distribution function of the activation energy when using the DAEM
G(α)	temperature integral used in some isoconversional methods
HHV	Higher Heating Value
h_k	the highest value of the decomposition rate during the experiment
i	number of the point of a curve that is currently being evaluated in the Least Square Method
j	number of the pseudo-component that is being currently considered in the least Square Method
KAS	Kissinger-Akahira-Sunose isoconversional method
k	number of the experiment that is currently being evaluated in the Least Square Method
κ(T)	temperature dependent rate constant

κ_1	primary cracking constant of char
κ_2	primary cracking constant of tar
κ_3	primary cracking constant of volatiles
M	the amount of the considered pseudo-components in the Least Square Method
M	Moisture content [%]
M_{char}	dry mass of char produced in the pyrolysis process at its final temperature [kg]
M_{feed}	mass of the feedstock measured at the end of the 105^{o}C heating stage [kg]
m_0	initial sample mass [kg]
m_T	remaining sample mass at T temperature [kg]
m_f	final mass [kg]
n	reaction order of decomposition process
n_i, n_j	reaction order of the decomposition process of the i^{th} or j^{th} pseudo-component
N_{exper}	number of experiments evaluated together in the lest Square Method
N_k	number of points considered at a given curve in the Least Square Method
OF	Objective Function in the Least Square Method
σ	deviation corresponding to the activation energy parameter when using the DAEM [kJ/mol];
σ_i, σ_j	deviation corresponding to the activation energy parameter of the i^{th} or j^{th} pseudo-component when using the DAEM [kJ/mol];
P_u	temperature integral for the Master-plots method
R	universal gas constant [8.314x10^3 kJ/mol];
reldev	relative deviation in the Least Square Method [%]
T	absolute temperature [K]
TGA	Thermogravimetric Analyzer
TGA curve	mass curve obtained from the Thermogravimetric Analyzer
$T_f(\beta)$	temperature at a fixed "f" value of the conversion degree, for a heating rate value of β
T_0	sublimit of the temperature integral
V_j	released mass fraction of the j^{th} pseudo-component in a certain moment of the process
V_j^*	total released mass fraction of the j^{th} pseudo-component in the whole process
VM	Volatile Matter content [%]
X	horizontal axis of the graphical methods
x	the fraction of volatiles that will be released from a certain T temperature until the end of the decomposition process, in reference to the total amount of volatiles released in the whole process
Y	vertical axis of the graphical methods
Y	sample mass normalized to the unity
Y_{char}	char yield [%]
$(yield\ of\ volatiles)_j$	amount of volatiles released form a unit mass of the j^{th} pseudo-component

1. Introduction

1.1. Scope and goals of the project

The main objective of this Master's Thesis is to develop a kinetic data set for thermal decomposition of woody biomass in the absence of oxygen. In addition, this project also looks at the effect of feedstock type and process parameters (feedstock particle size, initial mass, and the gas released during the decomposition) on the kinetics.

For collecting data of the thermal decomposition process of the different sample types, pyrolysis experiments were carried out in a Thermogravimetric Analyzer, TGA. The experiments were non-isothermal and were developed in an inert, nitrogen atmosphere. By means of the TGA instrument, all needed information regarding mass loss of the samples and their corresponding decomposition rates were constantly recorded during the whole pyrolysis process, providing us with the necessary data for developing the kinetic modeling.

Although the kinetic modeling of biomass, and specially of woody biomass, has been widely studied by many authors [1-15]**,** the novelty introduced by the study developed for this Master's Thesis is that, not only kinetic modeling of stem wood samples was been developed, but the behavior of forest residue samples was also simulated. The fact of modeling the kinetics of forest residue samples is quite rare and involves a higher level of difficulty in terms of achieving a good modeling of their behavior due to the high variability on the composition of forest residues and their heterogeneous nature. In short, in the current work it was deeply studied the comparison in terms of kinetic behavior and kinetic parameters between hardwood and softwood samples and between stem wood samples and forest residue samples, what involves the newness introduced by this Thesis.

Before going into the kinetic modeling process directly, a literature survey on the different and most commonly used kinetic models was developed, concluding with some models that were chosen as they were considered to be the most appropriate and accurate for the study of our samples behavior.

Besides, as previously said, one of the objectives of developing this kinetic modeling task was to observe the effect that some of the experimental parameters may have on the

kinetics of the samples. For carrying out this task, it was firstly studied how some of the experimental parameters are able to affect the kinetics behavior; based on this study, it was decided to carry out experiments with different sample mass and particle size, with the main goal of studying the effect that changing these parameters may have on the values of kinetic parameters.

Apart from the kinetic modeling and simulation, this thesis also pursued another important goal: to study how the charcoal yield of woody biomass carbonization can be improved by controlling the reaction environment, the sample mass and the feedstock particle size. For this, a new set of experiments was carried out by means of changing the decomposition atmosphere at which experiments took place, for studying how the environment affected the final char yields. Besides, comparison of solid yield of hardwood and softwood samples and of stem wood and forest residue samples was carried out.

1.2. Motivation for the study: biomass as key factor in the future global energy matrix

The main motivation of this project was based on the prediction of the evolution of the energy generation policies and measures which are needed to be taken by countries all over the world during the coming years, and which will force a rapid evolution and a wider implementation of renewable energy sources. Thus, the current global environmental concern and the spread awareness of the need to reduce the greenhouse gas emissions have led attention to the development and improvement of alternative energy sources that can substitute the dominant presence of fossil fuels in the global energy matrix.

As an example, the so-called 20/20/20 targets that the European Union countries have agreed on regarding climate change and energy involve that for 2020, the following should be achieved [16]:

- greenhouse gas emissions 20% lower than values from 1990 (this reduction will be of the 30% in case the conditions are good for it);
- 20% of energy needs from renewable energy; and
- 20% increase in energy efficiency.

At the same time, further and more challenging objectives based on the 20/20/20 goals have been established for 2030 by the same institution [17]:

- At least 40% of reduction in greenhouse gas emissions from 1990 levels
- 27% of energy needs from renewable energy
- 27% improvement in energy efficiency

The need for achieving these objectives involves that the politics of the countries within the European Union are obliged to follow a path where the presence, importance and efficiency of renewable energy sources will be dramatically and unavoidably increased. This global need was also reflected by the 2015 United Nations Climate Conference held in Paris, where the so-called Paris Agreement on the reduction of climate change was approved establishing measures to be taken in the same direction as the previously mentioned agreements from the European Union [18].

At the same time, this shift to a more eco-friendly way of energy production will have to cover the increasing energy demand all over the world, which between years 2010 and 2040, is expected to grow a 56% as far as The International Energy Outlook 2013 (IEO2013) [20,21]. For the moment, this increasing energy demand is mainly compensated by means of conventional energy sources such as coal, oil or natural gas, which are responsible for high levels of pollutants and greenhouse gas emissions and which are heading for an unavoidable, early extinction [21]. Therefore, for the implementation of a whole transformation in both, ways of energy generation and energy consumption, there is an urgent necessity of taking worldwide actions towards a global power generation system based on renewable and efficient energy sources. Besides, during the incoming decades they will be needed more sever energy generation policies that favor the reduction of the greenhouse gas and pollutant emissions.

In this context in which steps forwards are required to be taken for achieving a more sustainable energy outlook and where a diversification in energy supplies is compulsory in order to face the increasing energy consumption, bioenergy, meaning the energy obtained from biomass, stands as a renewable alternative with a high potential. Biomass is considered as a clean source of renewable energy whose exploitation contributes to the reduction of environmental pollution [22]. Biomass can be directly used for power generation, including electricity generation or heat power generation, or can be used to produce target products such as synthesis gas, liquid biofuels or solid charcoal [21,23]. The application of bioenergy covers the substitution of energy from fossil sources but it also competes with other renewable energy sources such as wind power and hydropower. Although there is a wide range of alternatives competing, bioenergy has been able to make a place for itself within the global energy scene and its presence has been continuously increasing recently, satisfying more than 14% of the world energy demand [19,23].

For the obtaining and utilization of the energy contained in the biomass, thermochemical conversion processes are considered to be effective, efficient and relatively simple procedures. Biomass counts with an outstanding advantage when undergoing thermochemical processes for energy generation or for obtaining target products, as its neutral nature in relation to greenhouse gas emissions and global warming is assumed [8]. This involves that the CO2 emissions produced when a

thermochemical process is applied to biomass is supposed to be balanced by the CO2 that the biomass has removed from the atmosphere during its life cycle, meaning that the equilibrium of the atmospheric carbon concentration is not altered. Among the existing thermochemical processes for conversion of biomass into energy or chemicals, the main and most applied conversion techniques are based on combustion, gasification, pyrolysis and liquefaction [24]. In those thermochemical conversion processes, devolatilization stands as the first decomposition step in which volatile matter initially contained in the feedstock is released and light and condensable gases escape from the solid matter [25]. Therefore, devolatilization stands as the key, initial process preceding further conversion steps and it is in this fact where its importance resides. This is why achieving to obtain a good description of the devolatilization process is highly important in biomass modeling.

Besides, still further development and improvement of both technically and economically feasible and therefore profitable systems for conversion of biomass to energy by means of thermochemical conversion processes is needed, what requires a deep understanding of the thermal properties of biomass and a broad study and understanding of the reaction kinetics [3].

Concretely, woody biomass is probably the biomass source with one of the highest potential in terms of exploitation and it currently stands as the most important renewable energy source [26]. In the year 2010, the use of woody biomass meant about the 9% of the world primary energy consumption, and this supposed the 65% of the world renewable primary energy consumption[20,26]. Although this figures are highly impressive and show the spread use and exploitation of woody biomass resources, they are still below the real potential this resource has. For instance, it has been foreseen that for the year 2050, all the existing and available woody biomass resources could cover between the 10% and the 40% of the expected primary energy needs and consumption of the world [26].

Therefore, it is undeniable the high potential and importance of woody biomass not only as a renewable energy source, but also as an energy source that covers a high percentage of the world's primary energy consumption and whose contribution to the global energy matrix is expected to grow.

As several types of biomass resources, woody biomass can be employed both, for energy generation and for bio-fuels production. Although the needed technology for a high-level exploitation of woody biomass resources has been available to be used for many years, its use has widely spread recently. This massive use of biomass was not introduced before because its use was not feasible in economic terms. But with the expected development of the world's energy production with focus on a more eco-friendly energy generation policy and with the highest support to the use of renewable energy sources in history due to worldwide legislation being obliged to include measures for reducing climate change, the use of woody biomass has spread and its contribution to the energy outlook is expected to continue increasing [27].

Thus, as previously said, among biomass energy resources woody biomass stands as the most important and promising energy resource with a high potential. Furthermore, the exploitation and utilization of woody biomass resources leads to some unique benefits that involve real and important advantages.

For instances, woody biomass has a more or less uniform distribution along the world's surface, which is a feature that cannot be attributed to, for example, finite fossil fuels. This worldwide availability involves a real possibility for many countries around the world to generate their own clean energy while reducing their energy dependence on other countries. This means a unique opportunity not only for national energy self-sufficiency, but also for regional and local energy self-sufficiency, while providing opportunities to rural population and farmers in the use of the regional or local potential for a sustainable development [28]. These benefits, together with the reduction of greenhouse gas emissions and the technologically and economically feasible nature of the needed resources for its exploitation, make woody biomass one of the ideal future energy sources which will play a decisive role in the future global energy outlook.

In this context, the knowledge of the kinetics of woody biomass materials when undergoing a certain thermal degradation process is important and can result useful in terms of the design of different thermochemical reactors, as for instance pyrolysis and gasification reactors, and also for the optimization of the process conditions of the different thermal processes.

Thus, it was considered that developing the kinetic modeling of woody biomass samples and studying their devolatilization behavior had the needed and valuable

motivation, aiming to make a contribution to the biomass kinetic modeling and simulation fields. Thus, the current Master's Thesis focused on analyzing and modeling the kinetics of woody biomass by means of running pyrolysis experiments in a Thermogravimetric Analyzer, TGA.

Another important motivation was also found for this study, due to the novelty that some of the analyzed feedstock involved in the kinetic modeling field: the analyzed feedstock included stem wood samples and forest residue samples, being the kinetic modeling and the study of the thermal decomposition of the latter quite rare. Thus, developing the study of a non-widely analyzed type of woody biomass means a newness itself that contributes to the motivation of the study.

Besides, related to the kinetic modeling task, experiments with different sample mass and different particle size were developed for studying the effect of the value of these parameters on the kinetics of the decomposition reactions.

It was also studied the effect of sample mass, particle size and devolatilization atmosphere on the char yield. The aim was to increase the char yield of the thermal process, by analyzing the effect of the mentioned parameters and also to identify the woody biomass sample types that favored higher char yield values. Although devolatilization of woody biomass samples by means of thermogravimetry has been widely studied by many authors [8,29,30,31,32], the thermogravimetric study of the effect of created volatiles atmosphere in devolatilization behavior and in the char yield is more rare. Besides, many of the pyrolysis studies previously developed focus on increasing the liquid yield of the process, but not many pursued as main goal increasing the char yield. Moreover, the analysis of devolatilization behavior and char yield of forest residue samples is not that common compared to the stem wood samples, meaning also a novelty

2. Literature survey

2.1. Thermochemical conversion processes of biomass: pyrolysis

Thermochemical conversion processes of biomass feedstock include a wide range of different processes that convert the initially considered biomass feedstock into fuels and chemical which are produced to give to them a specific use. This biomass feedstock undergoing thermochemical conversion processes can be employed in a solid form as solid fuel, or can undergo certain processes before suffering the thermochemical conversion, in order to convert the initial feedstock into liquid or gaseous fuel [33]. By means of the thermochemical conversion of these fuels, valuable products can be obtained, such as electricity, heat power, a wide amount of different chemicals or gaseous or liquid products which will be used as fuel in some other processes.

Among the thermochemical conversion processes, the following different processes can be distinguished: Pyrolysis, Gasification and Liquefaction [33].

In this case, pyrolysis experiments of woody biomass samples were carried out for the Master's Thesis and so, this is the thermochemical process that will be studied in depth.

Pyrolysis process consists of an endothermic reaction where cracking and conversion of hydrocarbon molecules take place in inert atmosphere. During pyrolysis process, successive devolatilization reactions result in conversion of initial fuel on solid, gaseous and liquid products. At first, free radicals are formed due to thermal cracking of the molecular bonds; after that, and by means of rearrangements of the atoms, those free radicals get stabilized. Tars products have unstable free radicals in their composition which also get recombined. Then, among the created stable species, the lightest species are released as volatiles and the heaviest ones form part of the composition of the solid char [34].

Concretely, biomass pyrolysis has become an outstanding thermochemical conversion process in the last years, especially in industrial applications. It consists of the thermal decomposition of the organic matter contained in biomass under non-oxidizing conditions, that is, in an oxygen-free atmosphere, which gives solid char, liquid bio-oil and non-condensable gases as products [24]. The obtaining of each of

those products will be highly dependent on the composition of biomass feedstock and the conditions of the pyrolytic process. The main steps during biomass pyrolysis process are: dehydration, primary reactions and secondary reactions. The primary decomposition region of biomass feedstock is generally assumed to be composed of dehydrogenation, depolymerization and fragmentation as mainly occurring reactions [24].

There are many parameters affecting the biomass pyrolysis process, which have effect on the obtaining yields and on the properties and characteristics of the end products. Among those parameters that affect pyrolysis process, the following are included: type of biomass used as feedstock; pre-treatments suffered by the biomass, which can be physical, chemical and biological, in case it undergoes any; reaction temperature; reaction atmosphere; heating rate; dimension of feed particles, and vapor residence time [35,36].

Concretely, depending on the values of the heating rate and the residence time applied to the process, pyrolysis can be classified into three main groups that pursue the maximization of either char or bio-oil yields: slow pyrolysis, which is the conventional pyrolysis process; fast pyrolysis; and flash pyrolysis [24,35,37].

Slow pyrolysis is also named as carbonization and has been conventionally and widely used for charcoal production, where the thermal decomposition of biomass is achieved by the application of very low heating rates. The slow pyrolysis process is provided with the needed time for enough repolymerization reactions to take place, what provokes an increase in the obtained solid, char yields. This involves that long residence time is needed so that the process takes place, sometimes even ranging from hours to days. Regarding the final temperature, low final temperatures are commonly used which range between 300-700ºC. This slow pyrolytic process accepts a wide range of particle sizes (5—50mm), unlike the other two types of pyrolysis processes where the requirements regarding particle dimensions are more strict [24]. Thus, when the process is accomplished under slow pyrolysis conditions, highest char formation is obtained, but the efficiency of the process is not very high giving as a result a quite low conversion of biomass into char [38,39].

On the contrary, fast pyrolysis is characterized by high heating rates (>10-200ºC/s) and much shorter residence times of only some seconds or even less: it could range

between 0.5-10s, but the most typical residence times for fast pyrolysis are shorter than 2 seconds. Regarding the particle size needed for the process, finely ground biomass feedstock is traditionally required. For accomplishing the fast pyrolytic process, a temperature around 500ºC is needed in the vapor phase; the strict control of this pyrolysis reaction temperature is necessary for accomplishing the process successfully [40]. Fast pyrolysis is mainly applied for obtaining bio-oil: the bio-oil yields can be about 50-70% in weight [24,40]. For obtaining the bio-oil product, it is required a fast cooling of the vapors generated during the pyrolysis process. When even higher bio-oil yields are required or pursued, flash pyrolysis is employed, which uses higher heating rates in the range of 1000-10,000ºC/s and residence times below 0.5 seconds obtaining between 75-80% of bio-oil yield [24].

Pyrolysis process of biomass can be described by the decomposition phases of its main components along the following main temperature regions [4], being those main components of biomass hemicellulose, cellulose and lignin:

- Below 120ºC, moisture is removed together with the release of some light volatiles.
- In the temperature range between 220ºC and 315º, most of the hemicellulose contained in the biomass decomposes.
- Between 315ºC and 400ºC, degradation of cellulose and lignin takes place.
- Lignin continues decomposing at temperatures above 450ºC. In this final, high temperature region the degradation of lignin dominates the process since the other two components have previously been completely decomposed at lower temperature ranges.

The pyrolysis experiments that will be presented as part of this project will be based on pyrolysis of stem wood and forest residues of three different tree species: spruce, birch and oak. Among the facts to study from the experiments that will be described in later sections, the study of the effects of devolatilization conditions on kinetic parameters and on char production (by means of the study of the char yield) will be analyzed. Besides, the influence of those conditions on further conversion will be studied too.

2.2. Charcoal production and applications

In this section, the main reasons which have motivated the study of how to obtain increasing char yields from the pyrolysis process of woody biomass samples are explained, by means of presenting the role that charcoal produced from pyrolysis processes plays nowadays.

During the last decades, pyrolysis processes have suffered deep improvements and renovation steps that have provided them with the required, optimal features for being used for charcoal production [41]. Because of these improvements, the employment of pyrolysis for charcoal production has been widely spread.

Charcoal produced after biomass feedstock undergoing pyrolysis process, together with light gases and pyrolytic gases or tars, also meets the advantage regarding neutral carbon contribution to the atmosphere due to its biological origin, just as it happens with woody biomass [38,39]. This is one of the main reasons why it stands as a promising energy resource which is applicable for electricity generation but which is also applicable in a wide range of industrial processes as a potential substitute of widely used fossil fuels as coke and coal: due to important similarities regarding their thermal behavior, charcoal can replace them by contributing with a reduction of net CO2 emissions to the atmosphere [42].

In fact, pyrolysis process, which has a long history of use, was precisely initially deeply developed and applied for charcoal production [24]. One of the main markets for charcoal utilization has traditionally been metallurgical industry, which still remains being the main final application of charcoal nowadays [42]. The application of charcoal in metallurgical industry is mainly based on its strong reducing properties: when being heated together with metallic ores that contain oxides and sulphides, the carbon combines with oxygen and sulphur favoring the extraction of the main metal. Both hardwood and softwood can be used as raw materials for charcoal production for being used in metallurgy [42]. Charcoal can be used in several applications and processes within metallurgical industry, such as in foundry operations, smelting and sintering iron ores, copper smelting, in production of ferrosilicon and pure silicon, in electrodes or as purification agent in smelting of non-ferrous metals [43]. The use of charcoal in metallurgy decreases the environmental load of this industry and so increases its sustainability. Besides, bio-based carbon materials as charcoal have fewer impurities

and less sulphur content compared to traditionally used fossil fuels. These specific characteristics bring about some advantages to the process: when being employed as reduction agent, the reduced impurity content of charcoal leads to improvements in the final product quality, whereas its reduced sulphur content results in reduction in SO2 emissions [44].

When it comes to choosing a reduction material, the most meaningful parameter is the specific price per mass unit (normally per tonne) of the fixed carbon. For the cases where the performance of the process itself is not deeply affected by the choice of the reduction material, the specific price of the fixed carbon determines the decision of which carbonic substance or material will be used [44]. Reduction materials of biological origin, such as charcoal or wood chips, have a much higher price of fixed carbon in comparison with coal or coke, meaning that their use is much more expensive. Thus, the price of charcoal is nowadays a critical factor for industry, being this one of the main causes why its massive use in metallurgy has not been widely developed yet. Therefore, there is a need of reducing costs related to charcoal production processes. This can motivate its massive use as substitute of coal and coke in metallurgy and lead to a more feasible utilization of charcoal in a wider range of applications and industries. An effective way of making costs decrease is increasing the char yield from the carbonization process by application of the best process technologies and by optimizing the process conditions [44]. It has been reported that higher char formation is obtained when process is accomplished under slow pyrolysis conditions [38,39]. Nevertheless, in order to obtain higher char yields, further development and improvement of both technically and economically feasible and therefore profitable systems for thermochemical conversion of biomass is needed, what requires a deep understanding of thermal properties and behaviors of biomass [3].

Apart from its utilization in the metallurgical industry as an alternative to fossil fuels, charcoal presents a wide range of possibilities regarding its applications. For instance, it is used for energy generation mostly by applying combustion processes, and has a high potential in a large amount of industrial processes apart from the mentioned metallurgical industry. For example, charcoal is employed in the production of chemical components as synthesis gas by means of undergoing a gasification process.

Based on this wide range of applications of charcoal produced during pyrolysis of biomass and taking into account the need of improving the efficiency and reduce the

costs of this process, the improvement of char yield was studied in the current work by means of changing some pyrolysis conditions.

2.3. Devolatilization kinetics

In this section, it is presented an overview of the kinetic methods and models that have been considered to be used for the simulation of the pyrolysis experiments of woody biomass in which this thesis is based on. The aim was to study the main methods that have been both, traditionally and recently used in kinetic modeling of biomass by different authors, and to evaluate the value, suitability and reliability of them in general and for this case concretely.

First, an introduction summarizing the basis of devolatilization kinetics is presented, where the basic fundamentals of the modeling task, conditions to be held during experiments and the main parameters used in the kinetic study are defined. Then, a survey on the different kinetic models is presented, composed of potential models and methods for being employed for the simulation of the experiments composing this Master's Thesis.

2.3.1. Basis of devolatilization kinetics and definition of main parameters

Information regarding kinetics of biomass decomposition is absolutely necessary for achieving to know the different mechanisms of thermal decomposition processes and for being able to simulate their behavior.

Decomposition of biomass is a highly complex process due to many reactions taking place at the same time, both in a parallel and in a series way. Thus, while a thermochemical decomposition process is taking place, the amount of components decomposing together is really large. Besides, the study of the process is even more complex due to already decomposed components affecting the decomposition of the remaining biomass fraction, by means of secondary reactions taking place among the vapors and gases generated as a consequence of biomass decomposition, and the solid fraction of non-decomposed biomass components.

Due to the large amount of compounds which get decomposed when biomass undergoing a thermochemical process, the modeling of all existing reactions taking place becomes an extensive, impossible task. This is why the value and reliability of simplified models is widely assumed and accepted for modeling of biomass reaction kinetics. There is a wide range of different simplified models for simulation of reaction

kinetics of biomass, among which the most reliable and suitable ones should be identified for the specific case of the experiments developed for this Master's Thesis.

Firstly, a first selection had to be done with the aim of delimiting the study area of the different and possibly applicable kinetic models; that way, the study could be developed considering only those models which meet the basic needed specifications and main characteristics for simulating the experiments carried out for the current work.

Kinetic controlled regime

In reality, pyrolysis of biomass particles is dominated by chemical reactions, together with heat transfer and mass transfer. This is why when analyzing the thermal decomposition behavior of biomass for obtaining the mathematical model which fits the process best, theoretically the following should be considered [45]:

a. Reaction kinetics
b. Mass transfer
c. Heat transfer

Nevertheless, the complexity of a mathematical model describing the thermal decomposition of the feedstock that takes into account those three facts is too high. For avoiding the high complexity which the pursued mathematical model is likely to achieve when considering reaction kinetics, mass transfer and heat transfer, some assumptions are accepted and some measures are also taken. For instance, simplifications are both used and considered acceptable, but for that, some minimum requirements are needed to be fulfilled regarding the experimental conditions.

For example, in many cases internal mass transfer is considered to be negligible during pyrolysis experiments compared to heat transfer [46,47]. Nevertheless, it has been studied that the effect of mass transfer is sometimes not taken into account mistakenly, as its effects are not as mild as they should be for neglecting them completely during the study [48].

But, as said before, consideration of mass and heat transfer limitations together with the study of the kinetics makes the difficulty of analyzing the process too high.

For the case of this Master's Thesis, from the very beginning the main goal of it was, as explained before, to carry out the kinetic modeling of the samples and thus, to be able to simulate the thermal behavior of the analyzed feedstock when it was decomposed during pyrolysis process. This is why, as the aim was related to decomposition kinetics, it was required that kinetically controlled experiments were carried out so that the simulation could be reliable.

It is important to point out the fact that, when a decomposition process is led by kinetic control regime, the process itself is independent on the heating rate, the particle size, the particle mass or the experimental temperature. Thus, reactions take place under kinetic regime conditions when the rate of reaction is only dependent on and determined by the intrinsic kinetics of the particles; this happens when the heat transfer to the particles composing the sample and the heat transfer within each of the particles is fast in comparison with the decomposition rate or reaction rate [45]. When these conditions do take place, it is acceptable to neglect heat transfer limitations as it is assumed that all particles get heated up so fast, that the temperature of all particles composing the sample will be the same as the temperature of the surrounding atmosphere, without temperature gradients appearing neither among different particles, nor within the same particle [45]. At the same time, mass transfer limitations are also assumed to be negligible when these conditions for kinetic modeling are assumed.

This necessity of maintaining the decomposition reactions that take place during pyrolysis process within a kinetically controlled regime, involves that some experimental conditions and some feedstock characteristics will be unavoidably affected: their values will be made conditioned to the objective of developing the experiments within the kinetic control limits, avoiding to the highest extent the effect of mass transfer and heat transfer limitations. Some of the experimental parameters which do deeply affect the nature of the reactions being kinetically controlled or, on the contrary, being affected by mass and heat transfer limitations, are [45]:

- Heating rate
- Particle size
- Particle mass
- Experimental temperature

By defining the values of these parameters that affect the nature of the reactions regime within acceptable limits and acceptable value ranges, so that the assumption of kinetic control is acceptable, the heat and mass transfer effects could be considered negligible during the analysis of the experimental part of this Thesis. Values for these experimental parameters will be discussed in a later section, where it will be decisive the need of searching for the parameter values which fit the best the conditions for maintaining the kinetic control regime during the experiments.

Non-isothermal experiments

Kinetic study is developed differently depending on decomposition process being isothermal or non-isothermal.

Isothermal experiments are those at which the temperature of the system is raised as fast as possible up to the decided experimental temperature; as the heating of the system takes place so rapidly, there is no enough time for the main decomposition process of the feedstock and thus, the main reactions, to take place [45]. Once the aimed experimental temperature is reached, main decomposition reactions start taking place, while the temperature is maintained constant during the whole process, being time the only variable changing along the decomposition process.

On the contrary, in non-isothermal experiments, decomposition reactions take place during the heating process of the system; this heating process happens much more slowly in comparison with isothermal experiments, and thus, feedstock goes decomposing while temperature is increasing. In this case, the decomposition state will depend on temperature and time parameters.

The main feature of the TGA experiments that were developed for this Master's Thesis is that they were non-isothermal experiments, meaning devolatilization of one sample under non-constant temperature conditions. Thus, kinetic models applicable for non-isothermal experiments will be studied in this section. Besides, all experiments will be developed under constant pressure conditions.

During the running of the TGA experiments under these non-isothermal conditions at constant pressure, the temperature increase and mass loss of one sample were recorded; those recorded signals defined the feedstock decomposition behaviors. The obtained signals from the TGA were used for the obtaining of kinetic parameters by applying

different kinetic models, as it will be presented later on in the current work. By this procedure, a good simulation of those signals from the TGA was pursued.

By defining the thermal decomposition of the feedstock for non-isothermal experiments, as it will be done in this section, the basis for the implementation of the specific kinetic models was established.

For non-isothermal decomposition experiments developed under constant pressure, the rate of the decomposition process taking place depends on the temperature, T, and on the degree of conversion, α. The degree of conversion, α, can be derived from the mass-loss experiments and is defined as follows [3,25]:

$$\alpha = \frac{m_0 - m_T}{m_0 - m_f} \qquad (1)$$

where:

- m_0 is the initial sample mass [kg];
- m_T is the remaining sample mass at T temperature [kg]; and
- m_f is the final mass [kg].

Thus, the thermal decomposition of the feedstock undergoing TGA experiments under the previously specified conditions is defined as [3,25]:

$$\frac{d\alpha}{dt} = \kappa(T)\, f(\alpha) \qquad (2)$$

where κ(T) is the temperature dependent rate constant and f(α) is the conversion function dependent on the reaction mechanism. It can be observed that this conversion function f(α) has a fixed value for an specific conversion degree α, regardless of the value of the temperature or the temperature regime, form where it can be inferred that the process mechanism is only dependent on the conversion degree. The form and function of f(α) will be discussed later, when dealing with the different kinetic models to be employed.

The rate constant is defined by the Arrhenius equation as follows [3,25]:

$$\kappa(T) = A\, e^{-\left(\frac{E}{RT}\right)} \qquad (3)$$

where:

- A is the pre-exponential factor or frequency factor [min^{-1}];
- E is the activation energy of the decomposition reaction [kJ/mol];
- R is the universal gas constant [$8.314x10^3$ kJ/mol];
- T is the absolute temperature [K].

The activation energy, E, is defined as the minimum energy required in order to activate molecules and atoms to a state at which they are able to undergo a chemical reaction; thus, it is the amount of energy that at least is required so that the reaction could start. Regarding the pre-exponential or the frequency factor, it means the frequency at which molecules of the reactant compounds do collide with each other. Although it is usually described as a temperature-independent parameter, it is related to temperature as it describes molecular collision frequency, and this frequency is dependent on temperature [3,25].

When it is assumed that the process follows a scheme of a first order reaction, the temperature dependent rate constant is the result of the sum of the separately considered primary cracking constants of char, tar and volatiles, being κ_1, κ_2 and κ_3 respectively:

$$\kappa(T) = \kappa_1 + \kappa_2 + \kappa_3 \qquad (4)$$

Thus, taking into account the definition provided by Equation (3), Equation (2) stays as:

$$\frac{d\alpha}{dt} = A\, e^{-\left(\frac{E}{RT}\right)} f(\alpha) \qquad (5)$$

At the same time, the decomposition rate equation can be written as [25]:

$$\frac{d\alpha}{dT} = \frac{d\alpha}{dt}\,\frac{dt}{dT} \qquad (6)$$

where the term $\frac{dT}{dt}$ refers to the value of the heating rate. For non-isothermal experiments that are developed under non-constant heating rate conditions, and thus, where the value of the heating rate is varying as function of time, it is not possible to

simplify Equation (5); but in case of non-isothermal experiments with linear, constant, heating rate, as the TGA experiments developed for this Master's Thesis, it is completely possible to rewrite that expression by defining the values of the constant heating rate:

$$\beta = \frac{dT}{dt}$$

Thus, Equation (6) can be written as:

$$\frac{d\alpha}{dT} = \frac{d\alpha}{dt}\,\frac{1}{\beta} \qquad (8)$$

Therefore, by applying this Equation (8), the decomposition rate equation can be expressed as function of temperature [25]:

$$\frac{d\alpha}{dT} = \frac{A}{\beta}\; e^{-\left(\frac{E}{RT}\right)} f(\alpha) \qquad (9)$$

Equation (9) is the equation used for describing the thermal decomposition of the feedstock for non-isothermal TGA experiments with constant heating rate, written in function of the reaction mechanism, f(α).

This Equation (9) represents the differential form of the non-isothermal rate law, and is the expression which is normally applied for the calculation of kinetic parameters of the samples. It can be seen that the decomposition rate of biomass at a certain temperature depends on the conversion degree at that temperature.

Thus, when working on the development of the kinetic analysis of the thermal decomposition process of the samples considered in the current work, the kinetic parameters presented in Equation (9) were searched for the specific case of each of the samples undergoing the non-isothermal decomposition experiments. Therefore, the aim which was pursued within this kinetic modeling process was to find the values of the pre-exponential factor, A and activation energy, E, when applying the chosen kinetic model. Nevertheless, prior to starting with the calculations, the reaction mechanisms needed to be carefully evaluated and identified, so that the conversion function f(α) could be substituted in Equation (9). Apart from the mentioned parameters and

coefficients, depending on which reaction mechanism and kinetic model was decided to be applied, it could be also required to calculate the values of some other unknown parameters. All this will be deeply studied in the next section.

2.3.2. Survey on kinetic models:

In this section, a survey on the different most used kinetic models is presented for biomass feedstock, with special attention to the case of woody biomass. They have been considered different types of methods and models:

a. Isoconversional methods: which are applicable regardless of the reaction mechanism.

1) The KAS method
2) The FWO method

b. Master-plots method: for determining the reaction mechanisms of decomposition reactions.

c. Direct assumption of the degrade mechanism f(α): $f(\alpha) = (1-\alpha)^n$

- Specific case: n=1

d. Assumption of $f(\alpha) = (1-\alpha)^n$: Graphical approach

- Direct Arrhenius Plot Method
- The graphical method: Coats and Redfern

e. Assumption of $f(\alpha) = (1-\alpha)^n$: Analytical approach. The Least Square Method

- Considering pseudo-components for biomass kinetic evaluation by the Least Square Method
- The Three pseudo-components model in wood kinetics
- Least Square Method assuming the three pseudo-components model and employing the Distributed Activation Energy Model: DAEM

Now, each of the mentioned methods will be presented in detail.

a. Isoconversional methods

By means of isoconversional methods, an estimation of the activation energy, E, is obtained regardless of the reaction mechanism. Therefore, no assumption for the reaction mechanism is needed as it will not be part of the calculations. These isoconversional methods have been widely and commonly used for describing the solid-state thermal decomposition processes. Although they do not allow a complete modeling of the thermal behavior of the samples, the calculation of the value of the activation energy involves an important step for studying the thermal behavior of the different species, while no consideration for the reaction mechanism is needed. In this section, the basis of this type of methods and the basis for their application will be explained.

Nevertheless, it is necessary to mention that the accuracy or suitability of employing isothermal methods for kinetic modeling has also been widely studied, having concluded in some drawbacks related to their use that will be presented later.

When applying a model-free isoconversional method for the kinetic modeling of a thermal process, the first initial steps follow the previously presented assumptions related to the formulation of the decomposition rate, recently described by Equations (5) and (9).

Starting from these expression, different isoconversional policies can be employed with two different approaches: for isothermal processes or non-isothermal processes [49,50]. In this case, and in agreement with the nature of the TGA experiments that were developed for this Master's Thesis, the approach for non-isothermal experiments will be considered.

For the case of non-isothermal experiments, it is necessary to define a set of temperatures that result in a concrete conversion degree for different heating rates. This obeys the name of the method itself: the term isoconversional involves that different experimental points with identical degree of conversion need to be considered. For that, the temperatures needed for achieving these experimental points with equivalent, fixed conversion degree are determined, for a range of different heating rates: $T_f(\beta)$, with letter "f" referring to a fixed value of the conversion degree. Thus, those different temperatures at which a set of specific values of conversion degree are achieved are defined as $T_f(\beta)$, along the whole conversion process [50,52].

Following that first step, there are two different ways of dealing with the modeling challenge by applying isoconversional methods for non-isothermal experiments:

1.) **By approximating the temperature integral [50]:**
One way consist of considering the integration of Equation (5) and applying an approximation in order to solve the temperature integral that is obtained; for this, it is only required a set of $T_f(\beta)$ temperatures. Among the equations and models which follow this trend for obtaining the kinetic parameters, they will be studied the KAS (Kissinger-Akahira_Sunose, 1957) and the FWO (Flynn and Wall, 1966, Ozawa, 1965) equations.

2.) **Without mathematical approach for solving the temperature integral [50]:**
The other alternative does not use any integral approach. It consists of defining different decomposition at a fixed value of the conversion degree, α. Regarding this way of isoconversional modeling, the Friedman method will be explained.

By means of using these isoconversional methods, a different value of the activation energy is obtained for each specific, considered value of the conversion degree (α). By means of evaluating the differences among the obtained values of the activation energy, it will be concluded if it is acceptable to consider a single-step reaction with a single, average value of the activation energy, or if the decomposition process can be divided into different regions regarding too different ranges of activation energy.

Now, a short overview about these two ways of solving the modeling issue by applying isoconversional methods will be presented.

1) By approximating the temperature integral [50]:

This approach is based on the integration of Equation (5) by means of the separation of the variables, as follows [50]:

$$G(\alpha) = \int_0^{\alpha} \frac{d\alpha}{f(\alpha)} = \frac{A}{\beta} \int_{T0}^{Tf} \exp\left(-\frac{E}{RT}\right) dT \approx \frac{A}{\beta} \int_0^{Tf} \exp\left(-\frac{E}{RT}\right) dT \qquad (10)$$

being the function G(α) representative of the integral form of Equation (5) with the separation of variables. Regarding the right side of the equation, the sublimit of the temperature integral, T_0, has been approximated to zero as decomposition reactions at temperatures below the ambient temperature are very low, and thus, this approximation is completely permitted.

The technique used for the approximation needed for resolving the temperature integral of Equation (10) will make the difference among the existing various methods based on this approach.

All those different methods that follow this way of solving the modeling problem involve a plotting task where the following is represented: $1/T_f$ is plotted against a logarithmic function which will vary depending on the specific method used, and which will be dependent on the value of the heating rate and in some cases, it will also depend on the temperature. The form that this logarithmic function will have will depend on the approach used for approximating that mentioned temperature integral.

As there are many different ways of mathematically approximating the temperature integral, they also exist a wide range of different methods for obtaining the activation energy following this approach.

Now the results derived from two different approaches for solving the temperature integral will be presented and their usefulness and accuracy will be also evaluated based on previous publications:

1.1. The KAS method: Kissinger-Akahira-Sunose, 1957 [3,25,52].

This method, also called as the Kissinger method, is the most known isoconversional method among those which employ an approximation of the

temperature integral. The final equation which is derived from the KAS approach is as follows:

$$ln\left(\frac{\beta}{T_f^2}\right) = ln\frac{AR}{EG(\alpha)} - \frac{E}{RT_f} \qquad (11)$$

where the term G(α) refers to the temperature integral presented in Equation (10).

As previously explained, these methods base the calculation of the parameter of the activation energy on a plotting step. Note that the term G(α) is only dependent on the conversion degree, α; thus, by considering fixed values of the conversion degree, the Equation (11) results in a straight line for each of the values of α considered, when defining the following Y and X parameters:

$$Y = ln\left(\frac{\beta}{T_f^2}\right) \qquad (12)$$

$$X = \frac{1}{T_f} \qquad (13)$$

1.2. The FWO method: Flynn and Wall, 1966; Ozawa 1965 [6,15,25,52,53,].

In this method, the equation obtained after solving the temperature integral is as follows:

$$ln\beta = ln\frac{0.0048AE}{RG(\alpha)} - 1.0516\frac{E}{RT_f} \qquad (14)$$

And in this case, the following Y and X parameters will be defined for the plotting of Equation (14) for fixed values of conversion degree, α:

$$Y = ln\beta \qquad (15)$$

$$X = \frac{1}{T_f} \qquad (16)$$

Just as happened for the KAS method, in this case the function G(α) will also have a constant value for a fixed value of α; that way, potting of Y vs. X, straight lines will also be obtained for constant conversion degree values.

Thus, for the KAS method and the FWO method, plotting of Y vs. X will give in both cases straight lines for constant values of conversion degree, with a slope of E/R. By building these plots and by means of evaluating the slope of the straight lines that will be obtained, the value of the activation energy, E, is obtained.

As it can be inferred from what has already been explained regarding these methods, there is no need of assuming any reaction mechanism for defining function f(α); this is what makes these isoconversional methods be free-model methods for obtaining the values of some of the kinetic parameters.

***<u>Example of KAS method</u>: kinetic analysis of one type of biomass samples having undergone TGA experiments at different heating rates* [25].**

In this example, the KAS method is employed for the calculation of the activation energy. Different values of α, the degree of conversion, are considered for 4 different heating rates. In Figure 1, they are represented the axes presented in Equations (12) and (13). From this figure, it can be seen that the method presents high linear correlations.

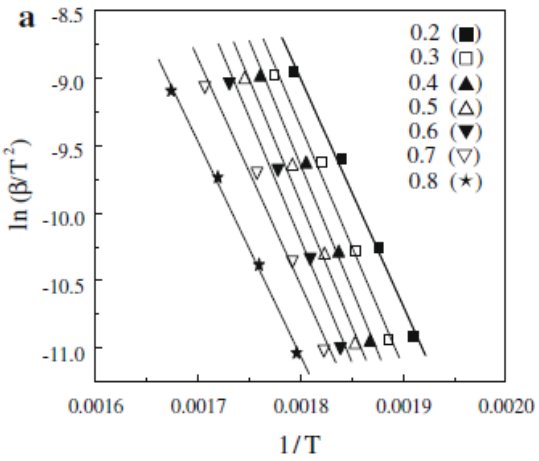

Figure 1. Y vs. X is plotted for the KAS method, for obtaining the value of the activation energy [25].

The slope of the lines will be: $-\frac{E}{R}$; so values of the activation energy, E, are obtained for each conversion degree (for each considered value of α). For the FWO method, the essentially same methodology would be employed, with the difference that the Y axis used in the plot would be the one defined by Equation (15) for this FWO method specifically.

For both, KAS and FWO methods, after obtaining different activation energy values as function of the conversion degree, a comparison among the values of the activation energies obtained for the different conversion degrees must be made; in case the differences are acceptable, the average value of the activation energy will be considered the final value. Predictably, the values of the activation energy that will be obtained for different constant degrees of conversion will not be similar as most of the solid-stage reactions are not single-step, but follow a more complex multi-step mechanism being the values of the activation energy dependent of the conversion degree [25].

2) Without mathematical approach for solving the temperature integral [55]:

Regarding the other alternative of isoconversional methods which use no mathematical approach or approximation for solving the temperature integral, they still need data about $T_f(\beta)$, that is, the value of the temperature at a certain heating rate at which an equivalent, fixed conversion degree is reached. It is also needed the value of the conversion rate at that $T_f(\beta)$ temperature.

Among the methods that are based on this approach, the Friedman method will be presented here. It is based on applying logarithms in Equation (5), resulting in [55]:

$$ln\left(\frac{d\alpha}{dt}\right) = ln[A\, f(\alpha)] - \frac{E}{RT_f} \qquad (17)$$

For applying this Friedman method, a set of experiments need to be run by applying different linear heating rates, β;for those experiments, there should be the possibility of registering the times at which an specific conversion degree is achieved for the different heating rates and the temperatures, T_f, at which that conversion degree is reached. That way, as the conversion function, f(α), only depends on the conversion degree, it will be constant for all experimental points considered.

Thus, as it can be inferred from Equation (17), by plotting ln(dα/dt) against $1/T_f$, a set of straight lines will be obtained, whose slope will be –E/R; from the value of the slope, the activation energy will be obtained for each of the conversion degrees considered. The axes for plotting and for obtaining the activation energy would be:

$$Y = ln\left(\frac{d\alpha}{dt}\right) \qquad (18)$$

$$X = \frac{1}{T_f} \qquad (19)$$

Nevertheless, it is normally much preferable to use the equation as function of the temperature derivative of conversion degree, defined by Equation (9), instead of using the time derivative of the conversion degree. This is why the following variation from Equation (17) will be employed in most cases, resulting in an expression dependent on the heating rate:

$$ln\left(\frac{d\alpha}{dT}\beta\right) = ln[A\, f(\alpha)] - \frac{E}{RT_f} \qquad (20)$$

When using Equation (20), the plot in this case will be ln(βdα/dt) against $1/T_f$:

$$Y = ln\left(\frac{d\alpha}{dT}\beta\right) \qquad (21)$$

$$X = \frac{1}{T_f} \qquad (22)$$

From the slope of the obtained lines, the values of the activation energy, E, will be calculated, without having to assume any type of reaction method for defining f(α). The method has, as previously said, no dependence on the reaction mechanism.

Evaluation of the studied isoconversional methods

The employment of isoconversional methods implies the necessity of running experiments using different heating rates; so in case this methods were decided to be employed for the calculation of the activation energy of the experiments run for the Master's Thesis, the experimental section would have to be designed taking into account this need of considering different heating rates.

By the employment of these isoconversional methods, it is not necessary to assume a reaction mechanism, what can be very time-consuming depending on the nature of the samples analyzed and on the amount of prior work and bibliography available regarding their kinetics; but on the other hand, only the value of the activation energy can be calculated by means of these methods. Thus, a real simulation of the decomposition behaviors of the samples is not possible by means of the only employment of the isoconversional methods.

In some previous studies, it has been reported the high level of inaccuracy of the Ozawa (FWO) method [50]. The reason why these methods, including the Ozawa (FWO) method, have been considered for this literature survey on kinetic modeling is that the most used and known methods were decided to be both, proposed and studied. Nevertheless, it has also been reported that, among the methods that approximate the temperature integral, there are actually methods which have a higher accuracy level than the best-known Kissinger (KSA) or Ozawa (FWO) methods, showing that no matter how widely used and known those methods are, more precise and better methods actually exist [50].

Regarding if it could involve an advantage the fact that some methods do not use a mathematical approach for solving the temperature integral, it has been reported in some previous publications that the approximations employed for solving the integral are highly precise and accurate, and that the approximations themselves do not involve a source of inaccuracies [50]. Precisely, it has been reported by Starink [50] that the methods which approximate the temperature integral for obtaining the value of the activation energy are more accurate in comparison to the Friedman-type methods, which do not use that approximation of the integral.

Nevertheless, other authors have also reported the higher level of accuracy of the Friedman-type methods, while the use of the widely employed integral model-free methods such as Kissinger's (KAS) or Ozawa's (FWO) could involve errors in the activation energy values [55].

b. Master-plots method

The Master-plots method is a method which leads us to the determination of the reaction mechanism based on the experimental behavior of the samples. By the employment of this Master-plots method, the suitability of the different potential conversion functions is studied graphically.

In addition, when being employed in combination with one of the previously presented isoconversional methods, from which only the value of the activation energy can be obtained, the value of the pre-exponential factor, A, can also be calculated by means of this Master-plots method.

This method is based on the integral form of the Arrhenius equation; thus, remembering the previously presented Equation (10):

$$G(\alpha) = \int_0^{\alpha} \frac{d\alpha}{f(\alpha)} = \frac{A}{\beta} \int_{T0}^{Tf} \exp\left(-\frac{E}{RT}\right) dT \approx \frac{A}{\beta} \int_0^{Tf} \exp\left(-\frac{E}{RT}\right) dT \qquad (10)$$

For the employment of the Master-plots method, the following designation is assumed [25]:

$$G(\alpha) = \frac{A}{\beta} \int_0^{Tf} \exp\left(-\frac{E}{RT}\right) dT = \frac{AE}{\beta R} P(u) \qquad (23)$$

where the function P(u) stands for the temperature integral as follows [25]:

$$P(u) = \int_{\infty}^{u} -(e^{-u}/u^2)\, du \qquad (24)$$

with the following definition of the u parameter [25]:

$$u = \frac{E}{RT} \qquad (25)$$

The temperature integral which function P(u) stands for has no analytical solution and can be expressed by an approximation. The Master-plots method employs the following approximation called the approximation of Doyle [25]:

$$P(u) = 0.00484\, e^{-1.0516u} \qquad (26)$$

Considering the decomposition process of biomass feedstock as a single step process with no variations in the expression of G(α), the analysis by the Masters-plot method leads us to a unequivocal choice of the most appropriate kinetic model [56]. Thus, a single-step model is employed in this case, involving that the activation energy, E, and the pre-exponential factor, A, will have a constant value during the whole decomposition process.

For applying the method, a reference point is used: let us assume that, for a single-step decomposition process, the degree of conversion of α = 0.5 will be considered as a reference, as it was employed by Shuping et. al. [25]:

$$G(0.5) = \frac{A}{\beta R} \, \mathrm{P}(u_{0.5}) \tag{27}$$

$$u_{0.5} = E/RT_{0.5} \tag{28}$$

As said before, A and E do not vary during the whole decomposition process when a single-step model is employed, so this involves that the following expression is fulfilled:

$$\frac{G(\alpha)}{G(0.5)} = \frac{P(u)}{P(u_{0.5})} \tag{29}$$

A plot where G(α)/G(0.5) against α is represented, corresponds to theoretical master plot of various G(α) functions. At the same time, plotting P(u)/P(u0.5) against. α involves drawing an experimental master plot from experimental data obtained at different heating rates.

From Equation (29), it can be observed that for a given α, the theoretically calculated G(α)/G(0.5) and experimental value P(u)/P(u0.5) are equivalent, when using the appropriate reaction model.

For evaluating the suitability of the different reaction models, some of the most frequently used models or mechanisms are evaluated within this Master-plots method, by comparison of the theoretical [G(α)/G(0.5)] and the observed [P(u)/P(u0.5)] master plots. The most suitable model will be that whose theoretical master-plot is the nearest to the experimental master plot.

Most frequently used mechanisms for solid state processes are presented in Table 1. There, the different mechanisms are both presented and defined by their correspondent f(α), the conversion dependence function. For each f(α), its corresponding integrated form, $G(\alpha) = \int_0^{\alpha} \frac{d\alpha}{f(\alpha)}$ (Equation 10) is defined.

For all considered mechanisms, their corresponding theoretical master plots are drawn against α, and the experimental master plot is also plotted against α in the same graph, as shown in Figure 2. The model which is the closest to fulfill Equation (29) will be the selected one.

Table 1. Most frequently used reaction mechanisms for solid stage processes [25].

Mechanisms	Symbol	$f(\alpha)$	$G(\alpha)$
Order of reaction			
First-order	F_1	$1-\alpha$	$-\ln(1-\alpha)$
Second-order	F_2	$(1-\alpha)^2$	$(1-\alpha)^{-1}-1$
Third-order	F_3	$(1-\alpha)^3$	$[(1-\alpha)^{-2}-1]/2$
Diffusion			
One-way transport	D_1	0.5α	α^2
Two-way transport	D_2	$[-\ln(1-\alpha)]^{-1}$	$\alpha+(1-\alpha)\ln(1-\alpha)$
Three-way transport	D_3	$1.5(1-\alpha)^{2/3}[1-(1-\alpha)^{1/3}]^{-1}$	$[1-(1-\alpha)^{1/3}]^2$
Ginstling-Brounshtein equation	D_4	$1.5[(1-\alpha)^{1/3}-1]^{-1}$	$(1-2\alpha/3)-(1-\alpha)^{2/3}$
Limiting surface reaction between both phases			
One dimension	R_1	1	α
Two dimensions	R_2	$2(1-\alpha)^{1/2}$	$1-(1-\alpha)^{1/2}$
Three dimensions	R_3	$3(1-\alpha)^{2/3}$	$1-(1-\alpha)^{1/3}$
Random nucleation and nuclei growth			
Two-dimensional	A_2	$2(1-\alpha)[-\ln(1-\alpha)]^{1/2}$	$[-\ln(1-\alpha)]^{1/2}$
Three-dimensional	A_3	$3(1-\alpha)[-\ln(1-\alpha)]^{2/3}$	$[-\ln(1-\alpha)]^{1/3}$
Exponential nucleation			
Power law, $n=1/2$	P_2	$2\alpha^{1/2}$	$\alpha^{1/2}$
Power law, $n=1/3$	P_3	$3\alpha^{2/3}$	$\alpha^{1/3}$
Power law, $n=1/4$	P_4	$4\alpha^{3/4}$	$\alpha^{1/4}$

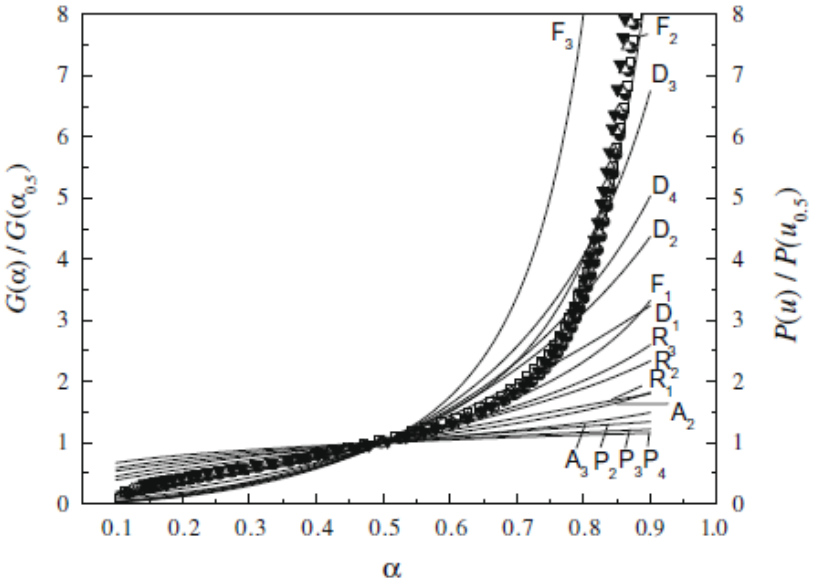

Figure 2. Theoretical and experimental master plots for the samples, against α, degree of conversion [25].

As previously said, this Master-plots method could be used after having employed an isoconversional method for the estimation of the activation energy: for a fast calculation of the activation energy, at first one of the isoconversional methods can be used; later on, if suddenly finding the reaction mechanism becomes an objective or a necessity, by means of the Master-plots method that reaction mechanism can be calculated. Once both, the reaction mechanism, and so the f(α) and G(α) functions are known, by using the average value of the activation energy calculated for different degrees of conversion by an isoconversional method, the value of the pre-exponential factor, A, can be calculated.

For that, for the corresponding reaction mechanism, Equation (23) is considered:

$$G(\alpha) = \frac{AE}{\beta R} P(u) \qquad (23)$$

Based on this equation, the pre-exponential factor A is evaluated by plotting G(α) against $\frac{EP(u)}{\beta R}$. The slope of the linear drawing will be the value of the pre-exponential factor, A.

Evaluation of the Master-plots method

The Master-plots method is a method for the determination of the reaction mechanism when this is completely unknown. When employing it, a wide range of different reaction mechanisms is considered and the mechanism which fits the best is finally chosen. Nevertheless, its nature of being an almost purely graphically performed method can create mistrust when it comes to the accuracy of the results. This high dependence on the graphical plotting and performance for obtaining the results can be considered as a drawback when deciding about the use of this method.

Besides, with the only use of this method, only the reaction mechanism can be estimated or determined; in order to obtain the values of the kinetic parameters such as the activation energy, E, or the pre-exponential factor, A, it is necessary the use of another type of method. One option could be, as previously stated in this section, to estimate the value of the average activation energy along the whole process by means of an isoconversional method; meanwhile, by means of the Master-plots method, the reaction mechanism can be determined graphically, and then, by the employment of Equation (23) from the Master-plots method and using the calculated value of the activation energy, the pre-exponential factor can be calculated graphically. All this means that the Master-plots method needs to be considered as a part of a wider kinetic analysis method, since if considered independently as a whole, it has an important lack regarding the calculation of the most important and meaningful kinetic parameters (E, A).

c. Direct assumption of the degrade mechanism f(α): $f(\alpha) = (1-\alpha)^n$

If talking about the modeling of the thermal decomposition behavior of some solid feedstock that has not been kinetically modeled in a broad, wide way, the direct, automatic assumption of the degrade mechanism and so, of the f(α) conversion function, is something beyond one's ability or means. In those cases, it is strictly necessary the evaluation of different degrade mechanisms in order to conclude which the one that fits the best is, following a technique that could be similar to the presented procedure of the Master-plots method, for instance.

Nevertheless, when the kinetics of certain feedstock undergoing a process have been widely modeled and studied, and if it has been concluded that a specific degrade mechanism is appropriate for describing the decomposition of the feedstock and for carrying on the modeling, it is completely acceptable to directly assume that degrade mechanism. And precisely, this is the case of the woody biomass feedstock undergoing pyrolysis experiments: the kinetics mechanisms of the woody biomass samples have been deeply studied putting a special attention to their degradation through thermal decomposition while pyrolysis process taking place. This is why it is acceptable and even the most appropriate decision, to directly consider the most widely used reaction mechanism for describing the woody biomass decomposition based on the criteria of previous authors and available literature.

In many publications where devolatilization behavior of biomass is studied, the conversion function f(α), which is dependent on the reaction mechanism, is assumed to be as follows [1-7]:

$$f(\alpha) = (1-\alpha)^n \tag{30}$$

where n refers to the reaction order of the decomposition process.

This conversion function corresponds to the case of the decomposition of polymer compounds when being submitted to a thermal process, just as it is the case of woody biomass feedstock, and is traditionally used for describing the decomposition behavior of many different types of biomass feedstock, including woody biomass samples.

Regarding the other previously presented methods, although in some cases the employment of model-free methods as the presented isoconversional methods can be a shortcut for estimating the values of activation energy, their employment does not make much sense for those cases for which in several previous publications a main reaction mechanism has already been identified and employed. Regarding the graphical method of the Master-plots, it can be useful for determining the appropriate reaction mechanism when there is no clue about it; it could be also used to confirm the suitability of one specific degrade mechanism in comparison to some others. Besides, the possible lack of accuracy and precision of these purely graphical methods is something to consider.

Thus, substituting Equation (30) in the general differential expression of the non-isothermal rate law presented by Equation (9), the following expression is obtained:

$$\frac{d\alpha}{dT} = \frac{A}{\beta}\ e^{-\left(\frac{E}{RT}\right)}(1-\alpha)^n \qquad (31)$$

This Equation (31) refers to the decomposition of biomass where degradation of polymers takes place; it can be seen that the decomposition rate of biomass at a certain temperature depends on the fraction of biomass that has not reacted at that point, (1-α), together with the reaction order, n. This expression will be applied for the calculation of kinetic parameters of the samples. Not only will be needed to calculate the activation energy, E, and the pre-exponential factor, A, but it will be also needed to work out the value of the unknown reaction order, n.

- **Specific case: n=1.**

In this section, it will be shortly presented the specific case of the assumed conversion function $f(\alpha) = (1-\alpha)^n$ for the thermal decomposition of woody biomass, when assuming a first order reaction mechanism instead of the previously presented general case with n-order reaction mechanism. Thus, for this specific case of first order reaction, the equation describing the reaction rate of the decomposition process will consist of:

$$\frac{d\alpha}{dT} = \frac{A}{\beta}\ e^{-\left(\frac{E}{RT}\right)}(1-\alpha) \qquad (32)$$

In this case, the only unknown parameters that need to be calculated will be the activation energy, E, and the pre-exponential factor, A, as the reaction order has already been assumed to be 1. This assumption of first order reaction mechanism is widely applied in the available literature for describing the decomposition of a wide range of biomasses, including wood samples [8-12].

Different ways of facing the resolution of the kinetic modeling, that is, the calculation of the kinetic parameters, by assuming n-order reaction mechanism (Equation (31)), including the specific case for n=1 (Equation 32), will be presented now. The ways of solving the kinetic problem with this conversion mechanism that will be presented next include both, graphical and analytical resolution methods.

c.1. Assumption of $f(\alpha) = (1-\alpha)^n$: Graphical approach

In this section, two different and widely used graphical methods that assume the $f(\alpha) = (1-\alpha)^n$ conversion function will be presented for the determination of the activation energy, the pre-exponential factor and the order of reaction. Those graphical methods are the Direct Arrhenius Plot Method and The Graphical Method by Coats and Redfern. From the employment of each of these methods, slightly different kinetic parameters are expected to be obtained; in case of applying these methods at the same time, the values of the parameters could be comparable in order to evaluate the accuracy of the methods and to determine whether the obtained results are reliable.

Direct Arrhenius Plot Method

The employment of the Direct Arrhenius Plot Method has its basis on taking logarithms of Equation 31; when doing so, the following expression is obtained [3,4]:

$$ln\left[\frac{1}{(1-\alpha)^n}\frac{d\alpha}{dT}\right] = ln\left[\frac{A}{\beta}\right] - \frac{E}{RT} \quad (33)$$

For an easier, further evaluation of the parameters and so that the graphical expression of Equation (33) could be achieved easier, the following X and Y parameters are defined:

$$Y = ln\left[\frac{1}{(1-\alpha)^n}\frac{d\alpha}{dT}\right] \quad (34)$$

$$X = \frac{1}{T} \quad (35)$$

So Equation (33) will result in:

$$Y = ln\frac{A}{\beta} - \frac{E}{R}X \quad (36)$$

➢ Determining the order of reaction, n: [3]

By plotting the parameters defined as Y and X (Equations (34) and (35)), as it is represented in Figure 3, the order of reaction n is evaluated as follows:

- The defined parameters in Equations (34) and (35), will be represented graphically by means of plotting Y vs. X., with the aim of determining the order of reaction, n.
- The parameter defined as Y by means of Equation (34) will be evaluated along the values of the X parameter (Equation (35)) by attributing different values to the order of reaction, n. Among the considered values of n, for its correct value, the plot of Y vs. X will give a straight line.
- Thus, all the data obtained for different values of n will be fitted, and the best-fit regression line, which has the highest correlation coefficient, will be determined. This way, the value of n that gives the best fit in relation to the straight line that should be obtained, will be considered as the correct value of the reaction order.

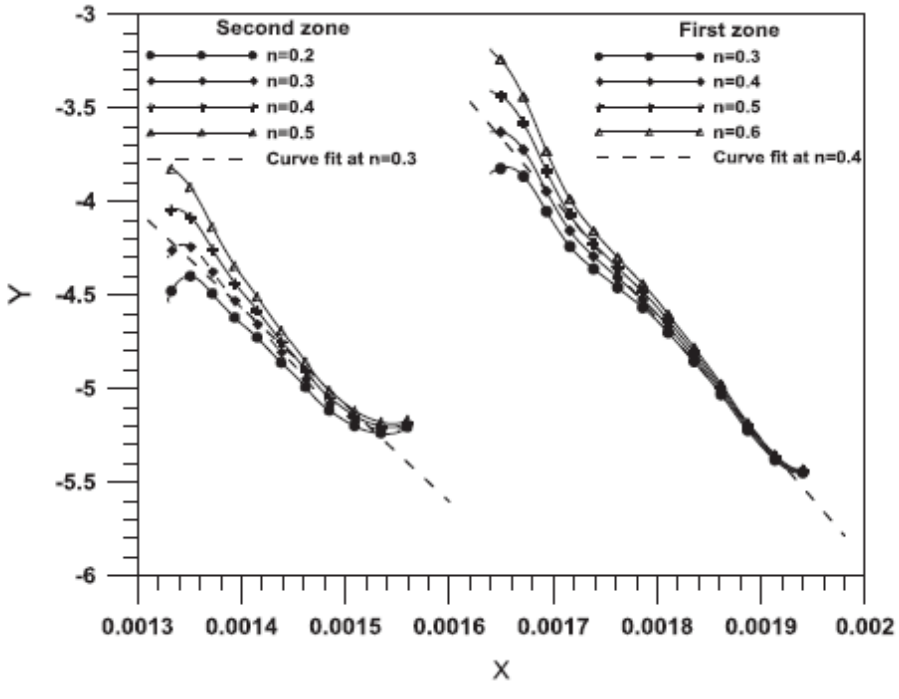

Figure 3. Determining the order of reaction, n, for direct method [3].

Once the reaction order has been estimated, the activation energy and the pre-exponential factor are calculated as follows:

- Activation energy, E: From Equation (36), it can be seen that the slope of the plot of Y vs. X is $-\frac{E}{R}$; therefore, the value of the actvation energy can be obtained graphically from the calculation of the slope.

- Pre-exponential factor, A: as it can be inferred from Equation (36), the value of the pre-exponential factor can be obtained from the intercept of the straight line with the vertical axis. That interception between the straight line corresponding to the decided order of reaction and the vertical axis takes place at the following value of the Y parameter:

$$Y_{interception} = ln\frac{A}{\beta} \qquad (37)$$

  Thus, the value of that interception point will be obtained from the graphic and the value of the pre-exponential factor will be calculated by substituting the known parameters in Equation (37).

The graphical method: Coats and Redfern

The other graphical method assuming the conversion function as $f(\alpha) = (1-\alpha)^n$ that will be presented is the so-called Graphical Method by Coats and Redfern, and it is used to evaluate kinetic data from thermogravimetric curves. This method has two different equations to be considered, depending on the assumption of n-order kinetics or on the assumption of first order reaction mechanism. Those equations are as follows [3,4,57]:

For $\boldsymbol{n \neq 1}$**:**

$$ln\left[\frac{1-(1-\alpha)^{1-n}}{T^2\,(1-n)}\right] = \ln\left[\frac{AR}{\beta E}\right] - \frac{E}{RT} \qquad (38)$$

For $\boldsymbol{n = 1}$**:**

$$ln\left[\frac{-ln(1-\alpha)}{T^2}\right] = \ln\left[\frac{AR}{\beta E}\right] - \frac{E}{RT} \qquad (39)$$

The following Y and X notation will be used for each case, just as it was made in the previous section [3,4,57]:

For $n \neq 1$:

$$Y = ln\left[\frac{1-(1-\alpha)^{1-n}}{T^2\,(1-n)}\right] \quad (40) \qquad \text{and} \qquad X = \frac{1}{T} \quad (41)$$

For $n = 1$:

$$Y = ln\left[\frac{-ln(1-\alpha)}{T^2}\right] \quad (42) \qquad \text{and} \qquad X = \frac{1}{T} \quad (43)$$

Thus, for both approaches, the following equation is fulfilled:

$$Y = ln\left[\frac{AR}{\beta E}\right] - \frac{E}{R}X \quad (44)$$

For the case of n-order reaction mechanism, the procedure for determining the order of reaction will be basically the same as the procedure used for the Direct Arrhenius Plot Method, but in this case, by plotting the corresponding Y and X parameters defined by Equations (42) and (43). That way, by the evaluation of V vs. X for different values of n, the order of reaction will be determined, as the correct value of that n parameter should give a straight line. Thus, all the data obtained for different values of n will be fitted and the best-fit regression line, which will have the highest correlation coefficient, will be determined.

On the contrary, when n=1 is assumed, this step is skipped; in this case, Y vs. X will be also plotted according to Equations (49) and (41) and an only straight line will be obtained.

As it was explained for the Direct Arrhenius Plot Method, by means of the obtained plots the values of the activation energy and pre-exponential factor will be obtained following the same procedure for the two approaches: n≠1 and n=1. By looking at Equation (44), the values of these parameters can be obtained as follows:

- Activation energy, E: From Equation (44), it can be seen that the slope of the plot of Y vs. X is $-\frac{E}{R}$ for both approaches (n≠1 and n=1); therefore, the value of the activation energy can be obtained graphically from the calculation of the slope.

- Pre-exponential factor, A: as it can be inferred from Equation (44), the value of the pre-exponential factor can be obtained from the intercept of the straight line with the vertical axis. That straight line will be the only line obtained for n=1 and the straight line corresponding to the decided order of reaction for the case of n≠1. The interception between the straight line and the vertical axis takes place at the following value of the Y parameter:

$$Y_{interception} = ln\frac{AR}{\beta E} \quad (45)$$

From this expression, the value of the pre-exponential factor is calculated.

c.2. Assumption of f(α) = (1-α)n: Analytical approach. The Least Square Method.

In this section, it is proposed an analytical kinetic evaluation by means of the non-linear Least Square Method. This method is based on the least square evaluation of the decomposition rate curves.

In this point, it is important to clarify some aspects related to the notation and naming used for the curves obtained from the TGA:

- **Y:** it is the sample mass normalized to the unity, and it is represented by the curve named as the TGA curve. This curve refers to the mass loss registered in the TGA software. From data obtained from this curve, the conversion degree named as α is calculated:

$$\alpha = \frac{m_0 - m_T}{m_0 - m_f} \quad (1)$$

- **-dY/dT:** is the curve also named as the DTG curve, and refers to the temperature derivative of the mass loss curve (first derivative of the sample mass curve, TGA curve, with negative sign). It gives information about the decomposition rate along the temperature range considered in the experiment. It is the same as representing the conversion degree rate: dα/dT:

Thus, as said in the beginning of this section, by means of the Least Square Method the experimentally obtained and the theoretically calculated decomposition rate curves or DTG curves will be evaluated: $(-dY/dT)_{exp}$ and $(-dY/dT)_{calc}$, referring to the experimental curves (exp) directly obtained from the TGA and the simulated, calculated curves (calc) by means of the employment of Equation (31) that defines the decomposition rate (dα/dT):

$$\frac{d\alpha}{dT} = \frac{A}{\beta}\ e^{-\left(\frac{E}{RT}\right)} (1-\alpha)^n \qquad (31)$$

When assuming a first order reaction mechanism, n=1 will be directly assumed in this Equation (31), resulting in the previously shown Equation (32).

By the employment of the least square method and for a set of initial values of the kinetic parameters, the best values of those parameters are calculated for minimizing the square differences between the set of experimental points corresponding to the experimentally obtained curves of the decomposition rate (exp) and the theoretically calculated points of the decomposition rate (calc) by means of Equation (31).

For employing this method, the following objective function is defined, which describes the square differences between experimental and simulated curves [13,58]

$$OF = \sum_{k=1}^{N_{exper}} \sum_{i=1}^{N_k} \left[\left(-\frac{dY}{dT}\right)_{k,i}^{exp} - \left(-\frac{dY}{dT}\right)_{k,i}^{calc} \right]^2 \qquad (46)$$

- N_{exper} is the number of experiments evaluated together
- N_k is the number of points considered at a given curve, which corresponds to the number of different temperature-points considered for evaluating a curve.
- $(-dY/dT)^{exp}$ refers to the experimental DTG curve obtained from the TGA; that is, the first temperature derivative of the mass loss curve (the first derivative of the mass curve, TGA curve, with negative sign).

- ***(-dY/dT)^{calc}*** refers to the decomposition rate calculated by means of Equation (31).

The methodology employed consists of finding the values of the kinetic parameters that minimize the defined objective function. For that, an initial value is attributed to each of the parameters whose value is pursued, so that the iteration process which aims the minimizing of that objective function can be started. Thus, an iterative process is performed with the aim of minimizing the value of the objective function, by means of giving different values to the kinetic parameters which are searched. This iteration process is easily optimized by means of computational methods, what makes feasible the process of finding the most suitable values of the parameters. Although the iteration process can be optimized, it is important to remark the high importance of the initial values attributed to each of the parameters for getting the iteration process started, as the results of the kinetic parameters obtained from the iteration process that minimizes the objective function will be highly dependent on those initial values used. This is the reason why it is highly recommended that for that initializing task of the parameters, values of the kinetic parameters from available literature sources and previous studies are employed.

The resulting fit quality of the simulation can be expressed for each curve that has been evaluated by means of the following expression:

$$FIT(\%) = 100\left(1 - \sum_{i=1}^{N_k}\left[\left(-\frac{dY}{dT}\right)_{k,i}^{exp} - \left(-\frac{dY}{dT}\right)_{k,i}^{calc}\right]^2 / N_k\right)^{0.5} / h_k \quad (47)$$

Where $\boldsymbol{h_k}$ is the highest value of the decomposition rate registered during the experiment, and is defined as follows [7,58]:

$$h_k = max\left(\frac{-dY}{dT}\right)_k^{exp} \quad (48)$$

Thus, the expression of the fit quality can be expressed as:

$$FIT(\%) = 100\left(1 - \sqrt{\frac{OF}{N_k}}\right)/h_k \tag{49}$$

Equally, the fit quality can be estimated by means of defining the relative deviation (reldev, %) of the calculations. This relative deviation is based on the root mean square difference between the experimental and the calculated values, and takes into account the value of the maximum peak of the experimental curve [7,13]:

$$reldev(\%) = 100\left\{\sum_{i=1}^{N_k}\frac{\left[\left(-\frac{dY}{dT}\right)_k^{exp} - \left(-\frac{dY}{dT}\right)_k^{calc}\right]^2}{N_k}\right\}^{0.5}/h_k \tag{50}$$

It can be observed that the following is fulfilled [7]:

$$reldev(\%) = 100\sqrt{\frac{OF}{N_k}}/h_k \tag{51}$$

Of course, the lowest the relative deviation, the highest the quality of the fit will be. Thus, the fit quality (Equation (49)) and the relative deviation term (Equation(50)) are expressing contrary parameters, and with defining one of them would be enough for determining the quality to the kinetic simulation process.

The use of this non-linear Least Square Method for the kinetic modeling of non-isothermal experiments was used by Broido and Weinstein as pioneers in their work [58,59]. Since this work was published, the Least Square Method for the kinetic evaluation of the curves has spread in a gradual form, having been employed in several kinetic studies and publications both, traditionally since that time and recently [2,3,6,7,11,13,58,60,61].

This Least Square Method for kinetic evaluation of biomass feedstock is widely employed by defining a number of pseudo-components among the composition of the biomass feedstock; for these cases, the kinetics of each of the pseudo-component is evaluated separately. Then, the whole decomposition rate considering the sum of the decomposition rates of all decomposed pseudo-components is submitted to the Least Square Method; the sum of the decomposition rates corresponding to each pseudo-component is done by using some parameters that attribute a “weight” to the released

volatiles fraction of each pseudo-component. This way, they are obtained the values of the kinetic parameters corresponding to each of the pseudo-components which minimize the least square differences. Now, the changes in the formulation of the reaction rate equations and in the employment of the Least Square Method will be presented, when considering the decomposition of pseudo-components instead of analyzing the decomposition process and kinetics of feedstock as a whole.

Considering pseudo-components for biomass kinetic evaluation by the Least Square Method.

As previously said, many different types of components get decomposed during biomass pyrolysis; although the description and study of the degradation process and kinetics of each of those components is something beyond our means, a simplification is assumed by grouping components with the same thermal behavior together in pseudo-components. The breakdown of these pseudo-components does actually define different decomposition zones in the decomposition curves obtained from the TGA.

It will be assumed that the degradation of each of the pseudo-components will contribute to the generation of a fraction of the total amount of volatiles released. That way, assuming M as the amount of the different pseudo-components considered, the total volatiles that will be emitted during the whole process will consist of M fractions. The release of each of the volatiles fractions and the degradation process of each those pseudo-components will have its own dynamics that will be determined independently [25], and therefore, the kinetic parameters will be defined separately for each of those identified decomposition zones.

The term pseudo-component refers to decomposing species while the thermal process is taking place, which are grouped together as their decomposition can be described by using the same values of kinetic parameters [7]. Thus, a pseudo-component is composed by different species which have similar decomposition kinetics and which can be described equally. It can occur that a large amount of reacting species might be attributed to a single pseudo-component. Species with very different reactivity values are thus grouped in different pseudo-components whose decomposition will be described by different activation energies.

As said, the decomposition of the different pseudo-components will be described separately, defining different zones; at each zone, the degradation process of one of the pseudo-components will be the main contributor to the decomposition process, but the effect of the decomposition of the other pseudo-components will also be visible. This is because the unavoidable overlap among the decomposition of the different pseudo-components in terms of temperature and time in the mass loss curve [14].

Considering the decomposition of different pseudo-components separately and studying and calculating their kinetics separately while being part of the whole decomposition process, is something that has been broadly employed for the case of thermal decomposition of biomass [7,8,9,11,13,14,60].

In all those mentioned publications the previously presented definition of the reaction rate, based on the Arrhenius equation, is assumed for each pseudo-component. Remembering the equation defining the decomposition rate when an only decomposition reaction was assumed for the whole feedstock:

$$\frac{d\alpha}{dT} = \frac{A}{\beta}\ e^{-\left(\frac{E}{RT}\right)} f(\alpha) \tag{9}$$

Assuming the conversion function defined by Equation (30) which is widely used for the case of biomasses, Equation (9) resulted in Equation (315):

$$\frac{d\alpha}{dT} = \frac{A}{\beta}\ e^{-\left(\frac{E}{RT}\right)} (1-\alpha)^n \tag{31}$$

When studying the decomposition kinetics of different pseudo-components, that final Equation (31) is applied to each of the pseudo-components considered, with some changes.

Considering M as the total number of pseudo-components, the equation defining the reaction rate of the j^{th} pseudo-component will be as follows [25]:

$$\frac{\mathrm{d}\alpha_j}{\mathrm{dT}} = \frac{A_j}{\beta}\ \mathrm{e}^{-\left(\frac{E_j}{\mathrm{RT}}\right)} (1-\alpha)^{n_j}\ ; \qquad j = 1, M \tag{52}$$

By means of this approach, it is assumed that the different pseudo-components decompose independently of each other, resulting in the following expression of the overall reaction rate [8,10]:

$$-\frac{dm}{dT} = -\frac{dY^{calc}}{dt} = \sum_{j=1}^{M} c_j \frac{d\alpha_j}{dT} \quad (53)$$

where:

- m and Y^{calc} refer to the sample mass divided by the initial sample mass, that is, the mass fraction normalized to the unity at its initial value; this Y^{calc} parameter takes values from 1 to $Y(t_\infty)$;
- the parameter c_j refers to the contribution that the j^{th} pseudo-component makes to the decomposition process. The definition of this c_j parameter is dependent on the concentration or mass fraction of the j^{th} pseudo-component in the sample considered [10]:

$$c_j = (concentration\ of\ component)_j\ (yield\ of\ volatiles)_j \quad (54)$$

The term $(\text{concentration of component})_j$ refers to the presence of the j^{th} pseudo-component in the initial sample and the term $(\text{yield of volatiles})_j$ refers to the amount of volatiles which are released or created form a unit mass of the j pseudo-component. This c_j component is difficult to be calculated as: although the term that refers to the mass fraction of that j^{th} pseudo-component can be easily calculated by means of the initial composition of the sample, the term referring to the fraction of volatiles attributed to the decomposition of each of the pseudo-components (the term $(\text{yield of volatiles})_j$) is not something that can be inferred directly from the experiments. This is why these c_j terms attributed to each of the pseudo-components are not assumed, but they are calculated during the kinetic modeling process together with the rest of the kinetic parameters [10].

The three pseudo-components model in wood kinetics.

For the case of kinetic modeling of woody species, a concrete case of the method of the Least-Square by assuming pseudo-components will be employed, based on the widely available literature on this regard [2,3,6,8,15,62]: the three pseudo-components model. This model refers to the three main pseudo-components of the woody biomass samples: cellulose, hemicellulose and lignin, and it assumes the decomposition of each of these pseudo-components can be considered, studied and modeled independently, following the path described for the Least Square method for a M number of pseudo-components. Thus, Equation (52) will be expressed for the case of M=3, resulting in:

$$-\frac{dm}{dT} = -\frac{dY^{calc}}{dt} = \sum_{j=1}^{3} c_j \frac{d\alpha_j}{dT} \tag{55}$$

This method could be broadened by means of integrated additional reactions which consider the low-temperature phenomena, that is, the decomposition of extractives. For that, it would be enough with considering two more fractions or decomposition zones [25], being 5 the total number of pseudo-components to be considered (M=5).

Least square method assuming the three pseudo-components model and employing the Distributed Activation Energy Model: DAEM.

So far, with the consideration of M pseudo-components decomposing in the process and the concrete case of the Three pseudo-components model, it has been considered that the activation energy has a constant value for each of the pseudo-components during the woody biomass decomposition process. Nevertheless, there is another approach which has been also widely employed recently called the Distributed Activation Energy Model (DAEM) [7,12,15], which presents some benefits in comparison with the models that consider a constant activation energy during the whole process. For example, when employing the DAEM, more information about the activation energy, E, which depends on temperature, is provided as a result of the modeling process.

The DAEM considers that the parameter of the activation energy follows a distribution function along the decomposition process. This distribution function could have different shapes, but the most used one is the Gaussian distribution. Therefore, in this document, when mentioning the DAEM, it will be assumed that the activation energy follows a Gaussian distribution function. That way, when by means of the Least Square Method, the unknown kinetic parameters are calculated for each of the pseudo-components, the value of the mean activation energy, E_0, is calculated, together with its corresponding deviation, σ. Therefore, this means that the values of the activation energy along the process will vary between ($E_0 - \sigma$) and ($E_0 + \sigma$).

The procedure that needs to be followed for the implementation of this Distributed Activation Energy Model is slightly more complicated compared to the constant activation energy model.

The general equation for the DAEM is as follows [15,63]:

$$1 - \frac{V_j}{V_j^*} = x_j = \int_0^\infty \exp\left(-A_j \int_0^t e^{-\frac{E_{0j}}{RT}} dt\right) f(E) dE \qquad (56)$$

Where V_j is the released mass fraction of the j^{th} pseudo-component in a certain moment of the process and V_j^* is the total released mass fraction of the j^{th} pseudo-component in the whole process. For the case of the Three Pseudo-components Model: j= 1,2,3. Expressing Equation (55) as function of temperature:

$$1 - \frac{V_j}{V_j^*} = x_j = \int_0^\infty \exp\left(-\frac{A_j}{\beta} \int_0^T e^{-\frac{E_{0j}}{RT}} dT\right) f(E) dE \qquad (57)$$

The term f(E) corresponds to the distribution function of the activation energy. As said before, a Gaussian activation energy distribution is assumed, so function f(E) is defined as follows [15,63]:

$$f(E) = \frac{1}{\sigma\sqrt{2\pi}} exp\left(-\frac{(E-E_0)^2}{2\sigma^2}\right) \qquad (58)$$

By employing the definition of the terms V and V^* [63]:

$$1 - \frac{V}{V^*} = \frac{V^* - V}{V^*} = \frac{m_T - m_f}{m_0 - m_f} = x \qquad (59)$$

where:

- m_0 is the initial sample mass [kg];
- m_T is the remaining sample mass at T temperature [kg];
- m_f is the final mass [kg]; and
- x is the fraction of volatiles that will be released from a certain T temperature until the end of the decomposition process, in reference to the total amount of volatiles released in the whole process.

Remembering the definition of the conversion degree parameter, α, by means of Equation (1):

$$\alpha = \frac{m_0 - m_T}{m_0 - m_f} \tag{1}$$

It can be observed that:

$$1 - \alpha = x \tag{59}$$

Remembering Equation (52) for the case of the Three pseudo-components model:

$$\frac{\mathrm{d}\alpha_j}{\mathrm{dT}} = \frac{A_j}{\beta}\, \mathrm{e}^{-\left(\frac{E_j}{\mathrm{RT}}\right)} (1 - \alpha_j)^{n_j} \; ; \quad j = 1, 2, 3 \tag{60}$$

The term $(1-\alpha_j)$ will be substituted by x_j which is defined by Equation (57). This way, by considering the decomposition rate of each of the pseudo-components and their corresponding c_j parameter, the expression of the simulated DTG curve can be obtained by means of Equation (53):

$$-\frac{dm}{dT} = -\frac{dY^{calc}}{dt} = \sum_{j=1}^{M} c_j \frac{d\alpha_j}{dT} \tag{53}$$

By means of the Least Square Method, all the unknown kinetic parameters can be calculated, including E_{0j}, the mean activation energy for each of the pseudo-components, and σ_j as the deviation corresponding to each pseudo-component.

The complexity of employing the Distributed Activation Energy Model resides in the need to solve the double integral from Equation (57), together with the fact that the variable E ranges from 0 to infinite. Many different simplifications have been proposed for solving that complex integral which cannot be calculated directly. In this case, it is proposed the employment of the Simpson's rule for solving the integral with the E variable.

For the case of assuming first order reactions, n=1, the procedure would be exactly the same but with one less unknown parameter per pseudo-component, making n=1 in Equation (60).

2.3.3. Determination of methods employed in the kinetic modeling for the Master's Thesis.

Before rushing into the justification behind the election of the kinetic methods that were finally decided to be employed in this Master's Thesis, a short summary of the different methods and models studied in the previous section is presented:

- **Summary and final conclusions on kinetic modeling methods:**

  a. Isoconversional methods

  They are model-free methods, that is, no assumption or calculation of the degradation mechanism is needed. By means of these methods, it is only possible to directly obtain the value of the activation energy, and it is needed to run experiments with different values of heating rate. The calculation of the activation energy is based on plotting the values of certain parameters in a graphic; it is a graphical method which bases the calculation of the activation energy on the linear correlation among some experimental points obtained. This will have the lack of accuracy attributable to the graphical methods in general.

  b. Master-plots method

  It is a method that leads to the determination of the reaction mechanism by following a graphical procedure. The suitability of the potential

conversion functions is proved graphically, and the theoretical function that fits the best the experimentally obtained curve is decided to be the one describing the reaction mechanism. So it is also a graphical method. Used in combination with some other methods, such as isoconversional methods which give us the value of the activation energy, the pre-exponential factor can be calculated. Thus, it can be obtained a complete calculation of kinetic parameters including the determination of the reaction mechanism. If Master-plots method is considered independently, it lacks the calculation of the most important and meaningful kinetic parameters (E, A).

c. Direct assumption of the degrade mechanism f(α): $f(\alpha)=(1-\alpha)^n$

The kinetics of woody biomass samples have been widely studied and this form of the function defining the degrade mechanism has been widely accepted. This is the reason why this assumption of f(α) becomes acceptable, makes us save time in calculations and even gain accuracy by means of avoiding graphical methods for the estimation of the degrade mechanism.

- **Specific case: n = 1.** The assumption of first order reaction mechanism involves an acceptable simplification for the case of woody biomass samples.

c.1. Assumption of $f(\alpha)=(1-\alpha)^n$: Graphical approach

Two different methods were presented for graphically obtaining the value of kinetic parameters by means of assuming the n^{th} order degrade mechanism. The largest problem this methods present is, once again, the graphical way of solving the kinetic problem and the lack of precision that can be attributed to this type of methods.

c.2. Assumption of $f(\alpha)=(1-\alpha)^n$: Analytical approach. The Least Square Method

By means of this widely used analytical approach for solving the kinetic problem and finding the values of main kinetic parameters, high

levels of precision and good approximations are obtained. It basically consists of finding the values of kinetic parameters that give the lowest difference between the experimental and simulated curves by employing an iteration procedure. Some specifications were also presented for this method:

- **Considering pseudo-components**
- **The three pseudo-components model in wood kinetics.**
- **Distributed Activation Energy Model: DAEM**

- **Determination of the kinetic method and models used in the Master's Thesis**

For the calculations and modeling developed for the current work, it was decided to assume that the conversion function dependent on the degrade mechanism was: $f(\alpha) = (1-\alpha)^n$. Thus, the n^{th} order $f(\alpha)$ conversion function was directly assumed as the reaction mechanism that described the best the thermal decomposition of the woody biomass feedstock analyzed in this Master's Thesis.

Besides, the Three pseudo-components model was also assumed by describing separately the decomposition processes of hemicellulose, cellulose and lignin by means of three parallel reactions. Each of the parallel reactions has its own and independent kinetic parameters, which were calculated for the case of the studied woody biomass samples. It was decided not to include the decomposition of the extractives at low temperature in the kinetic modeling carried out for the current wok, by betting on this Three-pseudo components model (M=3). The way of calculating the kinetic parameters corresponding to each of the three pseudo-components assumed was by the employment of the recently presented Least Square Method for the case of the Three pseudo-components model.

Three variations were suggested and employed when it came to modeling the decomposition behavior of each sample type, with the employment of the Least Square Method as assuming the following:

- **Constant E, n=1:** assumption of constant activation energy, E, and first order reactions for each of the pseudo-components.

- **Constant E, n≠1:** assumption of constant activation energy, E, and calculation of the reaction order, n, for each of the pseudo-components.

- **n=1, DAEM:** assumption of distributed activation energy model, DAEM, and first order reactions for each of the pseudo-components. It was decided to employ the DAEM but considering a first-order reaction kinetics to make the process slightly easier by reducing the number of unknown parameters and assuming directly that n=1. The solving process is exactly the same as the general case presented in the previous section, but with n=1.

2.3.4. Survey on kinetic parameters of woody biomass samples

In this section, they have been registered kinetic parameters of woody biomass samples which have been considered to be comparable to the species analyzed for the Master's Thesis.

The values of the kinetic parameters presented in this section have been collected from literature as a result of a survey developed with the aim of obtaining some reference values for the parameters. The goal was to have these comparable values to check against the results that would be obtained from the modeling.

Nevertheless, these comparable results from literature corresponding to the kinetic parameters of pyrolysis process of woody biomasses are only useful as illustrative values, as the conditions of the experiments, the origin of the samples, and in some cases even the sample types themselves, are not equal. So they will be considered as illustrative values of the kinetic parameters.

The results collected in the following tables were obtained in different publications by the employment of the Least Square Method and the assumption of the Three pseudo-components model. Results obtained by means of the application of some other method, such as the graphical methods presented in the literature survey on kinetic modeling, were not registered. Thus, by means of comparing results of kinetic parameters calculated by using the same calculation methods, more reliable comparison was aimed to be obtained. This makes the results from literature more comparable with the results obtained after treatment of experimental data.

In this case, c_i, E_i, A_i, n_i and σ_i are the kinetic parameters correspondent to each of the pseudo-components.

a.) n=1.

a.1.) Spruce wood.

Heating rate: 5K/min.

Table 2. Kinetic parameters for spruce wood, n=1 [8].

	Hemicellulose	**Cellulose**	**Lignin**
c_i	0.33	0.32	0.14
E_i (kJ/mol)	100	236	46
A_i (min^{-1})	1.51E+08	1.61E+19	2.28E+02

a.2.) Beech wood.

Heating rate: 5K/min

Table 3. Kinetic parameters for beech wood, n=1 [13].

	Hemicellulose	**Cellulose**	**Lignin**
c_i	0.25	0.38	0.13
E_i (kJ/mol)	100	236	46
A_i (min^{-1})	4.10E+08	1.75E+19	1.98+03

a.3.) Spruce stump wood.

Heating rate: 10K/min

Table 4. Kinetic parameters of spruce stump wood, n=1 [15].

Fit (%): 98.86	**Hemicellulose**	**Cellulose**	**Lignin**
$\mathbf{c_i}$	0.33	0.48	0.19
$\mathbf{E_i}$ **(kJ/mol)**	108.12	185.12	38.54
$\mathbf{A_i}$ **(min$^{-1)}$**	9.66E+08	3.936E+14	5.57E+01

b.) n≠1.

b.1.) Spruce stump wood.

Heating rate: 10K/min

Table 5. Kinetic parameters of spruce stump wood, n≠1 [15].

	Hemicellulose	**Cellulose**	**Lignin**
$\mathbf{c_i}$	0.35	0.46	0.20
$\mathbf{E_i}$ **(kJ/mol)**	108.4	185.18	38.49
$\mathbf{A_i}$ **(min$^{-1)}$**	9.66E+08	3.936E+14	5.57E+01
$\mathbf{n_i}$	1.16	1.01	1.37

c.) DAEM.

c.1.) Spruce stump wood.

Heating rate: 10K/min

Table 6. Kinetic parameters of stump wood, DAEM (Distribute Activation Energy Model) [15].

Fit (%): 98.60	**Hemicellulose**	**Cellulose**	**Lignin**
c_i	0.35	0.51	0.13
E_i (kJ/mol)	93.79	168.44	57.55
A_i (min^{-1})	4.86E+07	1.70E+13	9.84E+02
σ_i (kJ/mol)	27.58	13.63	25.09

2.3.5. Parameters affecting devolatilization kinetics

As previously mentioned, the yields of char, liquids and gases obtained from pyrolysis process are mainly dependent on the composition of the feedstock, dimension of particles, heating rate, pyrolysis temperature and reaction time [24,36]. Gas production is favored by higher temperatures and longer residence times, whereas by means of the employment of slower heating rates and lower temperatures, higher char yields are obtained from pyrolysis process [36]. Therefore, variations in experimental parameters result in different overall behaviors of the samples undergoing pyrolysis process giving different products and yields and having an impact on the values of the kinetic parameters.

In this section, the main parameters affecting decomposition behavior of woody biomass samples during pyrolysis process are analyzed with the aim of determining the impact these parameters have in terms of devolatilization behavior and devolatilization kinetics of the samples. The parameters that will be studied are:

- Heating rate
- Particle size and sample mass
- Final temperature

By studying their impact, the most suitable values of the analyzed parameters will be established for being applied during the experimental part. The two following objectives are pursued when evaluating the most suitable values or ranges of values for these parameters: firstly, the best experimental conditions are needed to be chosen so that the values of kinetic parameters obtained in the kinetic modeling part can be as reliable and good as possible; and secondly, by determining the values of the experimental parameters, char formation is wanted to be favored.

At the same time, not only an attempt to maximize char formation and the reliability of the results from kinetic modeling is wanted, but it is also pursued the analysis of how changes in key parameters of pyrolysis process may affect both, char formation and kinetic modeling. Therefore, firstly the most suitable and reliable values of the mentioned experimental parameters (heating rate, final temperature, particle size and sample mass) were investigated and determined for being employed in the experimental part of the work, and then, variations of some of these parameters were considered for studying the impact they have on the process.

- ***Heating rate***

The influence of the heating rate on the feedstock decomposition using thermogravimetry has been thoroughly and widely studied by many authors and publications [5,64,65]. For a wide variety of feedstock types that underwent pyrolytic TGA experiments, a shift of the region of maximum weight loss rate to higher temperatures has been registered when heating rate is increased [5]. This shift of the first derivatives of the weight loss curves, the DTG curves, is based on heat transfer effectiveness: the lower the heating rate, the higher the effectiveness of heat transfer to the particles. Then, the effect of DTG curves moving forward to higher temperature regions when heating rate is increased is based on the less effectiveness of heat transfer. That way, the achievement of higher temperatures is needed to provide the particles the minimum heat required so that their cracking starts, what provokes a certain delay in the process in terms of temperature.

Not only is the decomposition rate of the samples delayed or moved forward when changing the heating rate during biomass pyrolysis process, but other impacts of heating rate variations have been registered too. For instance, and as it has been previously mentioned, the distribution of char and volatiles is accepted to be very dependent on the

heating rate of the polymers composing the feedstock. For example, it has been reported that for higher heating rates, the obtained char yield is significantly reduced in comparison with pyrolysis experiments carried out with slower heating rates [66]. The reason of this happening is the following: when applying low heating rates with values below 10ºC/min, the structure of polymers composing biomass is not so much affected; while the weakest chemical bonds break because of the heating effect, there are many other stronger bonds that remain stable under the influence of those low heating rates applied. This favors rearrangement reactions giving as a result a more stable configuration in comparison with processes subjected to higher heating rates. This more stable nature inhibits volatiles release resulting in higher char yields. At the same time, with low heating rates the possibility of secondary reactions occurring can be significantly reduced. By means of applying low heating rates, it is also ensured that thermal cracking will not take place involving that higher char yields will be obtained.

On the contrary, high heating rates favor further fragmentation of biomass and increase the formation of liquid and gas products while limiting the production of solid char products. The employment of high heating rates increases depolymerization of biomass into primary volatile components which will have the effect of reducing char formation. When high heating rates are applied, (>100ºC/s), several bonds of many different types break at the same time favoring the extensive release of volatile compounds. In this case with pyrolysis performed at high heating rates, the breaking of the many different bonds takes place prior to the arrangements reactions taking place [67]. As there is no time for rearrangement reactions to happen, particles suffer a rapid shift to a non-stable structure that is not able to inhibit volatiles release, resulting in a large release of volatile material. At the same time, with high heating rates secondary pyrolysis reactions which can favor the formation of gas products do actually dominate the whole process resulting in a reduced char production. The effect that the application of high heating rates has on reduced char production is more severe with low pyrolysis temperatures [64].

Nevertheless, it is not the lower the heating rate, the higher the char yield. For example, in the range of slow heating rates that give higher char yields as a result, it has been observed that for wheat straw particles, higher final char yield values were obtained when increasing the heating rate from 5ºC/min to 20ºC/min [62]. The reason of this happening is assumed to be as follows: when applying slower heating rates, the

feedstock, which was wheat straw in this case, was heated up very slowly resulting in a very good heat transfer taking place among the sample particles. Due to this better transfer of heat, the heating of all particles was achieved in a much more effective and uniform way provoking a cracking that takes place in a more effective way and what gives as a result a more severe weight loss as a larger amount of volatiles is released. On the contrary, when the heating rate was increased up to 20ºC/min, the heat transfer taking place among the sample particles was not so efficient resulting in higher amount of solid residue or char in the end of the process [62]. Exactly the same effect was registered by Altun et al. when studying the effects of the heating rate on pyrolysis experiments of Silopi asphaltite [34].

Heating rate is also related to restrictions in kinetic control of the decomposition reactions. Different heating rates provoke different rates of heat transfer resulting in different temperature lag, different temperature differences and different temperature gradients in and among the particles. All this leads to variations in decomposition behaviors and also results in limitations in kinetic analysis [4]: when increasing the heating rate of a pyrolytic process, the existing gradient in biomass particles becomes higher, favoring the appearance of heating transfer limitations or at least, making their appearance easier. Heat transfer limitations will affect the pyrolysis process and therefore their effects need to be taken into account in the kinetic study of the sample behavior: when at high temperatures the kinetic rate of biomass decomposition exceeds the rate of heat transfer, it gives as a result restricted decomposition kinetics. Therefore, in these cases the application of transport models will be needed for describing the kinetic behavior.

Nevertheless, the exact effect that the heating rate has on biomass pyrolysis kinetics is still unresolved. Some evidence has been found regarding the small effect that the heating rate has on the pre-exponential factor used to define the pyrolysis kinetics [66]. Some other studies have found that when pyrolysis is developed under high heating rate conditions the reactions of biomass conversion are slower than when the process takes place under low heating rate conditions [10,66,68].

In this regard, Grønli et al. [69] developed a series of pyrolysis experiments with Avicel PH-105 microcrystalline cellulose for studying the effects of the heating rate on kinetic parameters, together with the effects of using different instruments as experimental setup. Heating rates of 5ºC/min and 40ºC/min were employed and small

sample mass was used for reducing the effects of heat and mass transfer (< 5 mg). They registered variations in the values of the activation energy, E, and pre-exponential factor, A; for instance, they reported how changes in the activation energy of cellulose were registered when changing the heating rate, decreasing from 242 kJ/mol at a heating rate of 5ºC/min down to 222 kJ/mol when shifting the heating rate to 40ºC/min [69]. It was concluded that these variations in the values of kinetic parameters were caused by the differences in thermal lag among the different instruments that were used and by the effect produced by the different heating rates used [69]. The same conclusions were also derived from other studies [70,71].

The reason behind this effect of the heating rate on kinetics is supposed to be that when increasing the heating rate, the diffusion limitations among particles result emphasized provoking reduction in kinetic rates [66]. The same effect of decreasing values of activation energy while increasing the heating rate were reported by El-Sayed et al. when using the Direct Method for analyzing kinetics of cotton stalks [4]. They concluded that the best way of calculating the activation energy of that sample type with the Direct Method would be by employing lower heating rates. At the same time, almost no effect of the heating rate was registered for the same sample type when the Integral Method was applied.

It is also remarkable the influence that factors such as the temperature interval of pyrolysis process or the mathematical method used for kinetic evaluation have in the obtained values of that activation energy [4].

- ***Particle size and sample mass***

As it has been previously mentioned, the thermal decomposition of solid biomass feedstock is deeply influenced by the transport limitations. Particle size and sample mass of the feedstock are some of the most affecting parameters when it comes to determining the effect of transport limitations and whether the pyrolysis reaction is being developed under kinetic control regime or under heat transfer control regime [72]. Thus, in this section, attention is paid to the effect of particle size and sample mass on the reaction regime and reasonable values of particles dimensions and sample masses are searched.

When evaluating the kinetics of biomass samples, it is assumed that uniform temperature is held within the whole solid matter of the sample. Nevertheless, this is not

completely true: temperature gradients do actually appear within biomass particles and among different particles of the sample itself. Depending on the magnitude of those temperature gradients, the assumption of temperature uniformity may not be acceptable. Samples with a non-uniform, variable temperature distribution do not react in a uniform way and so, the kinetic data obtained and the kinetic parameters calculated from these kinds of processes will be meaningless and can end up being even misleading for further analysis [66]. Related to this, the size of feed particles is a key factor that influences the ability of the biomass to be heated up quickly and so, it is a key factor affecting the temperature of each particle; in other words, the dimensions of the biomass particles affect the velocity at which the feed can be heated, when being subjected to a heat flux and so, they have an effect on the uniformity of heat distribution. The larger the particle size, the more influenced and controlled the pyrolysis process will be by heat transfer effects. Thus, a balance must be found between the necessity to reduce the mass and heat transfer effects and the costs of size reduction of particles, which can become significant [36].

At the same time, while pyrolysis process taking place, it moves forward to higher values of temperature and that increasing of reaction temperature gives as a result that, in the end, kinetic rates become faster than the associated internal and external heat transfer rates. When the process achieves these high temperatures and when the sample is composed by large particles, the decomposition of the biomass becomes limited by heat transfer. This means that all kinetic calculations and evaluations have to take the heat transfer limitations into account by means of including a transport model in the pyrolysis kinetics analysis.

The temperature range at which the shift from kinetic control to heat transfer control takes place is highly dependent on the particle size and dimensions of biomass feedstock. Models have been developed for determining the highest particle size that involves the limit for kinetic control regime at a determined reaction temperature [72].

The size of biomass particles undergoing pyrolysis process directly affects the temperature gradient and the magnitude and the grade of negligibility of it. For avoiding high temperature gradients appearing in the particles, it is desirable to keep the particle size as small as possible. In fact, the use of relatively small particles is not only desirable but also necessary so that the assumption of uniform temperature of biomass samples can be acceptable. It has been proved that the thermal degradation of biomass

feedstock with particle size up to 0.2mm (<200μm) should undergo kinetic evaluation up to a temperature of about 450-500ºC with internal heat transport restrictions being negligible [72]. And lower temperatures should be applied for the cases where heat transfer to the surface of the biomass particle is too slow [66]. This fact coincides with the fact that most of the pyrolysis processes (or at least, the main decomposition processes) do actually take place below that mentioned temperature limit involving that the kinetic studies developed up to or below that temperature are free of heat and mass transport limitations and also free of inaccuracies linked to those limitations for particle size in that range. In order to overcome the heat and mass transfer limitations in cases where large biomass particle sizes are considered, there have been developed studies that define kinetic models for describing the decomposition of large particles (up to 2cm) [66,73,74].

Regarding the effect of the particle size on the obtained char yield, it has been observed in the literature that, once particle size of the samples is small enough to ignore the effects due to transport limitations, char yield increases for increasing particle size values [62]. On the contrary, it has also been reported that reducing particle size of the solid samples leads to higher volatiles yields, especially for those small particles of less than 1 mm of diameter or thickness [67].

Equally, heat transport limitations are not only dependent on particle size of feedstock, but they are also dependent on the initial mass of the sample. For determining the initial weight requirements of biomass samples that will undergo the pyrolysis process for kinetic evaluation, similar conclusions than the ones applied for the particle size are considered. In order to assure a uniform heating of the whole biomass sample, that is, so that all the particles conforming the sample get heated similarly and at the same time, and in order to avoid temperature gradients as much as possible, small initial sample weights are needed. That way, heating transfer effects are minimized in sample level, and the assumption of uniform temperature within the considered sample becomes acceptable as it is closer to the real situation taking place.

In this regard, increasing the initial weight has been reported to cause diffusion resistance for devolatilization to take place. Thermal resistance is also likely to happen when increasing the initial sample mass [62]. Therefore, in thermogravimetric studies and with the aim of avoiding the effects of transport phenomena, small samples in the

range of milligram size are employed [69]. Nevertheless, even when samples below one milligram undergo pyrolysis experiments, unavoidably effects of diffusion have been registered [66,75]. As an example, when running pyrolytic experiments in a TGA for cellulose samples, effects of initial sample mass on kinetic parameters E and A have been reported: with sample masses below 1mg, when decreasing the initial sample mass, higher values of activation energy and pre-exponential factor were obtained. It was also proved that by decreasing the initial sample mass, the systematic error derived from the existing thermal lag was reduced, resulting in more reliable results of the kinetic parameters [34,69].

- ***Final temperature***

Final temperature of the pyrolysis process has a deep influence, combined with the heating rate and residence time of the vapors, in the final product yields obtained from the process. In available literature, it is concluded that the optimum final temperature for obtaining maximum liquid yields and solid product yields is about 400-500ºC [24].

Regarding the effect of final temperature on the kinetic analysis of pyrolytic processes, it is necessary to study the effect of temperature linked to the particle size of the samples. The reason of this is that the shift to heat transfer limited kinetic behavior is highly dependent on both, values of particle size and temperature.

Simmons et al. [72] studied the boundary for particle size in function of temperature that means the limit between pyrolysis reactions being kinetically controlled and being heat transfer limited: below the boundary, the reaction is kinetically controlled, whereas above the boundary, it is highly dominated by heat transfer. They proved that for a particle size of 100µm and so that heat transport limitations could be negligible, 500ºC would be the limit temperature: above that limit, internal heat transfer could lead to heat transfer limitations; for a particle size up to 200µm, kinetic evaluation could be developed up to a temperature of about 450-500ºC, without having heat transfer limitations [72].

Nevertheless, one of the aims of the current project was to study the decomposition of the three main pseudo-components of the woody biomass feedstock, having decided that the three pseudo-components model, optimized by the method of the least square differences, would be employed for the determination of the kinetic parameters corresponding to each of the pseudo-components: hemicellulose, cellulose and lignin.

For being able to study the complete behavior of the pseudo-component whose decomposition spreads up to the highest temperatures, which is lignin, and in order to be able to simulate its whole decomposition kinetics, it is necessary to run experiments up to a final temperature at which decomposition of lignin has already been finished.

Thus, if a final temperature of about 500ºC was set based on the previously gathered information related to the maximum limit of the final temperature, for assuring kinetic control during the whole decomposition, it would not be possible to model the whole decomposition process of lignin as it spreads up to temperatures around 800ºC or even higher.

Taking this into account, when it came to deciding the final temperature of the process, the complete analysis of the decomposition process of the three pseudo-components, including the whole decomposition of lignin, prevailed over the possibility of some effect of heat and mass transfer taking place.

2.3.6. Assessment of values of the parameters for the experimental part

In this section, they is presented the assessment of values of the main experimental parameters used in the experimental part.

Based on what has been expounded in the section prior to this, the values of the experimental parameters were decided to be as follows:

- **Heating rate: 10K/min**

  The same value of the heating rate was decided to be used for all the experiments. A low value of it was decided in order to favor high values of char yield during experiments and to avoid possible restrictions in kinetic control of the decomposition reactions.

- **Particle size: 63µm<d<100µm and d<1mm**

  Two different particle sizes were used for the experimental part. All species were ground down to these two different particle size values, in order to analyze the effect of this parameter on char yield and kinetics. Small particle size, 63µm<d<100µm was mainly chosen in order to assure kinetic control regime. By assessing a quite large value to the second particle size considered (d<1mm), the analysis of the effect of this parameter was wanted. The experiments with this larger value of particle size (d<1mm) could have some slight heat transfer limitations due to the particle dimensions; in case this happened, the experimental situation could be somewhere between full kinetic control and diffusion control regimes. This was analyzed by comparing the results from the kinetic modeling: in case the calculated kinetic parameters resulted highly affected due to the changes of particle size, heat and mass transfer limitations may be attributed to the case of larger particle size.

- **Sample mass: 1mg and 10mg**

  Two different sample masses were considered for analyzing how this parameter affected the behavior of the samples. The lower sample mass, of 1mg, is low enough for assuming complete kinetic control of the reactions, whereas 10mg could be a too high value for assuming as negligible the heat and mass transfer effects. For both sample masses, kinetically controlled reactions taking place were assumed for developing the kinetic modeling, but always bearing in mind the possible effect of the elevated mass of 10mg samples. With the experiments with high sample mass, the same procedure than for the large particle size was followed: it was developed a comparison of the kinetic parameters between 1mg and 10mg samples to evaluate the agreement level of them, and to determine the effect of the sample mass; from the conclusions obtained, it would be possible to determine if heat and mass transfer limitations did actually affect decomposition of the 10mg samples.

- **Final temperature: 800ºC**

  The main reason why this high final temperature was chosen was to assure that the decomposition of the three considered pseudo-components could be completely simulated. Due to the wide range of temperatures through which

lignin pseudo-component decomposes, being the effects of his degradation still visible at high temperatures in the decomposition rate curves obtained from the TGA, the final temperature of 800ºC was considered. Thus, that way it was possible to be modeled the whole decomposition process of lignin.

2.3.7. *Influence of devolatilization on further conversion with focus on gasification*

In this section, the influence that devolatilization and pyrolysis processes have on further gasification conversion will be shortly analyzed. This involves studying how the conditions of pyrolysis process can affect the further gasification of the char produced by means of the pyrolysis process. This analysis is motivated by the wide use of the char produced by means of pyrolysis in gasification processes for the obtaining of synthesis gas.

The reactivity and kinetics of coal and coal char gasification have been widely studied in literature [38,76,77,78], whereas the amount of studies developed in this sense for char produced from lignocellulosic materials is considerably smaller and weaker. Although similarities can be found in the behavior of coal and lignocellulosic char gasification, there are also important differences in their gasification behaviors; for instance, the reactivity of char produced from lignocellulosic feedstock is higher than the reactivity of coal [38].

Therefore, in this section they are analyzed the effect that different process parameters of pyrolysis have on further gasification of the char produced, such as the effect of the heating rate, residence time and temperature, or the composition of the char produced in the pyrolysis process.

Unlike to what happened for the pyrolysis of lignocellulose biomass, for the gasification process of char there is no clear relation between the rate of the gasification conversion of char produced from biomass and the gasification rates of the pseudo-components hemicellulose, cellulose and lignin; this lack of evidence could be motivated by the scarce studies in the field of biomass char gasification. Nevertheless, some effects of pyrolysis parameters have been observed on the gasification reactivity of the char produced from the pyrolysis process.

The reactivity of char is deeply dependent on its structure in terms of morphology, which for a certain fuel is mainly affected by its content in inorganic matter and by the pyrolysis conditions employed in the char formation process. In this sense, it has been observed that gasification reactivity gets increased when employing high heating rates in the pyrolysis process from which the char is produced [38,79,80], due to the effect that the heating rate has in the morphology of the char.

For pyrolysis developed at atmospheric pressure, when employing high heating rates in the process, the morphology and internal structure of the lignocellulosic biomass is completely altered. Thus, it can be considered that the initial morphology and cellular organization is lost. These alterations on the basic cellular structure make the structure of the produced char be mainly composed of macropores, which are pores of big dimensions which favor the gasification reactivity of the char [38].

On the contrary, when lower heating rates are applied during the char-forming pyrolysis process, the morphology and internal structure of the biomass samples is not altered as the release of volatiles takes place by means of the naturally existing pores in the biomass. This involves that, unlike for the case of high heating rates, the char formed in the pyrolysis process will have a structure mainly composed of micropores, which do not favor the gasification reactivity of the char, but provoke just the contrary effect [38].

Continuing with the effect of the cellular structure of char, its tipically directional structure can also provoke differences in the gasification rates in the two main directions of the char structure [81].

The heating rapidity of the pyrolysis process also affects the composition of the char produced. If the pyrolysis process is quickly heated, there is registered a decreasing content of carbon, while Oxygen and Hydrogen contents get increased. The increasing contents of both Oxygen and Hydrogen trigger the reactivity of the char. Nevertheless, it has been observed that while the pyrolysis temperature gets increased, the carbon content in the produced char also increases reducing the mentioned effect that the heating speed has on reducing the carbon content [38].

It has been considered the effect of the pyrolysis heating rate on further conversion of char by means of gasification, but it is remarkable the fact that the mentioned effect of the heating rate is also dependent on the particle size of the biomass samples.

Depending on the biomass particle size, the heating and decomposition of the particles during pyrolysis is different, as the way heating level could be different in the inner, central zones of the particles and on the surface of them. This possibility of a particle not being homogenously heated depends on many factors, but the most important factor is the heating rate employed in the process together with the dimensions of the particle. This different heating of the particles makes that the reactivity of the produced char decreases. Taking this into account, it is considered that in general, pyrolysis of large, thick, biomass particles result in chars with lower values of gasification reactivity.

They have been also observed that differences in the char produced are registered between the char that is formed by means of primary pyrolysis reactions taking place and the char resulting as consequence of secondary reactions [38].

It has also been reported that char gasification reactivity decreases when high pyrolysis temperatures are held during the pyrolysis process by means of which the car is produced [38]. Besides, the catalytic effect of inorganic matter contained in the char acts as a catalyst during gasification process, enhancing the reactivity and favoring gasification reactions. In this regard, ash forming elements which in theory act as catalysts during the gasification process increasing the reactivity, can also provoke the contrary effect by means of provoking a lower porosity of the char, and thus lowering its surface area and reducing the overall gasification reactivity [38].

After having analyzed some of the effects of devolatilization and pyrolysis conditions on char gasification reactivity, it is important to mention that the reactivity level of the gasification process is not completely defined by the previous pyrolysis conditions; moreover, the reactivity level of the char is not even maintained constant while gasification process takes place, but this reactivity changes and evolves during the gasification process. For instance, reactivity becomes higher while conversion of char increases within the gasification process itself. Thus, the mentioned effects of pyrolysis conditions will have a considerably important impact on further char gasification, but there will be also other parameters which influence the gasification process regardless of the char formation process.

3. Experimental setup and procedure

3.1. Description of main equipment: TGA

The experiments for the Master's Thesis were developed in the laboratory of the Department of Energy and Process Engineering at the Faculty of Engineering Science and Technology at NTNU.

The main objective of the laboratory work was to produce and collect the necessary decomposition data of the samples while pyrolysis experiments were taking place, for the modeling of their decomposition behavior.

For this aim, a thermogravimetric analyzer (TGA), TA Instrument SDT Q600 model, was used for studying the non-isothermal decomposition of the samples during pyrolysis process.

Figure 4. TA Instrument SDT Q600 for pyrolysis experiments

When running one experiments, either 1 or 10 mg sample was firstly loaded in an alumina crucible that was placed into the furnace. Nitrogen gas was used as purging gas and introduced into the TGA furnace with a volumetric flow rate of 100L/min for all the experiments.

The operation of the TGA was controlled by the Q Series Advantage Software; communication, interaction and precise control was maintained between Q Series

Instrument or what is the same, the TGA itself, and the Q Series Advantage Software, during the whole operation. By means of this software, the mass of the sample inside he TGA furnace was constantly recorded.

For analyzing and processing the data obtained in the Q Series Advantage Software from the TGA operations and experiments, the TA Universal Analysis software was used. With the TA Universal Analysis Software, the mass curves (TGA) derived from the experimental operation and the first (DTG) and second derivatives of the mass loss curves were obtained and treated.

Principal components in the TGA:

Now a short description of elements which compose the TGA instrument is presented.

- **Thermobalance:** it consists of a horizontal dual balance. It measures the weight signal as the difference between the sample that has been located inside the instrument and reference beams.

- **Furnace:** Horizontal furnace. It provides the experiments with precise heating rate ramps and isothermal behaviors.

- **Temperature control and measurements system:** it is composed by a thermocouple pair which measures and controls the temperature in the system during the run of each experiment.

- **Purge gas system:** horizontal purge gas system. It has dual digital purge gas mass flow controllers.

3.2. Equipment and procedure for feedstock characterization

The procedures that were employed for developing the characterization of the analyzed woody biomass samples are presented, together with a short description of the equipment used in each case.

- ***Proximate Analysis***

Proximate analysis classifies the composition of the feedstock in moisture (M), volatile matter (VM), ash (A) and fixed carbon (FC) content. For developing this analysis, the ASTM Standards for biomass samples were followed.

Ceramic sample holders as the ones in Figure 5 were employed for keeping the woody biomass samples for the proximate analysis.

Figure 5. Sample holders used for containing the biomass samples during Proximate Analysis.

A drier was used for measuring the moisture content of the feedstock, whereas a muffle furnace was utilized for measuring the volatile matter content and ash content of the woody biomass samples, as very elevated temperatures are needed for measuring these parameters. The value of the fixed carbon content is deduced from the other measured values.

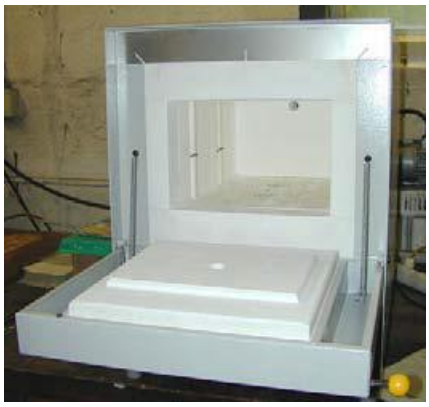

Figure 6. Muffle furnace for volatile matter content and ash content measurements.

The mentioned ASTM Standards which were followed for determining the Proximate Analysis of the feedstock are summarized in the following table:

Table 7. Summary of the ASTM Standards employed for Proximate Analysis of feedstock.

Content measured	Code of ASTM Standards	Experiment conditions	
		Temperature	Retention time
Moisture (M)	ASTM E871	103ºC	16h
Volatile matter (VM)	ASTM E872	950ºC	7min
Ash (A)	ASTM D1102	550ºC	12h

The steps listed below, based on weighing the sample in different moments through the process, were followed within the proximate analysis procedure:

1) First, moisture content measurement. The sample inside the crucible was weighed before and after its stay in the drier without the lid at 105ºC and for 16 hours. The mass that was removed during the process corresponded to the moisture content of the sample.
2) After the moisture content measurement, the volatile matter content was measured. For this, the crucible with the lid on was kept inside the muffle furnace, which had previously been heated up to 950ºC, for 7 minutes. The difference in mass before and after this action corresponded to the volatile matter content, in dry basis.
3) Finally, the ash content was measured by keeping the crucible without the lid inside the muffle furnace at 550ºC for 12 hours. The remaining mass inside the crucible after the process corresponded to the ash content in dry basis.
4) The fixed carbon content was calculated in dry basis by means of the values of obtained volatile matter and ash content:

$$FC = 100 - VM - A \tag{61}$$

- ***Ultimate Analysis***

Ultimate Analysis consists of determining the percentage of constituent elements of a substance. In this case, for the characterization of the elemental composition of the feedstock, results obtained prior to the start of this Master's Thesis by SINTEF Energy Research were used. By means of the Ultimate Analysis, the weight percentage of Carbon (C), Hydrogen (H), Nitrogen (N), Sulphur (S) and Oxygen (O) were

determined. The equipment used for the analysis of the elemental composition of the samples was a Eurovector EA 3000 CHNS-O Elemental Analyzer.

- ***Higher Heating Value measurement***

A bomb calorimeter was used for measuring the Higher Heating Value (HHV) of the feedstock. The model of the calorimeter used was IKA Labortechnik C5000, and the procedure followed was the one described by ASTM E711-87(2004). In the calorimeter, complete combustion of dried woody biomass samples took place and the higher or gross heating value of the analyzed sample was directly obtained.

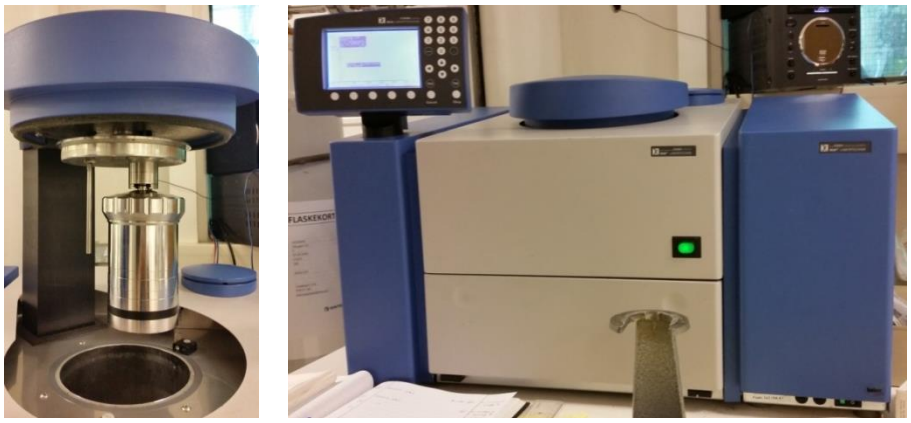

Figure 7. IKA Labortechnik C5000 bomb calorimeter used for Higher Heating Value measurements.

- ***Content of pseudo-components***

The corresponding percentage of each of the pseudo-components, hemicellulose, cellulose and lignin, in the different woody biomass species, was not experimentally measured for the Master's Thesis. Nevertheless, for having some reference values regarding the presence of each of the pseudo-components in the samples, a literature survey was carried out, whose results will be presented in the next section.

3.3. Feedstock characterization

Feedstock used in the TGA experiments came from spruce, birch and oak trees from Southern Norway. The mentioned tree species were separated into stem wood, bark and forest residues. Forest residues were composed of tops and branches from the mentioned tree types; the corresponding Norwegian acronym of tops and branches, GROT, was used for naming these forest residue samples. The exact localization from where the woody biomass samples were collected is available for spruce and birch:

- spruce was from South Norway, Latitude 59°38′N, Longitude 09°09′E;
- birch was from South Norway, Latitude 59°55′N, Longitude 10°89′E;
- for oak samples, there is no information available regarding the exact point from where the samples came from, apart from the place being also located in Southern Norway.

Concretely, for the pyrolysis experiments which were run for the Master's Thesis, stem wood samples and forest residue samples, GROT, were used.

The used wood samples can be classified regarding their nature of hardwood or softwood, as follows:

Table 8. Classification of the feedstock.

Origin tree	Wood type
Spruce	**Softwood**
Birch	**Hardwood**
Oak	

The classification between hardwood and softwood is mostly based on the way of plant reproduction of the trees. All trees reproduce by means of seeds, but there are important differences in the structure of the seeds, what makes the difference between hardwood and softwood: hardwood trees are angiosperms, with seeds having a cover, while softwood trees are gymnosperms, with seeds having no covering.

There are differences in the physical structures of hardwood and softwood in terms of both, microscopic level and surface level. At first glance, broad leaves are typical in hardwoods, while softwoods have needles and cones instead. At microscopic level,

hardwoods appear to be porous because of the vessel elements that are composing their structure, which have as their function the transportation of water through the wood. On the contrary, softwoods do not have those visible pores as they do not count on those vessel elements for water transportation, but they have medullary rays for this purpose, which do not involve any porous-kind microscopic structure.

There are also visible differences between hardwood and softwood species regarding the main chemical constituents, hemicellulose, cellulose and lignin, as presented later in this section in Table 9.

By means of analyzing both, hardwood and softwood species, a comparison of their decomposition behavior and kinetics will made, in case relevant differences could be identified.

Regarding characterization of each sample type, the previously mentioned experiments, following the previously indicated standards methods were developed for building the characterization of the samples. Besides, literature survey was developed for registering some of the characterization parameters whose measurement was not carried out in the laboratory.

In Table 9, the values of the Proximate Analysis, Ultimate Analysis and Higher Heating Value measurements are presented. Results from Proximate and Ultimate Analysis are presented as mass percentage (wt%) and were calculated in dry basis.

Table 9. Results from Proximate and Ultimate Analysis and Higher Heating Value (HHV) measurements of the samples.

Species	Proximate Analysis			Ultimate Analysis					HHV (J/g)
	VM (wt%)	FC (wt%)	A (wt%)	C (wt%)	H (wt %)	N (wt%)	S (wt%)	O (wt%)	
Spruce wood	78.0	21.4	0.6	49.6	6.4	0.1	0.0	43.8	19,642
Spruce GROT	72.1	25.4	2.5	51.7	6.1	0.7	0.0	41.5	20,632
Birch wood	81.4	17.8	0.8	49.9	6.7	0.36	0.0	43.1	19,567
Birch GROT	73.8	23.5	2.7	50.7	6.3	0.8	0.0	42.1	20,843
Oak wood	80.6	18.5	1.0	49.3	6.2	0.1	0.0	44.5	18,198
Oak GROT	74.0	23.7	2.3	50.2	5.9	0.8	0.0	43.1	19,139

Regarding the presence of pseudo-components in the samples, in the table below the range of values corresponding to the content of hemicellulose, cellulose and lignin is presented, separately for hardwood and softwood samples:

Table 10. Content of pseudo-components for hardwoods and softwoods [8,82].

Type of wood	Hemicellulose (wt%)	Cellulose (wt%)	Lignin (wt%)
Hardwoods	43±2	18-25	20-35
Softwoods	43±2	25-35	10-18

It was also developed a more specific literature survey in this regard, looking for the cellulose, hemicellulose and lignin content of the concrete species used in this Thesis. Although the chemical composition of exactly the same woody biomass was not possible to find, the composition of at least the same tree species as the ones used in the current work were found, with the aim of having some approximations and reference values regarding the composition of the samples used for this Master's Thesis.

Finding the composition of stem wood of spruce, birch and oak was quite easy. Nevertheless, it was harder to find the chemical characterization of the type of forest residues used in this work: due to the specific definition of the GROT samples, meaning tops and branches of the trees, it was not possible to get the characterization of a mix of tops and branches from literature. Therefore, for spruce and birch it was collected the chemical composition of branches only, whereas for oak, as composition of tops and/or branches was not found, the composition of the bark was decided to be included in the table, in case it could be useful as reference for the oak GROT composition.

Table 11. Hemicellulose, Cellulose, Lignin and Extractives composition of the samples.

Species	Hemicellulose	Cellulose	Lignin	Extractives
SPRUCE				
Stem wood [83]	42.0 (1.2)	27.3 (1.6)	27.4 (0.7)	2.0 (0.6)
Branches [83]	29.0	30.0	22.8 (1.7)	16.4 (2.6)
BIRCH				
Birch wood [83]	43.9 (2.7)	28.9 (3.7)	20.2 (0.8)	3.8 (1.3)
Birch branches [83]	33.3	23.4	20.8 (3.9)	13.5 (3.0)
OAK				
Oak wood (a.) [84]	38	29	25	4.4
Oak wood (b.) [85]	49.8	26.9	16.0	7.2
Oak bark [85]	30.0	20.5	19.6	26.9

For the case of spruce and birch, the values presented are medians of a wide literature survey made by Räisänen et al. [83] ; for the cases were more than two values obtained from literature were used for the calculation of the median value, the absolute deviation is presented in brackets. Regarding the concrete species whose chemical composition is presented in the table, they are as follows:

- values for spruce correspond to Norway spruce;
- values for birch correspond to Silver/Downy Birch; and
- values for oak correspond to : (a.) Europe oak, and (b.) Red oak.

3.4. Description of experimental conditions of pyrolysis experiments

The TGA experiments developed for the current work were non-isothermal pyrolysis experiments. The experiments were run in an inert atmosphere by means of using Nitrogen as flow gas, which was introduced into the TGA furnace with a flow rate of 100mL/min. The heating rate used was of 10K/min and was maintained constant for all the experiments. The final temperature was set in 800ºC. The summary of the experimental conditions which were kept constant during all the experiments is as follows:

- Gas used: Nitrogen (99.99% of pureness), with a flow rate of 100mL/min.
- Heating rate: 10K/min.
- Final temperature: 800ºC.
- Heating program: the same linear heating program was employed for all the experiments. It was composed of the following parts:
    1. Isothermal part for 30 minutes at room temperature.
    2. Heating up to a temperature of 105ºC, with 10K/min heating rate.
    3. Isothermal part for 20 minutes at 105ºC.
    4. This is the point in which the real experiment start, consisting of a ramp, defined by the same heating rate as before (10K/min), up to the final temperature of 800ºC.

As mentioned in previous sections, two different sample masses and two different particle sizes were considered, for studying the effect of these parameters in the decomposition behavior and kinetics:

- Sample mass: a. 1mg b. 10mg
- Particle size: a. 63µm<d<100µm b. d<1mm

It was also studied the effect of the decomposition atmosphere in the char yield value of the process by covering with a lid the crucible where the sample was kept during pyrolysis. This configuration of closed crucible was only employed for the 10mg samples, and not for the 1mg samples, whereas all samples underwent experiments with open crucible.

For kinetic modeling, only the experiments with the open crucible mode were used, where pyrolysis was developed in a pure nitrogen atmosphere without the interaction of the released volatiles. So, the experiments with closed crucible were only used for the analysis of char yield values: comparison of char yield values between experiments with and without the lid was developed. In experiments with the lid on, due to increasing retention times of released volatiles inside the crucible, secondary reactions were provoked, affecting the whole decomposition process and decomposition kinetics; due to these provoked secondary reactions, the modeling of the reaction kinetics of these experiments would have been meaningless.

It is now presented a short summary of the experiments developed for the current work, where the different values acquired by the variable parameters are presented, together with the task for which the results were used:

Table 12. Summary of the TGA experiments carried out for the Master's Thesis

Set of experiments	Sample mass	Particle size	Lid	Char yield analysis	Kinetic modeling
1)	1mg	63µm<d<100µm	Without lid	Yes	Yes
2)	10mg	63µm<d<100µm	Without lid	Yes	Yes
			With lid	Yes	No
3)	10mg	d<1mm	Without lid	Yes	Yes
			With lid	Yes	No

4. Results and discussion

4.1. Char yield

The char yield is defined as a non-devolatilized solid fraction of the biomass that remains after the experiment. It refers to the efficiency of pyrolysis and it is calculated as the fraction between the dry mass of char produced in the pyrolytic process and the initial dry mass of the biomass feedstock used for that charcoal production [44,86]:

$$Y_{char}(wt\%) = \left(M_{char}/M_{feed}\right)x100 \quad (62)$$

where Y_{char} corresponds to the char yield, M_{char} is the dry mass of charcoal produced in the process at its final temperature and M_{feed} is the mass of the feedstock measured at the end of the 105^{o}C heating stage.

As it was explained in the section prior to this, the effects that devolatilization atmosphere, the sample mass and the particle size have on the char yield were analyzed for stem wood and GROT samples. The calculated char yield values corresponding to the samples undergoing the pyrolysis process up to a final temperature of 800ºC are registered in Table 13.

Table 13. Values of char yield from the pyrolysis experiments.

	Y_{char}				
	Sample mass 1mg Particle size: 63µm<d<100µm	**Sample mass 10mg Particle size: 63µm<d<100µm**		**Sample mass 10mg Particle size: d<1mm**	
Species	**No lid**	**No lid**	**With lid**	**No lid**	**With lid**
Spruce wood	14.93	17.74	23.90	19.52	22.21
Spruce GROT	20.59	28.64	30.44	26.65	30.24
Birch wood	16.78	16.04	20.56	17.68	20.49
Birch GROT	14.93	25.14	32.89	21.96	29.39
Oak wood	29.36	26.75	30.92	20.54	24.89
Oak GROT	23.75	23.56	25.91	22.24	23.42

As previously said, for studying the impact of reaction environment in obtained char yield, experiments with two different reaction atmospheres were developed by changing the mode of the crucible employed for the experiments with 10mg of sample mass. With open crucible, released volatiles were removed by the nitrogen flow as they were generated, without interacting with the solid matter inside the crucible, whereas with closed crucible the volatiles remained inside the crucible affecting the evolution of the pyrolysis reaction and reacting themselves with solid matter contained in the crucible.

As it can be observed in Table 13, they were registered increasing char yield values when pyrolysis process took place in generated volatiles atmosphere, that is, with the lid of the crucible on, rather than in a pure, inert nitrogen atmosphere. This is in agreement with publications at which it has been reported the beneficial effects of increased vapor-phase resident times and increased vapor concentrations on favoring char formation and char yields [14,87]. The reason why the generated volatiles atmosphere provoked an increase in the value of the char yield is that keeping the released vapors and volatiles in contact with both the decomposing solid biomass and the solid mass products has the effect of gasses being absorbed onto the solid surface by means of secondary reactions that take place inside the crucible. By means of the absorption of those gas products by the solid surface, the amount of generated solid products increases in weight resulting in higher char yield values. The increment in the obtained char yield due to the effect of the generated volatiles atmosphere ranged between 6% for oak GROT and 36% for birch GROT: These both limit values correspond to the case of large particle size.

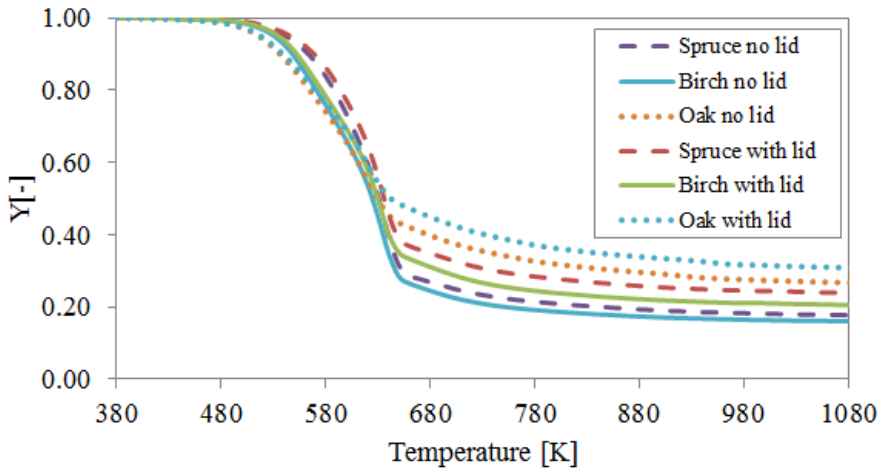

Figure 8. TGA curves of 10mg stem wood samples with small particle size (63µm<d<100µm). Comparison of experiments without the lid (pure Nitrogen atmosphere) and with the lid on (generated volatiles atmosphere).

The influence that the particle size could have in the obtained char yield was also analyzed, by considering, just as previously presented, different particle sizes for the analyzed 10mg samples: large particle size, d<1mm; and small particle size, 63 µm<d<100 µm. When reducing the particle size, increasing char yields were reported for majority of the woody biomass sample types, for the two modes of operation of the crucible, what is in agreement with a few previous studies [88]. This can be motivated by a higher presence of fines, i.e. fine dust and soil particles, in the reduced particle size samples, due to these fines falling down during sieving together with the small particles. This involves a higher content of inorganic compounds in the sample that contributes to give higher char yield values. This is known as fractionation of ash or effect of inorganic content in the solid fuel samples. This tendency of increasing char yield for smaller particle size was followed by all the GROT samples and some of the stem wood samples; nevertheless, some exceptions in behavior were reported among the stem wood samples, such as spruce and birch wood with open crucible and birch wood with closed crucible, for which increasing char yield values were registered for larger particle size. This effect, which was not the prevailing one in the experiments carried out, has been previously reported by many authors [13,14,87,89,90,91].

Comparison of TGA curves with different particle size and same sample mass (10mg) is presented in Figure 9, for both stem wood and GROT samples, for the experiments without the lid.

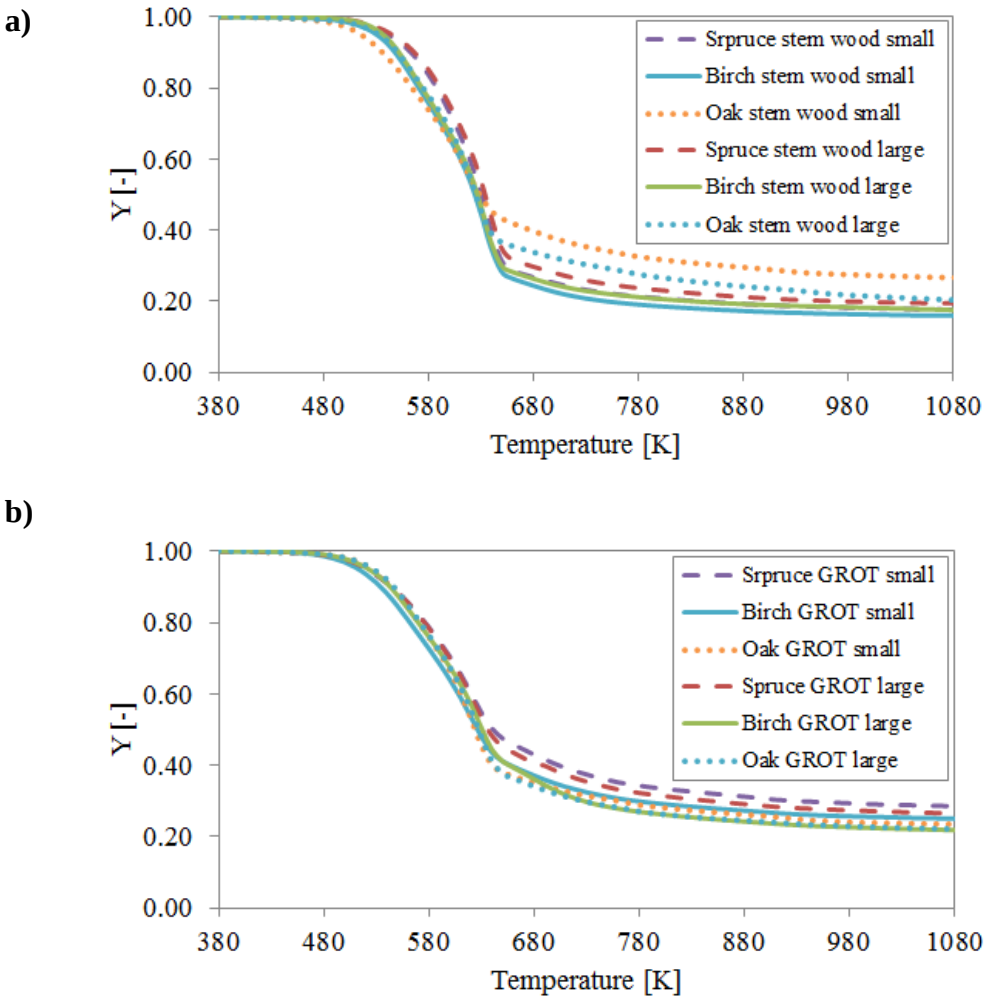

Figure 9. Comparison of TGA curves of 10mg samples and different particle size: small particle size (63µm<d<100µm) and large particle size (d<1mm), in pure nitrogen atmosphere (without the lid). a) Stem wood samples; b) forest residue (GROT) samples.

Regarding the effect of the sample mass, decreasing char yield values were observed when decreasing the sample mass, with the exception of oak wood.

Comparison of char yield values between wood and GROT samples was also developed: for the same tree species, GROT samples were the ones giving the highest char yield values for spruce and birch regardless of particle size, sample mass and devolatilization atmosphere. This rule observed for spruce and birch samples is in good agreement with the composition of the GROT forest residue samples: GROT samples have higher fixed carbon and ash content than their corresponding stem wood samples, meaning that higher char yield values are expected for them. This tendency was not maintained for oak samples: although higher fixed carbon and ash content values were also registered for oak GROT compared to wood samples, oak wood resulted in the

highest char yield for all experiments (with the exception of small particle size with open crucible).

About differentiation of hardwood and softwood samples, it was not possible to establish a final conclusion regarding the type of species giving the highest char yield values, as different results were obtained depending on particle size. For large particle size, the highest char yield values were obtained for softwood spruce GROT samples whereas for small particle size and for the two sample masses considered (10mg and 1mg), birch GROT and oak wood samples, both of them hardwood, were the ones giving the highest values.

Regarding the content of fixed carbon on the species, the highest value was registered for spruce GROT sample, which is among the highest char yield values at all experimental conditions, whereas the lowest fixed carbon content was for birch wood, giving the lowest char yield values in all cases. So for spruce and birch samples expectable, justifiable values of char yield were obtained. On the contrary, the case of hardwood oak is remarkable as this sample type gives one of the highest char yield values for all experimental conditions that were analyzed whereas it has one of the lowest fixed carbon content and ash content among all the samples considered. This can be graphically observed in Figure 9, for the case of experiments with 10mg sample mass.

a)

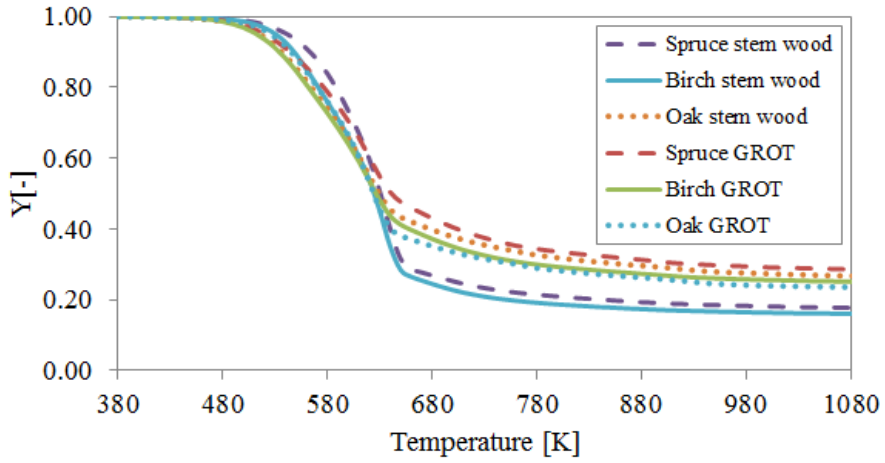

b)

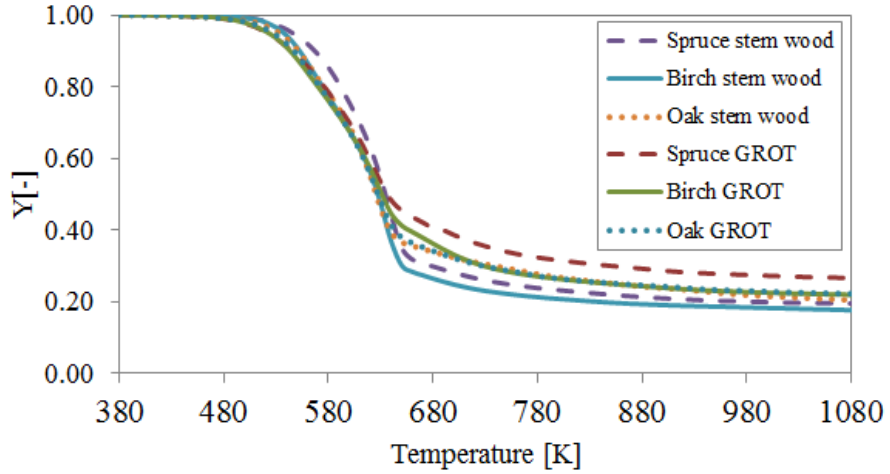

Figure 10. DTG curves of stem wood and forest residue (GROT) samples in pure nitrogen atmosphere (without the lid): a) sample mass: 10mg; particle size: 63µm<d<100µm; b) Sample mass: 10mg; particle size: d<1mm.

4.2. Kinetic modeling and simulation

In this section, the results derived from the kinetic modeling of the samples analyzed are presented. The values of the initially unknown kinetic parameters were obtained by means of the assumption of the Three pseudo-components model and the employment of the Least Square Method. Just as it was previously decided and justified in this Master's Thesis, the Least Square Method was employed for the case of first-order reactions (n=1) and non-first-order reactions (n≠1) assuming constant activation energies for each pseudo-component, and it was also used the Distributed Activation Energy Method assuming first-order reactions (n=1). Thus, three different sets of kinetic parameters were calculated and are presented in this section for each sample type, corresponding to the three different approaches employed for all the samples. Each of the sets of the kinetic results includes three different values for each of the kinetic parameters, each of one attributed to one of the pseudo-components considered: hemicellulose, cellulose and lignin, in that order.

Together with the kinetic parameters that were calculated for each sample type and for each of the method employed, the square differences (S.D.) and the fit (%) of each of the methods are also shown in the result tables in this section, so that the quality of the modeling can also be evaluated not only in terms of kinetic parameters being within an acceptable range, but also in terms of the accuracy of the calculated curves when imitating the real decomposition behaviors of the samples.

As it was mentioned in previous sections, the experiments whose kinetics were analyzed and modeled can be classified in 3 different set of experiments due to conditions related to sample mass and particle size, as follows:

Table 14. Classification of pyrolysis experiments whose kinetics were modeled.

SET 1 of experiments		
Sample mass: 1 mg	**Particle size: 63µm<d<100µm**	**Without the lid (pure Nitrogen atmosphere)**
Species:		
Spruce wood		
Birch wood		
Oak wood		
Spruce GROT		
Birch GROT		
Oak GROT		

SET 2 of experiments		
Sample mass: 10 mg	**Particle size: 63µm<d<100µm**	**Without the lid (pure Nitrogen atmosphere)**
Species:		
Spruce wood		
Birch wood		
Oak wood		
Spruce GROT		
Birch GROT		
Oak GROT		

SET 3 of experiments		
Sample mass: 10 mg	**Particle size: d<1mm**	**Without the lid (pure Nitrogen atmosphere)**
Species:		
Spruce wood		
Birch wood		
Oak wood		
Spruce GROT		
Birch GROT		
Oak GROT		

Regarding the curves obtained from the TGA for developing the modeling task, it was not possible to reproduce duplicates of all samples of the three set of experiments considered. This is the reason why the results are differently presented for the different set of experiments. Now, it will be shortly explained the way the modeling task was carried out for the different experiment sets:

- **Set 1 of experiments:** **(1mg; 63µm<d<100µm)**

  - **Wood samples:** two experiments were analyzed per each sample type. They were obtained good fittings for the same set of kinetic parameters for the two experiments considered for each sample type, meaning almost identical kinetic behavior of the samples when duplicating the experiments (Table 15). Thus, the same set of kinetic parameters was applicable to the two samples analyzed for each sample type. In Table 15, the results from kinetic modeling of 1mg stem wood samples are presented. For each sample type, the value of each of the kinetic parameters was calculated; besides, they were given the average values of the square differences (S.D.) and fitting (%) obtained by comparison of the simulated curve with the two real experimental curves used from the TGA for each sample type. Together with the average values of square differences and fitting, the standard deviation corresponding to each of those parameters was also calculated and the values are also presented for each sample type in Table 15.

  - **GROT samples:** two experiments per species were analyzed for Spruce and Birch GROT samples, whereas only one experiment was considered for Oak GROT as it was no duplicated. In this case, the kinetic parameters for the duplicated experiments were not in good agreement with each other: the best fitting for one of the experiments resulted in quite bad simulation of the other repetition of the same sample. When evaluating the kinetics of the two experiments of the same sample type together, bad fitting results were also obtained. For this reason, in Tables 18 and 19, they have been represented the best kinetic parameters for each of the experiments, with the values of the fitting and square difference obtained for the second repetition when using the kinetic parameters calculated for the first experiment. As it was considered that not good enough modeling could be obtained with one set of kinetic parameters for the two repetitions, results of kinetic parameters for each repetition were listed in Table 20 as the final results for these samples. The reason why it was no possible to achieve a good modeling of the two repetitions for each sample type with the same kinetic parameters could be that the GROT samples are residue samples of the trees, meaning that their composition may not be uniform for all the samples as it is for the stem wood chip samples; this could result in a not so uniform decomposition behavior and in not just identical kinetics.

- **<u>Sets 2 and 3 of experiments:</u> (10mg; 63µm<d<100µm and d<1mm)**

  - **Wood and GROT samples:** there was a lack of duplications for many of the experiments with large sample mass. Thus, one experiment was finally considered for kinetic evaluation of each sample (Tables 16,17,21 and 22).

In the tables presented now, all the results for the kinetic parameters have been listed. After the tables comments and discussion on those obtained results and on the observed behaviors are presented.

STEM WOOD SAMPLES

SET 1 OF EXPERIMENTS: SAMPLE MASS: 1 mg; SMALL PARTICLE SIZE: 63µm<d<100µm

Table 15. . Kinetic parameters of wood samples: sample mass 1mg, particle size 63µm<d<100µm. Two repetitions for each.

	n=1					n≠1						DAEM					
	c_i	E_i (kJ/mol)	A_i (min^{-1})	S.D.	Fit (%)	c_i	E_i (kJ/mol)	A_i (min^{-1})	n	S.D.	Fit (%)	c_i	E_{0i} (kJ/mol)	A_i (min^{-1})	σ (kJ/mol)	S.D.	Fit (%)
Spruce wood	0.31	108.92	1.68E+09			0.31	108.77	2.63E+09	1.01			0.28	98.65	4.63E+09	11.05		
	0.33	244.58	7.56E+19	5.78E-03	98.50	0.33	245.50	9.06E+19	1.01	5.94E-03	98.45	0.38	251.00	3.37E+21	29.12	2.07E-03	98.36
	0.19	32.93	2.03E+02			0.19	42.10	1.11E+03	1.80			0.10	52.00	5.85E+04	5.12		
			Deviation:	2.95E-03	0.37				Deviation:	3.00E-03	0.37				Deviation:	5.95E-04	0.24
Birch wood	0.37	88.07	5.43E+07			0.35	94.24	1.68E+08	1.12			0.30	92.33	2.37E+09	10.27		
	0.37	233.13	1.03E+19	6.00E-03	98.38	0.35	234.32	1.31E+19	1.01	5.25E-03	98.48	0.38	241.97	7.98E+20	28.24	2.49E-03	98.09
	0.14	41.46	6.02E+02			0.19	54.08	1.02E+02	2.19			0.10	56.11	1.22E+05	3.15		
			Deviation:	3.35E-04	0.06				Deviation:	2.00E-05	0.01				Deviation:	1.65E-04	0.08
Oak wood	0.23	80.22	1.74E+07			0.24	86.16	6.74E+07	1.18			0.23	95.67	1.23E+10	10.26		
	0.27	135.33	1.22E+11	2.35E-03	97.81	0.27	140.85	3.86E+11	1.16	1.41E-03	98.33	0.27	117.79	9.98E+10	13.16	1.80E-03	97.49
	0.17	45.97	9.95E+02			0.18	59.50	9.05E+03	1.84			0.18	58.36	1.25E+05	5.02		
			Deviation:	2.95E-04	0.16				Deviation:	4.54E-04	0.30				Deviation:	9.50E-05	0.13

STEM WOOD SAMPLES

SET 2 OF EXPERIMENTS: SAMPLE MASS: 10 mg; SMALL PARTICLE SIZE: 63µm<d<100µm

Table16. Kinetic parameters of wood samples: sample mass 10mg, particle size 63µm<d<100µm. One repetition for each sample.

	n=1					n≠1						DAEM					
	c_i	E_i (kJ/mol)	A_i (min^{-1})	S.D.	Fit (%)	c_i	E_i (kJ/mol)	A_i (min^{-1})	n	S.D.	Fit (%)	c_i	E_{0i} (kJ/mol)	A_i (min^{-1})	σ (kJ/mol)	S.D.	Fit (%)
Spruce	0.30	106.72	1.06E+09			0.29	114.02	4.49E+09	1.10			0.25	106.82	2.53E+10	11.87		
wood	0.31	258.52	1.21E+21	1.68E-03	99.16	0.30	265.85	4.99E+21	1.01	9.11E-04	99.38	0.38	256.82	1.66E+22	29.96	2.66E-03	98.07
	0.18	43.76	1.39E+03			0.23	52.00	8.38E+03	1.90			0.13	40.30	1.65E+04	4.00		
Birch	0.33	91.47	9.22E+07			0.31	100.58	6.41E+08	1.18			0.31	94.42	3.74E+09	10.33		
wood	0.32	241.70	6.02E+19	3.67E-03	98.64	0.31	245.17	1.19E+20	1.02	3.16E-03	98.73	0.38	249.61	3.73E+21	28.79	1.43E-03	98.46
	0.13	63.56	3.25E+04			0.17	50.50	4.28E+03	1.20			0.11	58.42	3.07E+05	2.50		
Oak	0.21	88.49	1.09E+08			0.22	94.02	3.98E+08	1.11			0.27	89.50	2.78E+09	9.47		
wood	0.28	142.92	5.70E+11	3.51E-03	99.78	0.31	140.77	3.92E+11	1.12	4.26E-03	99.75	0.36	151.87	6.82E+13	16.54	8.74E-04	99.79
	0.18	46.12	1.30E+03			0.14	63.00	1.71E+04	1.46			0.18	37.98	8.38E+03	3.00		

STEM WOOD SAMPLES

SET 3 OF EXPERIMENTS: SAMPLE MASS: 10 mg; LARGE PARTICLE SIZE: d<1mm

Table 17. Kinetic parameters of wood samples: sample mass 10mg, particle size d<1mm. One repetition for each sample.

	n=1					n≠1						DAEM					
	c_i	E_i (kJ/mol)	A_i (min^{-1})	S.D.	Fit (%)	c_i	E_i (kJ/mol)	A_i (min^{-1})	n	S.D.	Fit (%)	c_i	E_{0i} (kJ/mol)	A_i (min^{-1})	σ (kJ/mol)	S.D.	Fit (%)
Spruce	0.27	109.07	1.74E+09			0.27	112.91	3.82E+09	1.10			0.28	115.40	1.90E+11	12.5		
wood	0.31	263.01	2.65E+21	2.28E-03	99.02	0.31	262.11	2.23E+21	1.01	1.51E-03	99.20	0.33	219.72	1.01E+19	25.95	3.68E-03	97.67
	0.17	45.69	1.81E+03			0.20	47.97	2.87E+03	1.60			0.15	42.42	1.50E+04	4.00		
Birch	0.30	100.84	6.93E+08			0.31	109.56	4.58E+09	1.31			0.33	102.37	2.07E+10	11.13		
wood	0.33	237.82	2.88E+19	4.14E-03	98.58	0.31	240.83	5.03E+19	1.01	2.72E-03	98.75	0.38	243.41	1.18E+21	28.13	1.39E-03	98.40
	0.13	59.63	1.72E+04			0.17	56.34	1.10E+04	1.83			0.10	58.00	2.78E+05	2.32		
Oak	0.22	117.02	3.09E+10			0.24	117.02	3.09E+10	1.26			0.25	116.03	5.05E+11	12.77		
wood	0.33	211.75	3.27E+17	7.33E-03	99.79	0.33	211.75	3.27E+17	1.01	2.42E-03	99.88	0.34	209.34	3.40E+18	24.28	1.79E-03	99.81
	0.17	50.78	2.20E+03			0.17	50.78	2.20E+03	1.62			0.18	52.56	7.82E+04	4.20		

FOREST RESIDUE SAMPLES: GROT

In this case, two repetitions were considered for Spruce and Birch samples: Experiment 01 and Experiment 02 for each case. But as said before, no good agreement was found between the results for the two repetitions. Two different sets of kinetic parameters are presented for each sample type: a) and b). Each of the sets of kinetic parameters models quite well one of the experiments, while is far from giving a good fit for the other experiment. Square difference and fitting for the two different experiments are presented for each set of kinetic parameters in Tables 18 and 19.

As it can be seen in Tables 18 and 19, although for some of the cases not so bad agreement was found between the fitting values for the two different repetitions for Spruce and Birch GROT samples, in some cases the fitting values registered for one of the repetitions were very low when maximizing the fitting for the other experiment. It was decided that, as a whole, no good agreement was found for the two repetitions for each sample type and thus, that a joint solution of the kinetic parameters could not be reached. This is why the results for each of the experiments developed for each of the sample types are presented in Table 20, separately.

FOREST RESIDUE SAMPLES: GROT

SET 1 OF EXPERIMENTS: SAMPLE MASS: 1 mg; SMALL PARTICLE SIZE: 63µm<d<100µm

Table 18. Kinetic parameters of Spruce forest residue samples, Spruce GROT: samples mass 1mg, particle size 63µm<d<100µm. Two repetitions considered, 01 and 02, and two set of results of kinetic parameters considered, a) and b).

Spruce GROT	n=1			n≠1				DAEM			
a)	c_i	E_i (kJ/mol)	A_i (min^{-1})	c_i	E_i (kJ/mol)	A_i (min^{-1})	n	c_i	E_{oi} (kJ/mol)	A_i (min^{-1})	σ (kJ/mol)
	0.24	80.00	1.18E+07	0.27	72.95	2.69E+06	1.20	0.29	74.97	7.65E+07	7.76
	0.27	143.40	4.87E+11	0.27	150.52	2.15E+12	1.30	0.31	162.39	4.01E+14	17.62
	0.20	54.83	4.69E+03	0.18	53.00	3.10E+05	1.10	0.12	35.63	6.37E+03	3.78
Experiment number	S.D.	Fit (%)		S.D.	Fit(%)			S.D.	Fit (%)		
01	4.77E-03	97.44		3.34E-03	97.86			6.00E-04	98.34		
02	1.67E-02	95.04		1.07E-02	95.74			3.34E-03	95.64		
Deviation	5.97E-03	1.20		3.68E-03	1.06			1,37E-03	1,35		
b)	c_i	E_i (kJ/mol)	A_i (min^{-1})	c_i	E_i (kJ/mol)	A_i (min^{-1})	n	c	E_{oi} (kJ/mol)	A_i (min^{-1})	σ (kJ/mol)
	0.21	73.29	3.18E+06	0.23	93.02	2.00E+08	1.25	0.28	80.97	3.18E+08	3.50
	0.24	147.26	1.09E+12	0.24	159.54	1.21E+13	1.20	0.31	156.90	1.53E+14	16.94
	0.19	54.80	4.66E+03	0.20	61.10	1.29E+04	1.90	0.14	36.80	8.05E+03	1.83
Experiment number	S.D.	Fit(%)		S.D.	Fit (%)			S.D.	Fit(%)		
01	1.43E-02	95.56		1.98E-02	96.15			3.46E-03	96.01		
02	3.90E-03	97.42		4.13E-03	97.35			7.98E-04	97.87		
Deviation	5.20E.03	0.93		3.34E-06	0.60			1.33E-03	0.93		

FOREST RESIDUE SAMPLES: GROT

SET 1 OF EXPERIMENTS: SAMPLE MASS: 1 mg; SMALL PARTICLE SIZE: 63µm<d<100µm

Table 1917. Kinetic parameters of Birch forest residue samples, Birch GROT: samples mass 1mg, particle size 63µm<d<100µm. Two repetitions considered, 01 and 02, and two set of results of kinetic parameters considered, a) and b).

Birch GROT	n=1			n≠1				DAEM			
a)	c_i	E_i (kJ/mol)	A_i (min^{-1})	c_i	E_i (kJ/mol)	A_i (min^{-1})	n	c_i	E_{0i} (kJ/mol)	A_i (min^{-1})	σ (kJ/mol)
	0.30	75.63	5.88E+06	0.29	81.46	2.25E+07	1.07	0.24	79.72	3.33E+08	8.17
	0.28	145.81	8.16E+11	0.30	151.96	3.08E+12	1.21	0.31	141.79	8.69E+12	15.73
	0.20	44.90	1.04E+02	0.21	50.13	2.61E+03	1.52	0.12	39.77	1.11E+04	4.08
Experiment number	S.D.	Fit (%)		S.D.	Fit (%)			S.D.	Fit (%)		
01	3.14E-03	97.98		1.78E-03	98.48			7.01E-04	98.25		
02	6.84E-03	96.83		5.60E-03	97.13			1.99E-03	98.87		
Deviation	1.85E-03	0.58		1.91E-03	0.68			6.45E-04	0.69		
b)	c_i	E_i (kJ/mol)	A_i (min^{-1})	c_i	E_i (kJ/mol)	A_i (min^{-1})	n	c_i	E_{0i} (kJ/mol)	A_i (min^{-1})	σ (kJ/mol)
	0.27	79.20	1.31E+07	0.27	82.21	2.71E+07	1.06	0.24	78.07	2.14E+08	8.50
	0.27	145.00	7.25E+11	0.29	148.35	1.53E+12	1.17	0.33	152.30	6.13E+13	16.66
	0.19	42.69	7.88E+02	0.19	52.30	3.94E+03	1.65	0.15	38.80	8.57E+03	3.74
Experiment number	S.D.	Fit (%)		S.D.	Fit (%)			S.D.	Fit (%)		
01	7.12E-03	96.96		5.91E-03	97.23			1.94E-03	97.09		
02	3.01E-03	97.89		1.88E-03	98.34			7.79E-04	98.04		
Deviation	2.06E-03	0.47		2.02E-03	0.56			5.81E-04	0.48		

FOREST RESIDUE SAMPLES (GROT SAMPLES)

SET 1 OF EXPERIMENTS: SAMPLE MASS: 1 mg; SMALL PARTICLE SIZE: 63µm<d<100µm

Table 180. Kinetic parameters of GROT samples: samples mass 1mg, particle size 63µm<d<100µm. Separated results for each repetition

	n=1					n≠1						DAEM					
	c_i	E_i (kJ/mol)	A_i (min^{-1})	S.D.	Fit (%)	c_i	E_i (kJ/mol)	A_i (min^{-1})	n	S.D.	Fit (%)	c_i	E_{0i} (kJ/mol)	A_i (min^{-1})	σ (kJ/mol)	S.D.	Fit (%)
Spruce GROT 01	0.24	80.00	1.18E+07			0.27	72.95	2.69E+06	1.20			0.29	74.97	7.65E+07	7.76		
	0.27	143.40	4.87E+11	4.77E-03	97.44	0.27	150.52	2.15E+12	1.30	3.34E-03	97.86	0.31	162.39	4.01E+14	17.62	6.00E-04	98.34
	0.20	54.83	4.69E+03			0.18	53.00	3.10E+05	1.10			0.12	35.63	6.37E+03	3.78		
Spruce GROT 02	0.21	73.29	3.18E+06			0.23	93.02	2.00E+08	1.25			0.28	80.97	3.18E+08	3.50		
	0.24	147.26	1.09E+12	3.90E-03	97.42	0.24	159.54	1.21E+13	1.20	4.13E-03	97.35	0.31	156.90	1.53E+14	16.94	7.98E-04	97.87
	0.19	54.80	4.66E+03			0.20	61.10	1.29E+04	1.90			0.14	36.80	8.05E+03	1.83		
Birch GROT 01	0.30	75.63	5.88E+06			0.29	81.46	2.25E+07	1.07			0.24	79.72	3.33E+08	8.17		
	0.28	145.81	8.16E+11	3.14E-03	97.98	0.30	151.96	3.08E+12	1.21	1.78E-03	98.48	0.31	141.79	8.69E+12	15.73	7.01E-04	98.25
	0.20	44.90	1.04E+02			0.21	50.13	2.61E+03	1.52			0.12	39.77	1.11E+04	4.08		
Birch GROT 02	0.27	79.20	1.31E+07			0.27	82.21	2.71E+07	1.06			0.24	78.07	2.14E+08	8.50		
	0.27	145.00	7.25E+11	3.01E-03	97.89	0.29	148.35	1.53E+12	1.17	1.88E-03	98.34	0.33	152.30	6.13E+13	16.66	7.79E-04	98.04
	0.19	42.69	7.88E+02			0.19	52.30	3.94E+03	1.65			0.15	38.80	8.57E+03	3.74		
Oak GROT 01	0.25	97.33	4.55E+08			0.25	105.70	3.05E+09	1.21			0.29	99.14	1.63E+10	10-65		
	0.32	165.33	3.61E+13	3.74E-03	98.15	0.33	161.35	1.69E+13	1.02	2.86E-03	98.38	0.31	156.32	1.34E+14	17.81	9.59E-04	98.29
	0.17	41.58	5.19E+02			0.18	45.83	1.03E+03	1.41			0.15	42.32	1.18E+04	3.64		

FOREST RESIDUE SAMPLES (GROT SAMPLES)

SET 2 OF EXPERIMENTS: SAMPLE MASS: 10 mg; SMALL PARTICLE SIZE: 63µm<d<100µm

Table 191. Kinetic parameters of GROT samples: sample mass 10mg, particle size 63µm<d<100µm. One repetition for each sample.

	n=1					n≠1						DAEM					
	c_i	E_i (kJ/mol)	A_i (min^{-1})	S.D.	Fit (%)	c_i	E_i (kJ/mol)	A_i (min^{-1})	n	S.D.	Fit (%)	c_i	E_{0i} (kJ/mol)	A_i (min^{-1})	σ (kJ/mol)	S.D.	Fit (%)
Spruce GROT	0.21	72.31	2.68E+06			0.21	77.66	8.48E+06	1.10			0.27	80.25	2.60E+08	3.10		
	0.26	142.35	4.17E+11	5.54E-03	97.13	0.26	155.92	6.33E+12	1.22	4.64E-03	97.38	0.28	176.04	5.79E+15	19.27	7.92E-04	98.02
	0.19	51.03	2.73E+03			0.20	50.11	2.30E+03	1.24			0.18	40.35	1.58E+04	1.77		
Birch GROT	0.22	71.21	2.69E+07			0.25	81.48	2.18E+07	1.01			0.27	84.80	1.02E+09	2.56		
	0.28	121.03	1.54E+10	3.44E-03	97.64	0.26	163.38	3.17E+13	1.35	1.46E-03	98.47	0.30	140.90	7.98E+12	15.42	5.34E-04	98.31
	0.19	49.63	7.19E+02			0.18	55.30	6.84E+03	1.48			0.18	40.69	1.67E+04	2.18		
Oak GROT	0.26	72.83	2.68E+06			0.23	102.90	1.85E+09	1.20			0.27	104.60	6.13E+10	2.86		
	0.33	144.74	7.01E+11	8.59E-03	97.27	0.30	174.91	2.82E+14	1.08	8.04E-04	99.16	0.30	157.74	2.04E+14	18.00	6.12E-04	98.67
	0.14	52.83	2.73E+03			0.19	62.04	2.32E+04	2.28			0.18	37.59	7.43E+03	3.23		

FOREST RESIDUE SAMPLES (GROT SAMPLES)

SET 3 OF EXPERIMENTS: SAMPLE MASS: 10 mg; LARGE PARTICLE SIZE: d<1mm

Table 202. Kinetic parameters of GROT samples: sample mass 10mg, particle size d<1mm. One repetition for each sample.

	n=1					n≠1						DAEM					
	c_i	E_i (kJ/mol)	A_i (min^{-1})	S.D.	Fit (%)	c_i	E_i (kJ/mol)	A_i (min^{-1})	n	S.D.	Fit (%)	c_i	E_{0i} (kJ/mol)	A_i (min^{-1})	σ (kJ/mol)	S.D.	Fit (%)
Spruce	0.22	79.02	9.80E+06			0.20	80.89	1.68E+07	1.01			0.27	84.78	9.62E+08	3.98		
GROT	0.28	137.22	1.36E+11	5.12E+03	97.27	0.29	158.03	9.81E+12	1.40	2.11E-03	98.25	0.31	128.82	6.93E+11	14.08	5.91E-04	98.30
	0.19	47.58	1.40E+03			0.18	53.07	3.69E+03	1.26			0.17	38.92	1.11E+04	3.91		
Birch	0.24	85.12	4.07E+07			0.23	91.11	1.48E+08	1.01			0.24	93.26	5.38E+09	10.01		
GROT	0.28	154.47	3.86E+12	5.63E-03	97.41	0.29	162.09	1.83E+13	1.16	5.86E-03	97.37	0.31	152.90	6.58E+13	16.88	9.86E-04	98.03
	0.21	54.95	6.15E+03			0.18	58.77	1.21E+04	1.20			0.17	54.08	1.63E+05	5.81		
Oak	0.23	94.03	2.48E+08			0.24	101.85	1.31E+09	1.16			0.24	101.18	2.10E+10	10.88		
GROT	0.33	160.92	1.41E+13	2.47E-03	98.53	0.31	176.60	3.08E+14	1.12	1.38E-03	98.90	0.32	160.17	2.59E+14	18.13	6.51E-04	98.62
	0.18	49.38	2.30E+03			0.18	56.88	8.85E+03	1.54			0.17	49.02	5.42E+04	2.96		

From the results of kinetic parameters presented in this section, it can be stated that for all the sample types, good fitting was obtained with the 3 models applied, having obtained a good agreement between predictions and measured curves. This was reflected in the low values of the square differences (S.D. in the tables) obtained and in the high levels of fitting that was achieved for each of the samples; these values were considered as completely acceptable and in agreement with the fitting levels that have been traditionally obtained by previous authors in the field of kinetic modeling.

As a graphical example, a comparison between the experimentally obtained curve and the theoretically calculated curve is presented in Figure 11 for 1mg spruce stem wood sample with small particle size (63µm<d<100µm). In this case, the calculated curve corresponds to constant activation energy for each of the pseudo-components, and first-order reactions (n=1).

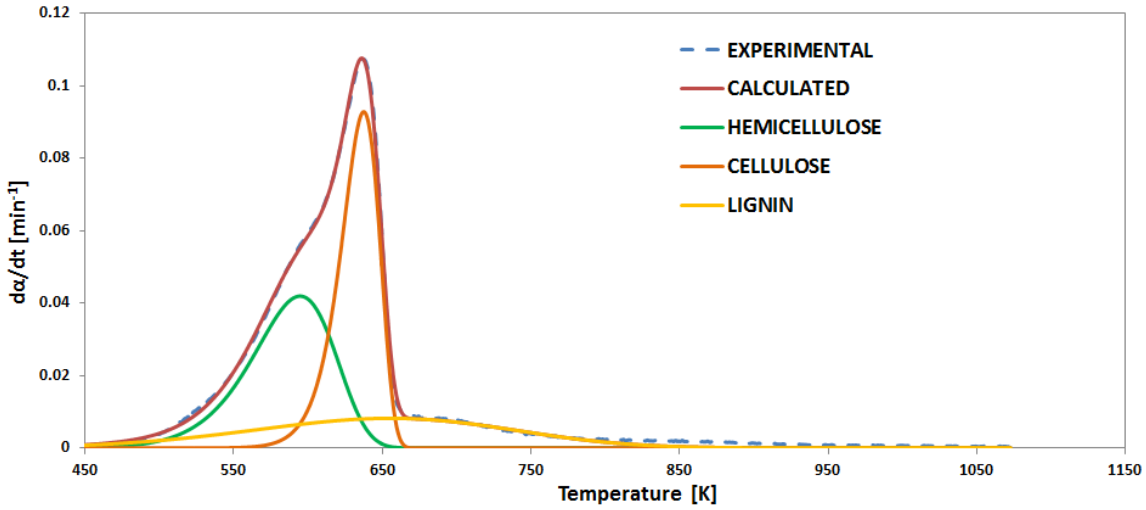

Figure 11. Comparison between the experimental and simulated curves of 1mg spruce stem wood sample with small particle size (63µm<d<100µm). Calculated curve: constant activation energy for each of the pseudo-components, first-order reactions (n=1).

Regarding the values of the kinetic parameters that were calculated by means of the Least Square Method, The obtained values and ranges of values of kinetic parameters are comparable with values from literature.

The differences between stem wood and GROT samples regarding the homogeneity and agreement of the kinetic parameters for the same sample type were remarkable. Among the duplicated experiments of stem wood samples that were kinetically evaluated, it was observed a high level of agreement in terms of kinetic parameters and thus, in terms of decomposition behavior, between experiments of the same sample type (same species and same mass and particle size conditions). This means that the same kinetic parameters modeled different experiments of the same sample type with acceptable, high fitting levels. On the contrary, for some forest residue (GROT) samples, especially for spruce GROT samples (for birch GROT samples the results were more acceptable), it was concluded that it was not possible to establish a set of common kinetic parameters for the two considered duplications with reasonable and acceptable levels of fitting. This is the reason why for the GROT samples whose experiments had been duplicated, it was decided not to present a commonly calculated set of kinetic parameters, as some of the results obtained this way would not fulfill the minimum fitting requirements; instead of that, the kinetic parameters were separately calculated and presented for each of the experiments analyzed.

Regarding differences between kinetic parameters of wood and GROT samples and among samples with different sample mass and particle size, some observations were made by pseudo-components. The aim of studying the values and the evolution of kinetic parameters by pseudo-components was to develop a deeper and a more-detailed analysis by considering effect of these variables on each of the pseudo-components. The remarkable observations are as follows:

Hemicellulose:

Much lower activation energy values of hemicellulose pseudo-component were obtained for GROT samples than for their counterpart stem wood samples for spruce and birch species. Nevertheless, for oak samples, the calculated activation energy values for hemicellulose were in the same range for both, stem wood and GROT type samples.

Some differences and tendencies in behavior found among the calculated values of hemicellulose activation energy for samples with different sample mass and different particle size are also remarkable. For instance, it was clearly observed the following tendency among the hemicellulose activation energy of stem wood samples: the higher the kinetic control level, that is, the lower the sample mass and/or the particle size, the lower the activation energy values corresponding to hemicellulose. Although this observation counts with some exceptions as it can be seen by comparing Tables 15, 16 and 17, two different conclusions could be obtained based on this observed tendency:

1. The first option could be that making higher the kinetic control level (lowering the sample mass and the particle size) favors the hemicellulose decomposition reaction, being needed lower energy for initiating the reaction and thus, resulting in lower activation energy values;

2. The other option which may explain the obtained differences could be based on the fact that increasing both sample mass and particle size of the samples distances the experimental situation from the ideal situation of a fully kinetically controlled reaction; this could make the calculations of the kinetic parameters for those cases with higher sample mass and higher particle size be not that reliable due to not fully kinetically controlled reactions taking place. The developed kinetic modeling process assumes kinetic control of the reactions taking place, but if this condition is not completely fulfilled, the reliability of the results obtained could be suspicious, and this could be the reason why different results were obtained for the different sample mass and particle size conditions.

For the hemicellulose activation energy of GROT samples, such a clear tendency regarding increasing or decreasing of the activation energy value when varying sample mass and particle size parameters was not observed; variation were registered regarding the activation energy values, but both increasing and decreasing values were obtained when making it higher the kinetic control level, depending on the samples.

If studying the hemicellulose pre-exponential factor, for one sample type the same order of magnitude was maintained among the values calculated by means of three different methods considered. The same order of magnitude was also maintained when varying the sample mass and particle size for one wood species or for one GROT

species. Nevertheless, important differences were observed between a certain wood species with concrete sample mass and particle size conditions, and its GROT counterpart: lower pre-exponential factors were registered for GROT samples than for their corresponding, equivalent stem wood samples.

Regarding the c parameter corresponding to the hemicellulose component (c_1), acceptable differences, and even sometimes identical values, were obtained for this parameter for each sample type when employing the three different calculation methods. Besides, the obtained values were very similar for the same stem wood species and also for the same GROT species, with no remarkable variations when varying the sample mass and the particle size. Important differences were observed between the equivalent stem wood and GROT samples of spruce and birch, whereas for oak samples, all c_1 values were maintained approximately in the same range and without high variations between stem wood and GROT sample types.

Cellulose:

Just as it was observed for hemicellulose, for cellulose pseudo-component much lower activation energy values were also registered for GROT samples than for their counterpart stem wood samples for spruce and birch species. Regarding the oak samples, when comparing certain stem wood sample with its corresponding GROT sample, the cellulose activation energy values were sometimes higher and sometimes lower, depending on the concrete sample type, and without that clear tendency observed for spruce and birch.

They are also remarkable the much lower values registered for the cellulose activation energy of oak stem wood, in comparison with spruce and birch stem wood samples. The huge existing gap between the cellulose activation energy values of oak stem wood and the other stem wood samples was not registered for the case of oak GROT samples, for which the obtained values were in the range of the other species.

Unlike what was observed for hemicellulose, no clear tendency of the activation energy of cellulose was observed when increasing the sample mass and/or the particle size of the samples. Variations in the obtained values were registered when these parameters changed, what could be in agreement with the second possible hypothesis

suggested for explaining the changes in the activation energy of hemicellulose, but without a concrete tendency being maintained.

Regarding the pre-exponential factor, good agreement was found among the three considered methods for each sample. Besides, no effects of the sample mass and particle size were fathomed in the values of the pre-exponential factor. Regarding stem wood samples, similar values, kept in the same range, were obtained for all sample types, whereas among the GROT samples, much lower values of the pre-exponential factor were obtained for oak samples in comparison with spruce and birch GROT samples. If comparing values of the pre-exponential factor of stem wood samples and their corresponding GROT samples, it was observed that for the case of spruce and birch, much lower values were obtained for GROT samples than for stem wood samples; regarding oak, variations in the pre-exponential factor were also registered between stem wood and the corresponding GROT samples, but with different tendencies (both higher and lower values were registered for GROT samples in comparison with stem wood samples, without a constant trend).

If the c parameter corresponding to the cellulose component is analyzed (c_2), for spruce and birch samples, they were presented decreasing values of these parameters for GROT samples in comparison with their corresponding stem wood samples. This tendency was not observed for oak samples; between oak stem wood samples and their corresponding GROT samples, differences were also registered in this c_2 parameter, but there was not maintained that tendency observed for spruce and birch. Besides, for spruce and birch samples good agreement was found in the values of the c_2 obtained by means of the three considered methods and also among the experiments developed with different sample mass and particle size conditions. It can be said that that previously mentioned as kinetic control level did not have influence on this parameters for spruce and birch, but such a good agreement was not maintained for the oak samples, for which higher variations in the c_2 parameter were observed when changing sample mass and particle size.

Lignin:

As it happened with the previously analyzed pseudo-components, they were obtained lower values of the activation energy of lignin for GROT samples compared to their corresponding stem wood samples.

Regarding the influence of the kinetic control level, that is, the sample mass and the particle size, on the values of the kinetic parameters, values within similar ranges were obtained for both, the activation energy and the c parameter which correspond to the lignin pseudo-component.

Regarding the pre-exponential factor corresponding to lignin, good agreement was achieved for the three considered methods, meaning that close enough values were obtained by means of the employment of the different kinetic approaches, making the results acceptable. Besides, approximately the same order of magnitude was maintained for each of the studied species, regardless of the sample mas and particle size; this observation also includes the comparison between the stem wood and their corresponding GROT samples, between which not relevant differences in the pre-exponential factor of lignin were observed.

In short, higher overall reactivity of GROT samples was observed for spruce and birch in comparison with their counterparts stem wood samples, due to the lower values of the activation energy registered for their GROT samples. The reason behind this can be found in the Proximate Analysis presented in Table 9. In this table, it can be seen that GROT samples have high content of ash forming elements, and if comparing the ash content of GROT and stem wood samples, GROT samples have higher content of ash forming elements. This higher amount of ash forming elements composing the GROT samples has a catalytic effect during the thermal conversion process. The fact that the higher amount of ash forming elements favors the decomposition reaction lowers the needed minimum energy amount for the reaction to get started. This means that the value of the activation energy decreases, while the reactivity of the samples increases.

5. Conclusions

Finally in this section, the main conclusions that have been obtained from the thermogravimetric analysis of some woody biomass species are presented. The thermogravimetric analysis was developed with the aim of 1) developing the kinetic modeling of some woody biomass samples when undergoing pyrolysis process, and 2) studying the char yield values with the pursue of improving them.

The woody biomass samples which were analyzed thermogravimetrically for this Master's Thesis were Norwegian spruce, birch and oak stem wood and forest residues; the latter were compose by tops and branches of the mentioned trees, and were named as GROT samples (the Norwegian acronym for tops and branches).

For a wide studying of both, the char yield values and the kinetics of the pyrolysis experiments carried out in a thermogravimetric analyzer, TGA (TA Instrument, SDT Q600 model), variations in the experimental conditions were applied: different values of sample mass and particle size were used for the char yield analysis and the kinetic simulation, and changes in the devolatilization environment were also applied for the char yield analysis.

From the analysis of the char yield values of the different samples, the most important conclusion that was obtained was related to the effect of the devolatilization atmosphere in the char yield of the process. It was experimentally proved that during the development of the pyrolysis process, if keeping the released volatiles inside the crucible where the remaining sample mass is still decomposing, has a clear effect of considerably increasing the obtained char yield value. Thus, in other words char yield values were proved to significantly increase when the thermal decomposition that takes place during the pyrolysis process was developed in a generated volatiles atmosphere. This generated volatiles atmosphere was created by covering with a lid the crucible where the sample was held during the experiment. When performing the pyrolysis experiments with the lid of the crucible on, the released volatiles which because of the effect of the lid were kept inside the crucible, were in contact with both, the solid biomass fraction that had not already been decomposed and with the already generated solid products; this favored secondary reactions taking place between the released

volatiles and the solid fractions, what in the end provoked the absorption by the solid matter of an important fraction of those released volatiles. This resulted in an increment in the solid fraction of the products generated in the process and thus, resulted in higher char yield values. This behavior was the most widely proved one, as all the analyzed samples, without exceptions, showed this tendency of increasing char yields in a generated volatiles atmosphere, in comparison with the char yields obtained in an inert atmosphere; thus, it can be considered a highly proved conclusion which found a total behavior agreement among all the sample types and for all the variations of the experimental parameters that were considered.

It was also experimentally proved the expected effect on increasing the char yield of the pyrolysis process that high ash content has. This was deduced from the comparison of the char yields obtained for stem wood and GROT samples of the same species: spruce and birch showed he expected behavior in this regard, with their GROT samples giving a higher char yield value than their corresponding stem wood samples. This was observed for all the combinations in terms of sample mass and particle size considered for spruce and birch samples. In this behavior, it was concluded that the higher ash content of the GROT samples compared to their counterparts stem wood samples was determining in the higher char yield values obtained, and thus, it was confirmed that the ash forming elements were responsible for favoring char formation. Besides, not only the higher presence of ash forming elements, but also the high fixed carbon content in was responsible for GROT samples resulting in the highest char yield values.

Nevertheless, a clear exception was observed in this regard with oak samples, for which stem wood samples were the ones giving the highest char yield values instead of their corresponding GROT samples. Only for the case of 10mg sample mass, large particle size (d<1mm) and without-lid configuration, oak GROT resulted in higher char yield value than its corresponding stem wood sample. For the rest of the experimental variations of oak samples, stem wood sample gave the highest char yields, what is not in agreement with the composition of oak stem wood and GROT samples: as it happened with spruce and birch species, higher content in ash formation elements and higher fixed carbon content is attributed to oak GROT compared to stem wood oak, and thus, the reasonable, expectable result should be that higher char yield was obtained for oak GROT.

No acceptable reason was found behind this odd behavior and unreasonable tendency observed for the oak samples, regarding char yield values obtained for stem wood and GROT samples: the results obtained just seem to be neither reasonable, nor expectable, nor even possible.

Even so, these odd, non-expected results observed for char yield values of oak, and for which no reasonable conclusions could be made, were not the only estrange observations made for this sample type, as it will be mentioned in next paragraphs.

For example, regarding the effect of the sample mass, for lower sample mass, lower char yield values were registered for all samples, with the exception of oak wood, which again followed a different tendency.

Regarding the effect of particle size on obtained char yield values, not complete agreement was found in the obtained results with two contrary behaviors having been observed. For all GROT samples and some stem wood samples (with the exception of spruce and birch stem wood with open crucible and birch stem wood with closed crucible), it was observed that reducing the particle size favored char formation, resulting in higher char yield values. It was concluded that this was provoked by the so-called fractionation of ash, or the effect of inorganic matter in solid fuels, provoked by the process of particle size reduction itself: when samples are sieved for getting their particle size reduced, significant amounts of fines fall down during the process together with the sample with reduced particle size. The filtering of these fines involves a higher proportion or content of inorganic matter in the sample that has just been sieved, that is, in the sample with reduced particle size. And this higher amount of inorganic content in the sample with smaller particle size has the effect of favoring char yield formation. Even so, not complete agreement among all samples was found in the effect of particle size in char formation, as for mentioned exceptions, just the contrary effect was reported, giving higher char yields when particle size was increased.

Regarding the part of the kinetic modeling, it was concluded that good agreement was found:

1) among the three different kinetic approaches used for solving the kinetic issue, by employing the Least Square Method assuming the Three pseudo-components

model: for n=1 and n≠1 with constant activation energy, and for DAEM assuming n=1; and

2) among the results of the kinetic parameters obtained in the current work, and the acceptable ranges of values for each parameter, based on available literature and prior publications and studies.

An important difference was observed when facing the modeling of the stem wood samples and the GROT samples. For the samples where two repetitions were modeled, identical kinetic behavior was registered for wood samples, whereas it was not that identical for the GROT samples. Thus, for the modeling of experiments performed with stem wood samples, good agreement was found regarding the fitting of the simulated curves and the experimentally obtained curves for the two repetitions, by using the same kinetic parameters. On the contrary, for GROT samples, this good agreement was not found between the two different repetitions of the same sample type: when trying to find a set of kinetic parameters that could fit the two experiments, it was only possible to achieve too bad fitting values. This is why kinetic parameters were calculated separately for each of the repetitions of GROT samples.

Regarding reactivity of the species, higher overall reactivity of GROT samples was observed, in comparison with wood samples, for Spruce and Birch species. This is caused due to the much higher content of ash forming elements in GROT samples than in wood samples; these ash forming elements act as catalysts during the thermal conversion, resulting in higher char yield values, as it was previously mentioned, and in a higher reactivity. Although this much higher content in ash forming elements is also registered for oak GROT samples than for Oak wood samples, this tendency regarding higher reactivity was not observed: oak GROT had higher reactivity than wood with 10mg sample mass and large particle size, whereas a lower reactivity of Oak GROT was registered with 1mg sample mass and small particle size; so no clear conclusion can be obtained from these observations.

Therefore, just as it happened with the char yield values of oak samples when comparing stem wood and GROT samples, the same odd, unexpected behavior was observed for oak reactivity.

It is thus remarkable the exceptionality of the oak samples behavior. Due to the impossibility of finding a reason behind these observed odd decomposition behaviors of the oak samples, which are completely illogical and in contrast with oak composition and its expectable behavior, it was concluded that the results obtained for oak were suspicious and thus, that conclusive assertions cannot be made regarding oak experiments. Therefore, due to their strange nature, these observed oak behaviors will not be generalized for oak species, but will be assumed as odd resolutions to be considered in next, further investigations in the field.

Regarding the comparison between hardwood-softwood samples, for the obtained values of both, char yields and kinetic parameters, relatively small differences were registered and the same tendencies were observed in cost of the cases when changing some experimental conditions or when shifting from stem wood samples to GROT samples.

Regarding the obtained values of the kinetic parameters calculated for different cases of sample mass and particle size, in the previous Results section they were identified differences in values and tendencies of the kinetic parameters when changing the sample mass and/or the particle size. From those observations previously presented, it can be concluded that the appreciated differences in the kinetic parameters of the same sample type under different sample mass and/or particle size conditions, which were not negligible, can be attributable to the effect of heat transfer limitations in the decomposition reactions. This effect of heat transfer limitations could were considered to become appreciable when increasing sample mass and particle size of the samples, provoking a shift from kinetically controlled reactions to reactions affected by heat transfer; for simulating the decomposition behavior of those samples, the proposed kinetic evaluation and modeling are not suitable as they assume fully kinetically controlled decomposition reactions, resulting in the obtained variations of the kinetic parameters for the different experimental conditions.

As proposal for further work, some points are suggested based on the conclusions obtained from the current work and on some of the suspicious behaviors observed:

- deeper, specific analysis of oak stem wood and GROT samples is needed, as the results obtained from the current work show an illogical behavior of this woody biomass type;

- deeper, wider confirmation of specially the kinetic results obtained is encouraged in order to completely ratify and confirm some of the obtained results;
- changes in other experimental conditions could be applied for studying their effect on the kinetic parameters and, if varying values were obtained, for having broader confirmation of the not fully kinetically controlled reactions as the cause of obtaining different values of the kinetic parameters.

6. References

[1] Conesa JA, Marcilla A, Caballero JA, Font R. *Comments on the Validity and Utility of the Different Methods for Kinetic Analysis of Thermogravimetric Data*. J. Anal. Appl. Pyrolysis 2001;617:*58-59*.

[2] Manyá JJ, Velo E, Puigjaner L. *Kinetics of biomass pyrolysis: a reformulated three-parallel-reactions model.* Ind. Eng. Chem. Res. 2003;42:434-441.

[3] El-Sayed SA, Mostafa ME. *Pyrolysis characteristics and kinetic parameters determination of biomass fuel powders by differential thermal gravimetric analysis (TGA/DTG).* Energy Conversion and Management 2014;85:165-172.

[4] El-Sayed SA, Mostafa ME. *Kinetic parameters determination of biomass pyrolysis fuels using TGA and DTA techniques.* Waste Biomass Valor 2015;6:401-415.

[5] Rajeshwar K. *The kinetics of the thermal decomposition of green river oil shale kerogen by non-isothermal tehrmogravimetry.* Thermochimica Acta 1981;45:253-263.

[6] Hu S, Jess A, Xu M. *Kinetic study of Chinese biomass slow pyrolysis: comparison of different kinetic models.* Fuel 2007;86:2778-2788.

[7] Tapasvi D, Khalil R, Varhegyi G, Tran K-Q, Gronli M, Skreiberg O. *Thermal decomposition kinetics of woods with emphasis on torrefcation.* Energy Fuels 2013;27:6134-6145.

[8] Grønli MG, Várhegyi G, Di Blasi C. *Themrogravimetric Analysis and Devolatilization Kinetics of Wood.* Ind. Eng: Chem. Res. 2002;1:4201-4208.

[9] Várhegyi G, Antal MJ Jr, Jakab E, Szabó P. *Kinetic modeling of biomass pyrolysis.* J. Anal. Appl. Pyrolysis 1997;42:73-87.

[10] Antal Jr MJ, Várhegyi G. *Cellulose pyrolysis kinetics: the current state of knowledge.* Ind. Eng. Chem. Res. 1995;34:703-717.

[11] Órfao JJM, Antunes FJA, Figueiredo JL. *Pyrolysis kinetics of lignocellulosic materials-three independent reactions model.* Fuel 1999;78:349-358.

[12] Conesa JA, Caballero JA, Marcilla A, Font R. *Analysis of different kinetic models in the dynamic pyrolysis of cellulose.* Thermochimica Acta 1995;254:175-192.

[13] Branca C, Albano A, Di Blasi C. *Critical evaluation of global mechnaisms of wood devolatilization.* Thermochimica Acta 2005;429:133-141.

[14] Di Blasi C. *Modeling chemical and physical processes of wood and biomass pyrolysis.* Progress in Energy and Combustion Science 2008;34:47-90.

[15] Tran K-Q, Bach Q-V, Trinh TT, Seisenbaeva G. *Non-isothermal pyrolysis of torrefied stump- A comparative kinetic evaluation.* Applied Energy 2014;136:759-766.

[16] *Europe 2020: Europe's growth strategy* (2012) European Comission. European Comission president Barroso.
Available at: http://ec.europa.eu/europe2020/pdf/europe_2020_explained.pdf

[17] *Climate Action: 2030 Climate & Energy Framework.* (2014) European Comission. Available at:
http://ec.europa.eu/clima/policies/strategies/2030/index_en.htm

[18] *Climate Action: Paris Agreement.* (2015) European Commission. Available at: http://ec.europa.eu/clima/policies/international/negotiations/paris/index_en.htm

[19] Paschalidou A, Tsatiris M, Kitikidou K. *Energy crops for biofuel production or for foof? – SWOT analysis (case study: Greece).* Renewable Energy 2016;93:636-647.

[20] Internation al Energy Outlook, 2013. Available at:
http://www.eia.gov/forecasts/ieo/pdf/0484(2013).pdf

[21] Saxena RC, Adhikari DK, Goyal HB. *Biomass-based energy fuel through biochemical routes: a review.* Renew Sust Energy Rev 2009;13:167-178.

[22] Akash B. *Thermochemical Depolymerization of Biomass*. The 5th International Conference on Sustainable Energy Information Technoogy (SEIT 2015). Procedia Computer Science *2015;52:827-834.*

[23] Soria-Verdugo A, Goos E, Arrieta-Sanagustín J, García-Hernando N. *Modeling of the pyrolysis of biomass under parabolic and exponential temperature increases using the Distributed Activation Energy Model.* Energy Conversion and Management 2016;118:223-230.

[24] Kan T, Strezov V, Evans TJ. *Lignocellulosic biomass pyrolysis: A review of product properties and effects of pyrolysis parameters*. Renewable and Sustainable Energy Reviews 2016;57:1126-1140.

[25] Shuping Z, Tulong W, Minde Y, Chun L. and Junmao, T. *Pyrolysis charactristics and kinetics of the marine mricroalgae Dunaliella tertiolecta using thermogravimetric analyzer.* Biosurce Technology 2010; 101: 359-365.

[26] Lauri P, Havlík P, Kindermann G, Forsell N, Böttcher H, Obersteiner M. *Woody biomass energy potential in 2050.* Energy Policy 2014;66:19-31.

[27] White EM. *Woody Biomass for Bioenergy and Biofuels in the United States- A Briefing Paper.* United States Department of Agriculture, Forest Service. Available at:
http://www.fsl.orst.edu/lulcd/Publicationsalpha_files/White_pnw_gtr825.pdf

[28] Zafar S. *Woody biomass resources*. Alternative Energy News. Available at: http://www.alternative-energy-news.info/woody-biomass-resources/

[29] Hu M, Chen Z, Wang S, Guo D, Ma C, Zhou Y, Chen J, Laghari M, Fazal S, Xiao B, Zhang B, Ma S. *Thermogravimetric kinetics of lignocellulosic biomass slow pyrolysis using distributed activation energy model, Fraser-Suzuki deconvolution, and iso-conversional method.* Energy Conversion and Management 2016;118:1-11.

[30] Zobel N, Anca-Couce A. *Influence of intraparticle secondary heterogeneous reactions on the reaction enthalpy of wood pyrolysis.* Journal of Analytical and Applied Pyrolysis 2015;116:281-286.

[31] Gao Z, Fan Q, He Z, Wang Z, Wang X, Sun J. *Effect of biodegradation on thermogravimetric and chemical charcateristics of hardwood and softwood by brown-rot fungus*. Bioresource Technoogy 2016;211:443-450.

[32] Johansen JM, Gadsbøll R, Thomsen J, Jensen PA, Glarborg P, Ek P, De Martini N, Mancini M, Weber R, Mitchell RE. *Devolatilization kinetics of woody biomass at short residence times and high heating rates and peak temperatures.* Applied Energy 2016;162:245-256.

[33] (2009) *Biofuels. Securing the Planet's Future Energy Needs.* Retrieved from: http://link.springer.com/chapter/10.1007/978-1-84882-011-1_6

[34] Altun NE, Hicyilmaz C, Kök MV. *Effect of particle size and heating rate on the pyrolysis of Silopi asphaltite.* Journal of Analytical Applied Pyrolysis 2003;67:369-379.

[35] Balat M, Balat M, Kirtay E, Balat H. *Main routes for the thermos-conversion of biomass into fuels and chemicals. Part 1: pyrolysis systems.* Energy Convers Manag 2009; 50:3147-3157.

[36] Vamvuka D. Bio-oil, solid and gaseous biofuels from biomass pyrolysis processes – an overview. Int. J. Energy Res. 2011;35:835–862.

[37] Demirbas MF, Balat M. *Biomas Pyrolysis for liquid fuels and chemicals: a review*. J. Sci. Ind. Res. India 2007;66:797-804.

[38] Di Blasi, C. *Combustion and gasification rates of lignocellulosic chars*. Progress in Energy and Combustion Science 2009;35:121-140.

[39] Monsen B, Tangstad M, Midtgaar H. *Use of charcoal in silicomanganese production*. ISBN: 0-9584663-5-1, INFACON X, 2004; 392-404. Retrieved from: http://www.pyrometallurgy.co.za/InfaconX/009.pdf

[40] Bridgwater AV, Meier D, Radlein D. *An overview of fast pyrolysis of biomass.* Organic Geochemistry 1999;30:1479-1493.

[41] Mohan D, Pittman CU Jr, Steele PH. *Pyrolysis of wood/biomass for bio-oil: a critical review.* Energy&Fuels, 2006;20:848-889.

[42] *Industrial Charcoal Production CP/CRO/3101 (A). Development of a sustainable charcoal industry.* The FAO project. June 2008, Zagreb, Croatia.

[43] *Industrial charcoal making.* FAO Forestry Paper 63. Mechanical Wood Products Branch. Forest Industries Division. FAO Forestry Department. Food and agriculture organization of the United Nations. Rome, 1985. M-37. ISBN 92-5-102307-7.

[44] Monsen B, Grønli MG, Nygaard L, Tveit H. *The use of biocarbon in Norwegian ferroalloy production.* Available at:

https://www.researchgate.net/publication/259572787_The_Use_of_Biocarbon_in_Norwegian_Ferroalloy_Production

[45] Willner T, Brunner G. *Pyrolysis kinetics of wood and wood components.* Chem. Eng. Technol. 2005;28(10):1212-1225.

[46] Chan W-C R, Kelborn M, Krieger BB. *Modelling and experimental verification of physical and chemical processes during pyrolysis of a large biomass particle.* Fuel 1985;64:1505-1513.

[47] Kansa EJ, Perlee HE, Chaiken RF. *Mathematical model of wood pyrolysis including internal forced convection.* Combustion and Flame 1977;29: 311-324.

[48] Boronson ML, Howard TB, Longwell JP, Peters WA. *Heterogeneous cracking of wood pyrolysis tars over fresh wood char surfaces.* Energy Fuels 1989;3:735-740.

[49] Simon P. *Isoconversional methods.* Journal of Thermal Analysis and Calorimetry 2004;76:123-132.

[50] Starink MJ. *The determination of activation energy from linear heating rate experiments: a comparison of the accuracy of isoconversional methods.* Thermochimica Acta 2003;404 163-176.

[51] Starink MJ. *On the applicability of isoconversion methods of obtaining the activation energy of reactions within a temperature-dependent equilibrium state.* Journal of Materials Science 1997;32:6505-6512.

[52] Slopiecka K, Bartocci P, Fantozzi F. *Thermogravimetric analysis and kinetic study of poplar wood pyrolysis.* Third International Conference on Applied Energy 2011:167-1698.

[53] Poletto M, Zattera A, Santana RMC. *Thermal decomposition of wood: kinetics and degradation mechanisms.* Bioresource Technology, 2012;126:7-12.

[54] Venkatesh M, Ravi P, Tewari SP. *Isoconversional Kinetic Analysis of Decomposition of Nitroimidazoles: Friedmas method vs Flynn-Wall_Ozawa Method.* The Journal of Physical Chemistry 2013;117:10162-10169.

[55] Criado JM, Sánchez-Jiménez PE, Pérez-Maqueda LA. *Critical study of the isoconversional methods of kinetic analysis.* Journal of Thermal Analysis and Calorimetry 2008;92:199-203.

[56] Gotor FJ, Criado JM, Malek J, Koga N. *Kinetic analysis of solid-state reactions: the universality of master plots for analyzing isothermal and* nonisothermal experiments. Journal of Physical Chemistry 2000;104:10777-10782.

[57] Ebrahimi-Kahrizsangi R, Abbasi MH. *Evaluation of reliability of Coasts-Redfern method of kinetic analysis of non-isothermal TGA.* Trans. Nonferrous Met. Soc. China 2008;18:217-221.

[58] Várhegyi G, Szabó P, Jakab E, Till F. *Least square criteria for the kinetic evaluation of thermoanalytical experiments. Examples from a char reactivity study.* Journal of Analytical and Applied Pyrolysis 2001;57:203-222.

[59] Broido A, Weinstein M. *Kinetics of solid-phase cellulose pyrolysis*, in: Wiedeman (Ed.), Proceedings of the 3rd International Conference on Thermal Analysis, Birjhauser Verlag, Basel, 1971, pp.285-296.

[60] Várhegyi G. *Aims and methods in non-isothermal reaction kinetics.* J. Anal. Appl. Pyrolysis 2007;79:278-288.

[61] Branca C, Di Blasi C. *Global kinetics of wood char devolatilization and combustion.* Energy & Fuels 2003;17:1609-1615.

[62] Mani T, Murugan P, Abedi J, Mahinpey N. *Pyrolysis of wheat straw in a thermogravimetric analyzer: effect of particle size and heating rate on devolatilization and estimation of global kinetics.* Chemical engineering research and design 2010;88:952-958.

[63] Cai J, Ji L. *Pattern search method for determination of DAEM kinetic parameters from nonisothermal TGA data of biomass.* Journal of Mathematical Chemistry, Vol 42 2007;3:547-553.

[64] Tripathi M, Sahu JN, Ganesan P. *Effect of process parameters on production of biochar from biomass waste through pyrolysis: A review.* Renewable and Sustainable Energy Reviews 2016;55:467-481.

[65] Sensöz S, Angin D. *Pyrolysis of safflower (Charthamus tinctorius L.) seed press cake: part 1. The effect of pyrolysis parameters on the product yields.* Bioresur. Technol 2008;99:(13):5492-5497.

[66] White JE, CatalloWJ, Legendre BL. *Biomass pyrolysis kinetics: a comparative critical review with relevant agricultural residue case studies.* J Anal Appl Pyrol 2011;91:1–33.

[67] Collard FX, Blin J. *A review on pyrolysis of biomass constituents: Mechanisms and composition of the products obtained from the conversion of cellulose, hemicellulose and lignin.* Renewable and Sustainable Energy Review 2014;38:594-608.

[68] Brown AL, Dayton DC, Daily JW. *A study of cellulose pyrolysis chemistry and global kinetics at high heating rates.* Energy & Fuels 2001;15:1286-1294.

[69] Grønli MG, Antal MJ Jr, Várhegyi G. *A round-robin study of cellulose pyrolysis kinetics by thermogravimetry*. Industrial & Engineering Chemistry Research 1999;38:2238-2244.

[70] Antal MJ, Várhegyi G. *Impact of Systematic Errors on the Determination of Cellulose Pyrolysis Kinetics.* Energy & Fuels 1997;11:1309-1310.

[71] Antal MJ, Várhegyi G, Jakab E. *Cellulose Pyrolysis Kinetics: Revisited* Ind. Eng. Chem. Res. 1998;37:1267-1275.

[72] Simmons GM, Gentry M. *Particle size limitations due to heat transfer in determining pyrolysis kinetics of biomass.* Journal of Analytical and Applied Pyrolysis 1986;10:117-127.

[73] Bryden KM, Ragland KW, Rutland CJ. *Modeling thermally thick pyrolysis of wood.* Biomass & Boenergy 2002;22:41-53.

[74] Hagge MJ, Bryden KM. *Modeling the impact of shrinkage on the pyrolysis of dry biomass.* Chemical Engineering Science 2002;57:2811-2823.

[75] Czarnecki, Sesták J. *Practical thermogravimetry.* Journal of Thermal Analysis and Calorimetry 2000;60:759-778.

[76] Hurt RH, Calo JM. *Semi-global intrinsic kinetics for char combustion modeling.* Combust Flame 2001;125:1138-1149.

[77] Smith IW. *The combustion rates of coal chars: a review.* In : Nineteenth symposium (international) on combustion, Pittsburgh, p: The Combustion Institutte; 1982. P. 1045-65.

[78] Laurendeau NM. *Heterogeneous kinetics of coal char gasification and combustion.* Prog Energy Combust Sci 1978;4:221-270.

[79] Mermoud F, Salvador S, Van de Steene L, Golfier F. *Influence of the pyrolysis heating rate on the steam gas gasification rate of large wood char particles.* Fuel 2006;85:1473-1482.

[80] Kumar M, Gupta RC. *Influence of carbonization conditions on the gasification of acacia and eucalyptus wood chars by carbon dioxide.* Fuel 1994; 73: 1922-5.

[81] Standish N, Tanjung FA. *Gasification of single wood charcoal particles in CO_2.* Fuel 1988;67:666-672.

[82] Hon DN-S,Shiraishi N. (2001) *Wood and cellulosic chemistry. Second edition, revised and expanded.* Available at: https://books.google.es/

[83] Räisänen T, Athanassiaadis D. *Basic chemical composition of the biomass components of pine, spruce and birch.* Forest Refine. Available at: http://www.biofuelregion.se/UserFiles/file/Forest%20Refine/1_2_IS_2013-01-31_Basic_chemical_composition.pdf

[84] The composition of oak. Available at: http://homedistiller.org/oak.pdf

[85] Jin W, Singh K, Zondlo J. *Pyrolysis kinetics of physical components of wood and wood-polymers using isoconversion method.* Agriculture 2013;3:12-32.

[86] Trubetskaya A, Jensen PA, Jensen AD, Steibel M, Spliethoff H, Glarborg P. *Influence of fast pyrolysis conditions on yield and structural transformation of biomass chars.* Fuel Processing Technology 2015;14:205-214.

[87] Wang L, Skreiberg Ø, Grønli M, Specht P, Antal Jr MJ. *Is elevated pressure required to achieve a high fixed-carbon yield of charcoal from biomass? Part 2: The importance of particle size.* Energy Fuels 2013;27:2146-2156.

[88] Aguilar G, Muley PD, Henkel C, Boldor D. *Effects of biomass particle size on yield and composition of pyrolysis bio-oil derived from Chinese tallow tree (Triadica Sebifera L.) and energy cane (Saccharum complex) in an inductively heated reactor.* AIMS Energy 2015;3(4):838-850.

[89] Lu H, Ip E, Socott J, Foster P, Vickers M, Baxter LL. *Effect of particle shape and size on devolatilization of biomass particle.* Fuel 2010;89:1156-1168.

[90] Gaston KR, Jarvis MW, Pepiot P, Smith KM, Frederick WJ Jr, Nimlos MR. *Biomass pyrolysis and gasification of varying particle sizes in a fluidized-bed reactor.* Energy&Fuels 2011;25:3747-3757.

[91] Bennadji H, Smith K, Serapiglia MJ, Fisher EM. *Effect of particle size on low-temperature pyrolysis of woody biomass.* Energy&Fuels 2014;28:7527-7537.

7. Appendix

Risk assessment

In this section, the risk assessment is presented. It consist of the official document for risk assessment from NTNU where the possible, potential risks that could happen when developing the tasks related to the Master's Thesis are considered, analyzed and classified, together with the measures for avoiding the happening of those risks and for mitigating their effects in case they happened.

NTNU HSE	Hazardous activity identification process	Prepared by	Number	Date
		HSE section	HMSRV2601E	09.01.2013
		Approved by		Replaces
		The Rector		01.12.2006

Unit: *(Department)* **Deparment of Energy and Process Engineering** **Date: 06/07/2016**

Participants in the identification process (including their function)**: Maria Zabalo Alonso as the student who will deveop the laboratory activities and Liang Wang, from SINTEF Energy Research, as responsible for laboratory work.**

Short description of the main activity/main process: Master project for student: Maria Zabalo Alonso. Project title: *Thermogravimetric Analysis of Woody Biomass.*

Is the project work purely theoretical? (YES/NO): NO *Answer "YES" implies that supervisor is assured that no activities requiring risk assessment are involved in the work. If YES, briefly describe the activities below. The risk assessment form need not be filled out.*

Signatures: *Responsible supervisor:* *Student:* 

ID nr.	Activity/process	Responsible person	Existing documentation	Existing safety measures	Comment
1	Pyrolysis experiments of woody biomass samples in the TGA- Thermogravimetric analyser.	Liang Wang (SINTEF Energy Research)	TGA brochure and instructions manual. SDT online help. http://www.tainstruments.com/wp-content/uploads/sdt.pdf http://mrllibrary.mrl.illinois.edu/rootfolder/1-Device%20Fabrication%20Core/FabFacility/DSC_TGA_Training_Module_01.pdf	General safety measures applied at the Laboratory of Energy and Process Engineering. Hard previous training: general training having to pass a safety course, and specific training on the TGA instrument. Discipline when running the experiments for avoiding problems with the instrument.	For this activity, the existing risk, as can be seen in the next section, was economical and related to machine damages. The security of the people involved is never put into risk. This is why the safety measures in order to avoid machine breakdown are based on prior training of the used and on following a strict discipline when dealing with the machine, always respecting manufacturer's advice.

ID nr.	Activity/process	Responsible person	Existing documentation	Existing safety measures	Comment
2	Proximate Analysis of woody biomass	Liang Wang (SINTEF Energy Research)	ASTM Standards. https://www.astm.org/	General safety measures applied at the Laboratory of Energy and Process Engineering. Gloves, lab coat and protection glasses compulsorily used when running the experiments Discipline when running the experiments for avoiding security problems (for example, being injuried).	For this activity, the existing risk, as can be seen in the next section, was related to human beings, their security and safety due to experiments at high temperatures were run. Specially important to avoid incidents in this activity due to the human damages that may be caused.
3	HHV measurements in bomb calorimether IKA Labortechnik C5000	Liang Wang (SINTEF Energy Research)	ASTM Standards. https://www.astm.org/ IKA Labortechnik C5000 brochure and user's manual.	General safety measures applied at the Laboratory of Energy and Process Engineering. Discipline when running the experiments for avoiding problems with the instrument. Discipline when running the experiments for avoiding human mistakes that may cause injuries due to working with a highly pressurized instrument.	For this activity, the existing risk, as can be seen in the next section, was human, economical and related to machine damages. The security of the people involved could be put into risk. Specially important to avoid incidents in this activity due to the human damages that may be caused. Besides, safety measures are also focused in avoiding machine breakdown: prior training of the user and following a strict discipline when dealing with the machine, always respecting manufacturer's advice.

NTNU HSE/KS	Risk assessment	Prepared by	Number	Date
		HSE section	HMSRV2603E	04.02.2011
		Approved by		Replaces
		The Rector		01.12.2006

Unit: *(Department)* **Derpartment of Energy and Process Engineering** **Date: 06/07/2016**

Participants in the identification process (including their function)**:): Maria Zabalo Alonso as the student who will deveop the laboratory activities and Liang Wang, from SINTEF Energy Research, as responsible for laboratory work.**

Short description of the main activity/main process: Master project for student Maria Zabalo Alonso. Project title: *Thermogravimetric Analysis of Woody Biomass.*

Signatures: *Responsible supervisor:* *Student:*

Activity from the identification process form	Potential undesirable incident/strain	Likelihood:	Consequence:			Risk Value (human)	Risk Value (environ.)	Risk Value (economy)	Comments/status Suggested measures
		Likelihood (1-5)	Human (A-E)	Environment (A-E)	Economy/ material (A-E)				
1: Pyrolysis experiments of woody biomass samples in the TGA-Thermogravimetric analyser.	Failure of the instrument, for human or technical reasons.	3	A	A	C	A3	A3	C3	Acceptable human and environment risks; assessment range for economy risk. **Suggested measures:** intensive training period before starting the experiments for minimizing human impact on the operation of the instrument.
2: Proximate Analysis of woody biomass	Incident when dealing with the furnaces at very high temperatures (600ºC-950ºC)	2	D	B	A	D2	B2	A2	Assessment range for human risk; acceptable environment and economic risks. **Suggested measures:** intensive training period before starting the proximate analysis for minimizing human risk. Use of protective clothing when dealing with high temperature furnaces: lab coat, gloves.
3: HHV measurements in bomb calorimether IKA Labortechnik C5000	Failure of the instrument, for human or technical reasons.	3	C	A	C	C3	A3	C3	Assessment range for human risk; acceptable environment risks; assessment range for economy risk. **Suggested measures:** same as 1. Discipline for avoiding mistakes that may cause serious injuries as working with high pressures.

Likelihood, e.g.:
1. *Minimal*
2. *Low*
3. *Medium*
4. *High*
5. *Very high*

Consequence, e.g.:
A. *Safe*
B. *Relatively safe*
C. *Dangerous*
D. *Critical*
E. *Very critical*

Risk value (each one to be estimated separately):
Human = Likelihood x Human Consequence
Environmental = Likelihood x Environmental consequence
Financial/material = Likelihood x Consequence for Economy/materiel

Potential undesirable incident/strain

Identify possible incidents and conditions that may lead to situations that pose a hazard to people, the environment and any materiel/equipment involved.

Criteria for the assessment of likelihood and consequence in relation to fieldwork

Each activity is assessed according to a worst-case scenario. Likelihood and consequence are to be assessed separately for each potential undesirable incident. Before starting on the quantification, the participants should agree what they understand by the assessment criteria:

Likelihood

Minimal 1	Low 2	Medium 3	High 4	Very high 5
Once every 50 years or less	Once every 10 years or less	Once a year or less	Once a month or less	Once a week

Consequence

Grading	Human	Environment	Financial/material
E Very critical	May produce fatality/ies	Very prolonged, non-reversible damage	Shutdown of work >1 year.
D Critical	Permanent injury, may produce serious serious health damage/sickness	Prolonged damage. Long recovery time.	Shutdown of work 0.5-1 year.
C Dangerous	Serious personal injury	Minor damage. Long recovery time	Shutdown of work < 1 month
B Relatively safe	Injury that requires medical treatment	Minor damage. Short recovery time	Shutdown of work < 1week
A Safe	Injury that requires first aid	Insignificant damage. Short recovery time	Shutdown of work < 1day

The unit makes its own decision as to whether opting to fill in or not consequences for economy/materiel, for example if the unit is going to use particularly valuable equipment. It is up to the individual unit to choose the assessment criteria for this column.

Risk = Likelihood x Consequence

Please calculate the risk value for “Human”, “Environment” and, if chosen, “Economy/materiel”, separately.

About the column ”Comments/status, suggested preventative and corrective measures”:

Measures can impact on both likelihood and consequences. Prioritise measures that can prevent the incident from occurring; in other words, likelihood-reducing measures are to be prioritised above greater emergency preparedness, i.e. consequence-reducing measures.

MATRIX FOR RISK ASSESSMENTS at NTNU

CONSEQUENCE						
	Extremely serious	E1	E2	E3	E4	E5
	Serious	D1	D2	D3	D4	D5
	Moderate	C1	C2	C3	C4	C5
	Minor	B1	B2	B3	B4	B5
	Not significant	A1	A2	A3	A4	A5
		Very low	Low	Medium	High	Very high
		LIKELIHOOD				

Principle for acceptance criteria. Explanation of the colours used in the risk matrix.

Colour		Description
Red		Unacceptable risk. Measures must be taken to reduce the risk.
Yellow		Assessment range. Measures must be considered.
Green		Acceptable risk Measures can be considered based on other considerations.